AD_____

Award Number: DAMD17-99-1-9564 Volume IV

TITLE: Role of Angiogenesis in the Etiology and Prevention of Ovarian Cancer

IV: Prevention of Ovarian Carcinoma Dissemination by Inhibiting Cell Adhesion

PRINCIPAL INVESTIGATOR: Sundaram Ramakrishnan, Ph.D.

CONTRACTING ORGANIZATION: University of Minnesota
Minneapolis, MN 55455-2070

REPORT DATE: October 2003

TYPE OF REPORT: Annual

PREPARED FOR: U.S. Army Medical Research and Materiel Command
Fort Detrick, Maryland 21702-5012

REPORT DOCUMENTATION PAGE

Form Approved OMB No. 074-0188

1. AGENCY USE ONLY (Leave blank)	2. REPORT DATE	3. REPORT TYPE AND DATES COVERED
	October 2003	Annual (1 Oct 2002 - 30 Sep 2003)

4. TITLE AND SUBTITLE

Role of Angiogenesis in the Etiology and Prevention of Ovarian Cancer
IV: Prevention of Ovarian Carcinoma Dissemination by Inhibiting Cell Adhesion

5. FUNDING NUMBERS

DAMD17-99-1-9564

6. AUTHOR(S)

Sundaram Ramakrishnan, Ph.D.

7. PERFORMING ORGANIZATION NAME(S) AND ADDRESS(ES)

University of Minnesota
Minneapolis, MN 55455-2070

E-Mail: sunda001@tc.umn.edu

8. PERFORMING ORGANIZATION REPORT NUMBER

9. SPONSORING / MONITORING AGENCY NAME(S) AND ADDRESS(ES)

U.S. Army Medical Research and Materiel Command
Fort Detrick, Maryland 21702-5012

10. SPONSORING / MONITORING AGENCY REPORT NUMBER

11. SUPPLEMENTARY NOTES

This is Volume IV of IV

12a. DISTRIBUTION / AVAILABILITY STATEMENT

Approved for Public Release; Distribution Unlimited

12b. DISTRIBUTION CODE

13. ABSTRACT (Maximum 200 Words)

The purpose of this project to evaluate the mechanism by which ovarian cancer cell spread with in the peritoneal cavity. Ovarian cancer cells adhere to mesothelial cells and their extracellular matrix lining the peritoneum. Characterizing the cell surface molecules involved in this interaction will facilitate development of methods to inhibit ovarian cancer spread and perhaps limit their growth as well.

14. SUBJECT TERMS

Ovarian Cancer

15. NUMBER OF PAGES

125

16. PRICE CODE

17. SECURITY CLASSIFICATION OF REPORT	18. SECURITY CLASSIFICATION OF THIS PAGE	19. SECURITY CLASSIFICATION OF ABSTRACT	20. LIMITATION OF ABSTRACT
Unclassified	Unclassified	Unclassified	Unlimited

Table of Contents

(4) INTRODUCTION:

Epithelial cancer of the ovary spreads by implantation of tumor cells onto the mesothelial cells and their associated extracellular matrix lining the peritoneal cavity. Our earlier data indicated that ovarian carcinoma cells adhere to mesothelial cells and their associated extracellular matrix (ECM) by use of CD44 and the β1 integrin subunit [1]. We hypothesized that CD44 and the β1 integrin subunit play a fundamental role in the formation of secondary tumor growths in ovarian carcinoma by promoting the adhesion, migration, and invasion of the ovarian carcinoma cells to the mesothelial cells that line the peritoneal cavity. Ovarian carcinoma patients frequently develop a malignant peritoneal ascites fluid containing single and aggregated tumor cells, or spheroids. Spheroids have been used as models of tumor microenvironments, and have been demonstrated to be resistant to many therapies, but their potential to contribute to ovarian cancer dissemination has not been determined. We have since shown that CD44 and β1 integrin mediate ovarian carcinoma cell migration toward extracellular matrix molecules [2] and that the β1 integrin subunit regulates the formation and adhesion of ovarian carcinoma multicellular spheroids [3]. By inhibiting these steps of secondary tumor growth, we will attempt to prevent the dissemination of ovarian carcinoma to organs within the peritoneal cavity. During the past year, we have addressed the following aims: (i) determine the role of CD44 and the β1 integrin subunit in the adhesion, migration, and invasion of a primary ovarian carcinoma cell line, specifically in the shape of multicellular aggregates or spheroids, toward mesothelial cells and their associated ECM; (ii) evaluate the role of CD44 and the β1 integrin subunit in ovarian carcinoma cell adhesion, migration, and invasion using populations of ascites cells isolated from patients with ovarian carcinoma; and (iii) determine whether ovarian carcinoma cells isolated as "floaters" from ascites fluid have different growth properties when cultured on monolayers of mesothelial cells.

(5) BODY:

Task #1: Determine the role of CD44 and the β1 integrin subunit in the adhesion and invasion of ovarian carcinoma cell lines toward mesothelial cells and their associated extracellular matrix.
This task has essentially been completed for single cell suspensions of ovarian carcinoma cell lines. However, based on the exciting results that we obtained in years #1-3, we expanded these studies to examine the migration and invasion of spheroids generated from an ovarian carcinoma cell line. Furthermore, in an effort to identify novel molecules that could serve to inhibit the dissemination of ovarian carcinoma, we also analyzed gene expression data. The data described below is unpublished; some results will need to be repeated prior to submission for publication.

Task #1a: Evaluate reagents for their ability to inhibit the adhesion of ovarian carcinoma cells to extracellular matrix components and/or monolayers of mesothelial cells.
In an attempt to identify novel proteins that are specific to ovarian carcinoma that could potentially serve as inhibitors of cell adhesion, migration, and invasion, we analyzed gene expression data. Through a collaboration with Gene Logic Inc. and the Cancer Center's Tissue Procurement Facility (for which I served as Director from 1995 until June 2002), researchers at the University of Minnesota were allowed access to the gene expression database that Gene Logic Inc. had compiled using tissues supplied by the University of Minnesota. We analyzed the Affymetrix HU_95 gene expression data for tissues from 20 ovarian carcinomas, 19 metastases

of ovarian carcinoma, 50 normal ovaries, and over 300 other tissues. We found 46 genes that were specifically upregulated in the ovarian carcinoma tissues. For seven of the genes, we performed immunohistochemistry on ovarian carcinoma and normal ovary tissues. The proteins for three of these genes were specific to the ovarian carcinoma tissues. We have submitted these findings for publication in the *American Journal of Pathology* [4; Appendix #3]. Future experiments will be performed to determine whether we can inhibit cell adhesion, migration, and invasion with these novel ovarian carcinoma proteins.

Task #1b: Evaluate reagents for their ability to inhibit the migration of ovarian carcinoma cells through extracellular matrix components.

We have assessed the ability of spheroids to disseminate and migrate. To determine their ability to disaggregate, spheroids generated from the human ovarian carcinoma cell line NIH:OVCAR5 were placed on a variety of extracellular matrix components. While laminin, fibronectin, and type IV collagen stimulated minor cell migration out of the spheroid, 5 μg/ml of type I collagen caused complete spheroid disaggregation. A blocking antibody against the β1 integrin subunit significantly inhibited this outgrowth. This data is still preliminary and has not been published yet.

Task #1c: Evaluate reagents for their ability to inhibit the invasion of ovarian carcinoma cells through a monolayer of mesothelial cells.

- We designed a cell-based invasion assay in which human LP9 peritoneal mesothelial cells were grown to confluence in tissue culture wells. The LP9 monolayers were: (i) live, (ii) irradiated so that they could not proliferate, or (iii) fixed with methanol. NIH:OVCAR5 ovarian carcinoma spheroids were added atop the mesothelial cell monolayers. Ovarian carcinoma spheroid cell invasion through the mesothelial cells was monitored daily for up to 7 days. Within 24 hours, the OVCAR5 spheroids adhered and disseminated on the mesothelial monolayers, and rapidly established foci of invasion, resulting in a 200-fold change in area within one week. Invasion of live and irradiated monolayers occurred at the same rate and to the same degree. NIH:OVCAR5 spheroid invasion of fixed monolayers was similar to live and irradiated, but large pile-ups of cells were noticeable at the edges of the invasive fronts.
- Inhibitors of invasion were added to the NIH:OVCAR5 spheroid suspensions in the cell-based invasion assay described above. Ovarian carcinoma spheroid cell invasion through live, irradiated, and fixed mesothelial cell monolayers was inhibited by the addition of a blocking mAb against the β1 integrin subunit. This suggests that β1 integrins may participate in ovarian carcinoma invasion *in vivo*.
- Invasion was also significantly blocked by GM6001, a broad-spectrum inhibitor of matrix metalloproteinases (MMPs). ε-amino-N-caproic-acid, a serine protease inhibitor, slightly reduced the ability of NIH:OVCAR5 spheroid cells to invade mesothelial monolayers. These data suggest that protease activity significantly contributes to the ability of NIH:OVCAR5 spheroid cells to invade.

Task #3: Evaluate the role of CD44 and the β1 integrin subunit in ovarian carcinoma cell adhesion and invasion using populations of ascites cells isolated from patients with ovarian carcinoma that express either high levels or nondetectable levels of CD44 and/or and the β1 integrin subunit.

This aim is essentially complete. We have presented this data at seven different conferences (see Reportable Outcomes, below). We have recently submitted these experiments as a manuscript for publication in *Gynecological Oncology* [5; Appendix 4].

Task #3b: Determine whether differences in adhesion and/or invasion to ECM components and/or mesothelial cells are observed depending upon the expression of CD44 and/or β1 integrins on ascites cells.

- We have determined that spheroids recovered from eleven stage III ovarian carcinoma patients adhere to laminin, fibronectin, type I collagen, and type IV collagen, partially through β1 integrin interactions. Patient ascites spheroids also adhered to live mesothelial cell monolayers via β1 integrins.
- We determined the ability of ovarian carcinoma spheroids to adhere to glycosaminoglycans commonly found in cell ECMs: hyaluronan, hyaluronan fragments, and chondroitin sulfate. Patient ascites spheroids demonstrated variable adhesive abilities: a highly adherent group (30-60% adhesion); a moderately adherent group (10-20% adhesion); and a non-adherent group (0-5% adhesion). Soluble hyaluronan was able to competitively inhibit NIH:OVCAR5 spheroid adhesion to slides coated with hyaluronan. However, a blocking antibody against CD44 failed to inhibit adhesion, suggesting that spheroid cell adhesion to hyaluronan may occur via another receptor.
- We previously reported that blocking mAbs against integrin subunits inhibited NIH:OVCAR5 spheroid adhesion to ECM proteins [3]. Taking the four most adhesive patient spheroid samples, we were able to significantly inhibit their adhesion to all ECM proteins by adding a β1 integrin-subunit blocking antibody. This implies ovarian carcinoma spheroid adhesion to ECM proteins is mostly mediated by β1 integrins.
- We have demonstrated that spheroids obtained from ovarian carcinoma patient ascites samples adhered to live mesothelial cell monolayers grown on glass chamber slides. In serum-free conditions, maximum adhesion of patient spheroids to ECM proteins was observed at 2 hours. Taken together, these results imply that the spheroids found in patients' ascites fluid can demonstrate an adhesive capability, though not as great as those of single cells.
- Using the four patient ascites spheroid samples most adhesive to mesothelial cells, we inhibited their adhesion to mesothelial monolayers by adding a β1 integrin-subunit blocking antibody. Blocking β1 integrin reduced ascites spheroid adhesion to live mesothelial monolayers by about 50%. CD44 blocking antibodies had no effect on adhesion. These data indicate that β1 integrins play a partial role in mediating spheroid adhesion to the mesothelium, but other cell adhesion molecules are also likely involved.

Task #4: Determine whether ovarian carcinoma cells that are isolated from tumor nodules present in the peritoneal cavity have different levels of expression of CD44 and β1 integrin, growth properties, or levels of apoptosis compared to ovarian carcinoma cells isolated as "floaters" from the ascites fluid of patients.
This aim has almost been completed.

Task #4c. Quantitate the growth of ovarian carcinoma cells on mesothelial cells.

- We developed a cell-based assay to study ovarian carcinoma spheroid cell invasion described in Task #1c. We have observed that ovarian carcinoma spheroid cells usually invade mesothelial cell monolayers, unless they are also incubated with protease inhibitors. In those cases, on fixed mesothelial monolayers, the OVCAR5 spheroid cells will attach to and spread on top of the monolayers, but will not invade. Otherwise, if proteases are not inhibited, the ovarian carcinoma spheroid cells will grow to confluence while invading and displacing the mesothelial cell monolayers. The growth is quantitated by measuring the surface area occupied by cells. We are still in the process of finalizing these studies.

Status of Project Schedule:

Task #1 (months 1-18): This task has been completed. Successful results have prompted us to expand the studies initially proposed for this task.
Task #2 (months 1-48): This task has proven to be unfeasible and will not be completed.
Task #3 (months 6-48): Tasks 3a and 3b have been completed. Task 3c will not be completed due to lack of CD44-negative ovarian carcinoma cells from patients' ascites.
Task #4 (months 24-48): Tasks 4a, 4b, 4c, and 4f have been completed, although the constant influx of additional primary patient samples will result in periodic updating of our results. Tasks 4d and 4e remain to be completed.

(6) KEY RESEARCH ACCOMPLISHMENTS:

- We confirmed our preliminary observations that NIH:OVCAR5 and patient ascites spheroids adhered to confluent monolayers of live mesothelial cells. Interestingly, the spheroids adhered to the mesothelial cell monolayers at a higher rate than to ECM components. Also, the patient samples adhered to live, but not fixed, mesothelial cell monolayers, indicating that either receptor conformation or signaling between the mesothelial and tumor cells is necessary for optimal adhesion.
- We confirmed our preliminary observations that patient ascites spheroids adhered to hyaluronan, hyaluronan fragments, and chondroitin sulfate. Soluble hyaluronan could prevent spheroid adhesion to hyaluronan coated on a glass slide, but a CD44 antibody did not block this adhesion. This implicates glycosaminoglycans as another source of attachment for ovarian carcinoma spheroids *in vivo*.
- When plated on type I collagen, NIH:OVCAR5 spheroids completely disaggregated. Outgrowth of cells from NIH:OVCAR5 spheroids was also induced by laminin, type IV collagen, and fibronectin, although to a much lesser extent. Blocking β1 integrins significantly inhibited this outgrowth; implicating that β1 integrin interaction with type I collagen can facilitate cell migration out of an NIH:OVCAR5 spheroid.
- We developed a cell-based assay to study ovarian carcinoma spheroid invasion and found that NIH:OVCAR5 spheroids could rapidly invade both live and fixed mesothelial monolayers. NIH:OVCAR5 spheroid invasion was inhibited by a blocking mAb against the β1integrin subunit. Preliminary studies indicate that inhibition of proteases such as MMPs and serine proteases may significantly inhibit NIH:OVCAR5 spheroid invasion into mesothelial monolayers. These results suggest that spheroid invasion occurs via a β1 integrin-mediated event that stimulates protease production.

(7) REPORTABLE OUTCOMES:

Manuscripts:

1. Casey, R.C., Oegema Jr., T.R., Skubitz, K.M., Pambuccian, S.E., Grindle, S.M., and **Skubitz, A.P.N.** (2003) Cell membrane glycosylation mediates the adhesion, migration, and invasion of ovarian carcinoma cells. Clinical and Experimental Metastasis 20:143-152.
2. Casey, R.C., Koch, K.A., Oegema, T.R., Jr., Skubitz, K.M., Pambuccian, S.E., Grindle, S.M., and **Skubitz, A.P.N.** (2003) Establishment of an *in vitro* assay to measure the invasion of ovarian carcinoma cells through mesothelial cell monolayers. Clinical and Experimental Metastasis 20:343-356.
3. Hibbs, K., Skubitz, K.M. Pambuccian, S., Casey, R.C., Burleson, K.M, Oegema, T., Jr., Thiele, J.J., Grindle, S.M., Bliss, R., and **Skubitz, A.P.N.** "Gene expression in ovarian carcinoma: Identification of β8 integrin, claudin-4, and S100A1 as potential biomarkers" (Submitted to the American Journal of Pathology).
4. Burleson, K.M., Casey, R.C., Skubitz, K.M., Pambuccian, S.E., Oegema, T.R., and **Skubitz A.P.N.** "Ovarian carcinoma ascites spheroids adhere to extracellular matrix components and mesothelial cell monolayers" (Submitted to Gynecologic Oncology).

Abstracts and Presentations:

1. Burleson KM, Casey RC, Grindle S, Pambuccian SE, Skubitz KM, Oegema TR, **Skubitz, APN**. Ovarian carcinoma ascites spheroids are capable of adhesion to extracellular matrix proteins and mesothelial monolayers. Presented at the AACR special conference in Cancer Research, "Proteases, Extracellular Matrix, and Cancer" at Hilton Head Island, SC on October 9-13, 2002.
2. Burleson, K.M., Casey, R.C., Grindle, S.M., Pambuccian, S.E., Skubitz, K.M. Oegema, T.R., and **Skubitz, A.P.N.** "Adhesion of Patient Ascites Spheroids in Ovarian Carcinoma." The Molecular, Cellular, Developmental Biology and Genetics Fall 2002 Poster Session and Retreat. The results from this study were presented as a poster presentation in Minneapolis, MN on November 12, 2002.
3. Burleson KM. "Multicellular Spheroid Adhesion in Ovarian Carcinoma." Molecular, Cellular, Developmental Biology & Genetics Interactive Television seminar. The results from these studies were presented as a televised seminar in Minneapolis and St. Paul, MN on November 14, 2002.
4. Burleson, K.M., Casey, R.C., Grindle, S.M., Pambuccian, S.E., Skubitz, K.M. Oegema, T.R., and **Skubitz, A.P.N.** "Ovarian Carcinoma Ascites Spheroids Adhere to Extracellular Matrix Proteins and Mesothelial Monolayers" 4th Annual University of Minnesota Cancer Center Spring Poster Session & Symposium. The results from these studies were presented as a poster session in Minneapolis, MN on May 15, 2003.
5. **Skubitz, A.P.N.** "Role of extracellular matrix proteins in ovarian carcinoma cell adhesion, migration, and invasion" Oral presentation at R&D Systems, Inc., Minneapolis, MN on June 17, 2003.
6. Burleson, K.M., Casey, R.C., Grindle, S.M., Pambuccian, S.E., Skubitz, K.M. Oegema, T.R., and **Skubitz, A.P.N.** "Multicellular spheroids from ovarian carcinoma ascites samples adhere to extracellular matrix molecules and mesothelial monolayers." The results from this study were published in the *Proceedings of the American Association for Cancer Research*; Vol. 44, pg 226, March 2003, and presented as a poster presentation at the 94th

Annual Meeting of the American Association for Cancer Research in Washington, D.C. on July 11-14, 2003.

7. Burleson KM. "Spheroids in ovarian cancer dissemination." Molecular, Cellular, Developmental Biology & Genetics Interactive Television seminar. The results from these studies were presented as a televised seminar in Minneapolis and St. Paul, MN on September 22, 2003.

Funding Applied for Based on Work Supported by this Award:

07/01/03 - Graduate School Grant-in-Aid of Research, Artistry, and Scholarship
01/15/05 "Metastatic potential of ovarian carcinoma spheroids"
P.I.: Amy P.N. Skubitz
5% effort
Direct costs: $29,039 (salary for graduate student)

05/15/03 - Minnesota Medical Foundation
05/14/04 "Ovarian carcinoma: The metastatic potential of patients' ascites cells"
P.I.: Amy P.N. Skubitz
1% effort
Direct costs: $15,000 (supplies)

05/15/03 - Minnesota Medical Foundation
05/14/04 "Role of multicellular spheroids in the spread of ovarian carcinoma"
P.I.: Amy P.N. Skubitz
1% effort
Direct costs: $4,815 (computer)

08/01/03 - Minnesota Ovarian Cancer Alliance
07/31/04 "Improving the treatment of ovarian cancer: Understanding the role of spheroids in the spread of ovarian carcinoma"
P.I.: Amy P.N. Skubitz
20% effort
Direct costs: $64,000 (personnel, equipment, supplies)

Pending research grant support:

11/01/03 - U.S. Army Medical Research and Material Command
10/31/06 "Discovery of novel biomarkers to be used in the early detection of ovarian carcinoma"
P.I.: Amy P.N. Skubitz
35% effort
Direct costs requested: $375,000
Date of submission: 04/23/03
Date of notification: 10/03

04/01/04 - National Institutes of Health

03/31/09 "Biomarkers with biological function in ovarian carcinoma"
P.I.: Amy P.N. Skubitz
40% effort
Direct costs requested: $1,050,000
Date of submission: 06/01/03
Date of notification: 01/03

12/01/03 – Marsha Rivkin Center for Ovarian Cancer Research
12/01/04 "Screening for ovarian cancer: Detection of novel cell adhesion proteins in patients' sera"
P.I.: Amy P.N. Skubitz
5% effort
Direct costs requested: $41,608
Date of submission: 08/31/03
Date of notification: 11/03

Employment or Research Opportunities Applied for and/or Received Based on Experience/Training Supported by this Award:

Kate Hibbs was a graduate student in my laboratory who conducted her thesis research as part of this project. She was graduated from the University of Minnesota with a M.S. degree from the Clinical Laboratory Sciences Program. She is currently a M.S. student at the University of Minnesota working toward a degree in genetic counseling.

(8) CONCLUSIONS:

We have designed a cell-based invasion assay that can serve as an *in vitro* model to examine the invasion of ovarian carcinoma cells into monolayers of mesothelial cells. We have identified potential inhibitors of invasion with this new assay. We have also identified novel ovarian carcinoma proteins via gene expression array analysis and immunohistochemistry. These studies may lead to the development of reagents that can prevent the further spread of ovarian carcinoma *in vivo*.

(9) REFERENCES:

1. Lessan, K., Aguiar, D.J., Oegema, T., Siebenson, L., and Skubitz, A.P.N. (1999) CD44 and the β1 integrin mediate ovarian carcinoma cell adhesion to peritoneal mesothelial cells. American Journal of Pathology 154:1525-1537.
2. Casey, R.C. and Skubitz, A.P.N. (2000) CD44 and β1 integrins mediate ovarian carcinoma cell migration toward extracellular matrix proteins. Clinical & Experimental Metastasis 18:67-750.
3. Casey, R.C., Burleson, K.M., Skubitz, K.M., Pambuccian, S.E., Oegema, T.R., Ruff, L.E., and Skubitz, A.P.N. (2001) β1 integrins mediate the formation and adhesion of ovarian carcinoma spheroids. American Journal of Pathology 159:2071-2080.

4. Hibbs, K., Skubitz, K.M. Pambuccian, S., Casey, R.C., Burleson, K.M, Oegema, T., Jr., Thiele, J.J., Grindle, S.M., Bliss, R., and Skubitz, A.P.N. "Gene expression in ovarian carcinoma: Identification of β8 integrin, claudin-4, and S100A1 as potential biomarkers" (Submitted to the American Journal of Pathology).
5. Burleson, K.M., Casey, R.C., Skubitz, K.M., Pambuccian, S.E., Oegema, T.R., and Skubitz A.P.N. "Ovarian carcinoma ascites spheroids adhere to extracellular matrix components and mesothelial cell monolayers" (Submitted to Gynecologic Oncology).

(10) APPENDICES:

1. Casey, R.C., Oegema Jr., T.R., Skubitz, K.M., Pambuccian, S.E., Grindle, S.M., and **Skubitz, A.P.N.** (2003) Cell membrane glycosylation mediates the adhesion, migration, and invasion of ovarian carcinoma cells. Clinical and Experimental Metastasis 20:143-152.
2. Casey, R.C., Koch, K.A., Oegema, T.R., Jr., Skubitz, K.M., Pambuccian, S.E., Grindle, S.M., and **Skubitz, A.P.N.** (2003) Establishment of an *in vitro* assay to measure the invasion of ovarian carcinoma cells through mesothelial cell monolayers. Clinical and Experimental Metastasis 20:343-356.
3. Hibbs, K., Skubitz, K.M. Pambuccian, S., Casey, R.C., Burleson, K.M, Oegema, T., Jr., Thiele, J.J., Grindle, S.M., Bliss, R., and **Skubitz, A.P.N.** "Gene expression in ovarian carcinoma: Identification of β8 integrin, claudin-4, and S100A1 as potential biomarkers" (Submitted to the American Journal of Pathology).
4. Burleson, K.M., Casey, R.C., Skubitz, K.M., Pambuccian, S.E., Oegema, T.R., and **Skubitz A.P.N.** "Ovarian carcinoma ascites spheroids adhere to extracellular matrix components and mesothelial cell monolayers" (Submitted to Gynecologic Oncology).

Appendix 1

Clinical & Experimental Metastasis **20**: 143–152, 2003.

Cell membrane glycosylation mediates the adhesion, migration, and invasion of ovarian carcinoma cells

Rachael C. Casey[1], Theodore R. Oegema Jr.[2], Keith M. Skubitz[3], Stefan E. Pambuccian[1], Suzanne M. Grindle[4] & Amy P.N. Skubitz[1]

Departments of [1]Laboratory Medicine and Pathology, [2]Orthopaedic Surgery, and [3]Medicine, and the [4]Tissue Procurement Facility, University of Minnesota, Minneapolis, Minnesota, USA

Received 27 June 2002; accepted in revised form 14 October 2002

Key words: cell adhesion, cell invasion, cell migration, cell membrane glycosylation, gene expression, ovarian carcinoma, proteoglycans

Abstract

We have previously shown that ovarian carcinoma cell adhesion to mesothelial cell monolayers and migration toward fibronectin, type IV collagen, and laminin is partially mediated by CD44, a proteoglycan known to affect the functional abilities of tumor cells. The purpose of this study was to determine the role of cell membrane glycosylation in the metastatic abilities of ovarian carcinoma cells. NIH:OVCAR5 cells were treated with glycosidases to remove carbohydrate moieties from molecules on the cells' surface. The ability of the treated cells to adhere to extracellular matrix components or mesothelial cell monolayers, migrate toward extracellular matrix proteins, and invade through Matrigel was assessed. We observed that the loss of different carbohydrate moieties resulted in altered ovarian carcinoma cell adhesion, migration, and/or invasion toward extracellular matrix components or mesothelial cell monolayers. Gene array analysis of NIH:OVCAR5 cells revealed the expression of several proteoglycans, including syndecan 4, decorin, and perlecan. In tissue samples obtained from patients, altered proteoglycan gene expression was observed in primary ovarian carcinoma tumors and secondary metastases, compared to normal ovaries. Taken together, these results suggest that ovarian carcinoma cell proteoglycans affect the cells' ability to adhere, migrate, and invade toward extracellular matrix components and mesothelial cell monolayers. Thus, the carbohydrate modifications of several proteoglycans may mediate the formation and spread of secondary tumor growth in ovarian carcinoma.

Abbreviations: ECM – extracellular matrix; EHS – Engelbreth–Holm–Swarm; FBS – fetal bovine serum; PBS – phosphate buffered saline

Introduction

Proteoglycans are major components of the extracellular matrix (ECM) that mediate interactions with other ECM and cellular components. Proteoglycans have been shown to regulate cell adhesion [1], cell signaling [2], and apoptosis [3]. In cancer, altered glycosylation is a common feature of malignancy, and some of these alterations contribute to metastatic processes, including cell adhesion, migration, and invasion.

CD44, a proteoglycan found on ovarian carcinoma cells [4–6], binds the ECM glycosaminoglycan hyaluronan with high affinity [7] and also has a weak affinity for fibronectin, type IV collagen, and laminin [8]. Hyaluronan is a high molecular weight glycosaminoglycan that is present in the ECM of the mesothelial cells that line the peritoneum [9]. We have previously reported that ovarian carcinoma cell adhesion to mesothelial cell monolayers and migration toward the ECM proteins fibronectin, type IV collagen, and laminin is partially mediated by interactions between CD44 and hyaluronan [6, 7]. Interactions between CD44 and hyaluronan affect cell adhesion [6], migration [5, 7], and tumor growth [10] in ovarian carcinoma cells. In some ovarian carcinoma cell lines, CD44 is heavily glycosylated, and the removal of carbohydrate moieties from the cells' surfaces resulted in altered cell adhesion to hyaluronan [11].

Other proteoglycans have also been implicated in cancer cell functions. Syndecan-1, a heparan sulfate proteoglycan, has been shown to mediate the invasion of myeloma cells [12]. Ovarian carcinoma cell adhesion to fibronectin and type I collagen is mediated by heparan sulfate and chondroitin sulfate proteoglycans synthesized by the cells [13]. Versican, a chondroitin sulfate proteoglycan, contains a hyaluronan-binding domain [14], stimulates cell growth, and inhibits human melanoma cell adhesion to fibronectin and type I collagen [15], possibly facilitating tumor cell detachment and proliferation. Decorin, another chondroitin sulfate

Correspondence to: Dr Amy P.N. Skubitz, Department of Laboratory Medicine and Pathology, University of Minnesota, MMC 609, 420 Delaware St. S.E., Minneapolis, MN 55455, USA. Tel: +1-612-625-5920; Fax: +1-612-625-1121; E-mail: skubi002@umn.edu

proteoglycan that binds collagen fibrils, has been shown to inhibit the growth of ovarian cancer cells [16]. Clearly, proteoglycans and their carbohydrate residues mediate many tumor cell functions; however, their exact roles in cancer metastasis are poorly understood.

The purpose of this study was to examine the roles of cell membrane glycosylation upon the adhesive, migratory, and invasive abilities of ovarian carcinoma cells. Our results suggest that proteoglycans, particularly those with chondroitin sulfate or sialic acid moieties, may affect the ability of ovarian carcinoma cells to interact with mesothelial cells and proteins found in their ECMs, and thus may affect the ability of ovarian carcinoma tumor cells to metastasize.

Materials and methods

Unless otherwise stated, all standard reagents and materials were obtained from Sigma Chemical Company (St. Louis, Missouri). Unless otherwise specified, all experiments were performed a minimum of three times.

Cell culture

The human ovarian carcinoma cell line NIH:OVCAR5, which mimics the progression of ovarian carcinoma when injected into *in vivo* mouse models [17], was maintained in RPMI 1640 medium, 10% fetal bovine serum (FBS), 2 mM glutamine, 0.2 U/ml insulin, and 50 U/ml penicillin G/streptomycin. The ovarian carcinoma cell line NIH:OVCAR5 was originally established by Dr Thomas Hamilton (Fox Chase Cancer Center) [18] and obtained from Dr Judah Folkman, Harvard Medical School. The human peritoneal mesothelial cell line LP9 (Coriell Cell Repositories, Camden, New Jersey) was maintained in a medium containing a 1:1 ratio of M199 and MCDB 10 media, 15% FBS, 2 mM glutamine, 5 ng/ml epidermal growth factor, 0.4 μg/ml hydrocortisone, and 50 U/ml penicillin G/streptomycin. Both cell lines were maintained in 75-mm^2 tissue culture flasks in a humidified incubator with 5% CO_2 at 37 °C.

Human tissue samples

Tissue samples from 50 normal ovaries, 20 primary ovarian carcinomas, 17 secondary omental metastases, and 7 normal omenta were obtained from the Tissue Procurement Facility of the University of Minnesota Cancer Center. Samples were obtained using protocols approved by the University of Minnesota Institutional Review Board. All samples were identified, dissected, and snap frozen in liquid nitrogen within 30 min of removal from the patient. Tissue sections of each sample were prepared before freezing, and were examined by a pathologist by light microscopy after H&E staining to confirm the pathologic nature of the sample. None of the samples were necrotic.

ECM molecules

Type IV collagen, isolated from mouse Engelbreth–Holm–Swarm (EHS) tumors, was purchased from Trevigen, Gaithersburg, Maryland. Mouse EHS laminin, prepared as previously described [19], was provided by Dr Leo Furcht, University of Minnesota. Human plasma fibronectin, purified as described [20], was provided by Dr James McCarthy, University of Minnesota. Human umbilical cord hyaluronan, chondroitin sulfate A, and ovalbumin were purchased from Sigma. Matrigel was purchased from Becton Dickinson, Bedford, Massachusetts.

Glycosidase treatment

Chondroitinase ABC from *P. vulgaris*, hyaluronidase from bovine testes, and neuraminidase from *C. perfringens* were purchased from Sigma Chemical Company. NIH:OVCAR5 cells were grown in monolayer cultures, released with 0.5% trypsin, 2 mM ethylenediaminetetraacetic acid as previously described [21], and resuspended in base medium at a concentration of 10^6 cells/ml. The cells were incubated in the presence of chondroitinase ABC (0.5 U/ml), hyaluronidase (200 U/ml), or neuraminidase (10 mU/ml) in base medium for 30 min at 37 °C prior to their use in further assays. Chondroitinase ABC was used to remove chondroitin sulfate resides and neuraminidase was used to remove terminal sialic acid residues. Bovine testicular hyaluronidase primarily cleaves hyaluronan, but also may cleave chondroitin sulfate residues. Heat-inactivated enzymes had no effect on cell adhesion, migration, or invasion (results not shown).

Cell–ECM adhesion assay

The ability of the glycosidase-treated ovarian carcinoma cells to adhere to ECM components was quantified as previously described [5]. Clear-bottom 96-well plates were coated with 5 μg/ml fibronectin, type IV collagen, or laminin, or with 1 mg/ml ovalbumin, chondroitin sulfate A, or hyaluronan in phosphate buffered saline (PBS) for 16 h at 37 °C. Nonspecific binding sites were blocked with 2% ovalbumin in PBS. NIH:OVCAR5 cells were radiolabeled with L-[^{35}S]methionine for 24 h, trypsinized, washed, and subjected to glycosidase treatment. The cells (10^5 cells/100 μl) were added to the coated 96-well plates and incubated for 30 min. Nonadherent cells were removed by washing and the radioactivity was counted. These experiments were performed three times each in eight replicates.

Cell–cell adhesion assay

The ability of glycosidase-treated ovarian carcinoma cells to adhere to monolayers of the human mesothelial LP9 cell line was determined as previously described [5]. The assays were performed as described above in the cell–ECM assay, except that the clear-bottom 96-well microtiter plates were coated with LP9 cells grown to confluence for 48 h in complete medium. Prior to the addition of ovarian carcinoma cells, the mesothelial cell monolayers were rinsed twice with

RPMI 1640 medium. These experiments were performed three times each in eight replicates.

Cell migration assay

Chemotaxis of glycosidase-treated ovarian carcinoma cells in response to ECM molecules was quantitated in modified Boyden chambers, using 8 μm pore size polycarbonate polyvinylpyrrolidine-free filters (Fisher Scientific, Itasca, Illinois) as previously described [6]. Base medium containing fibronectin (5 μg/ml), type IV collagen (2.5 μg/ml), or laminin (5 μg/ml) was added to the lower compartments. Glycosidase-treated NIH:OVCAR5 cells (10,000 cells/50 μl) were added to the upper chamber compartments. After a 5-h incubation at 37 °C, the filters were stained with Diff-Quik (Dade Behring, Newark, Delaware) and nonmigratory cells were removed from the tops of the filters. The number of migrating cells is expressed as the sum of cells counted in five fields at a 40× magnification.

Cell invasion assay

The ability of glycosidase-treated ovarian carcinoma cells to invade through Matrigel was assessed. Glycosidase-treated cells were washed, resuspended at 10^5 cells/100 μl in base medium containing 1% FBS, and applied atop Transwells® (Corning Inc., Bloomington, Minnesota) coated with 1 mg/ml Matrigel. The bottom chambers were filled with 10 μg/ml fibronectin, type IV collagen, or laminin in base medium. After a 20-h incubation at 37 °C, the filters were stained with Diff-Quik and noninvasive cells were removed from the tops of the filters. The number of invading cells is expressed as the sum of cells counted in five fields at a 40× magnification.

Gene expression analysis of NIH:OVCAR5 cells

The gene expression of NIH:OVCAR5 cells was determined using protocols described in the Affymetrix GeneChip® Expression Analysis Manual. Briefly, total RNA was isolated from NIH:OVCAR5 cells using the RNeasy Total RNA Isolation kit (Qiagen Inc., Valencia, California). Double-stranded cDNA was synthesized from 8 μg of total RNA using the Superscript Choice system (Gibco BRL, Gaithersburg, Maryland). First-strand cDNA synthesis was primed with a T7-(dT_{24}) oligonucleotide primer (Genset Corp., La Jolla, California). The cDNA was then extracted with phenol/chloroform and precipitated with ethanol. From 10 μg of cDNA, cRNA was synthesized and biotinylated using the BioArray™ HighYield™ RNA Transcript Labeling kit (Affymetrix, Santa Clara, California). The resulting cRNA was purified according to the RNeasy Mini kit protocol (Qiagen) and then fragmented in 40 mM Tris-Acetate, pH 8.1, 30 mM magnesium acetate, and 100 mM potassium acetate for 35 min at 94 °C. The fragmented cRNA was applied to Affymetrix GeneChip® U_133 arrays representing more than 39,000 transcripts derived from approximately 33,000 well-substantiated human genes or EST sequences. The subsequent processing, scanning, and quality control of the fragmented cRNA were performed by the Biomedical Genomics Center, University of Minnesota, according to Affymetrix protocols. The data was analyzed using Microarray Suite, version 5.0 (Affymetrix), and GeneData Analyst, version 3.1 (GeneData AG, Basel, Switzerland). This experiment was performed in quadruplicate.

Gene expression analysis of human tissues

RNA was prepared from the human tissue samples described above (50 normal ovaries, 20 primary ovarian carcinomas, 17 secondary omental metastases, and 7 normal omenta) and gene expression was determined at Gene Logic Inc. (Gaithersburg, Maryland) using Affymetrix GeneChip® U_95 arrays containing approximately 12,000 known genes and 48,000 ESTs. Gene expression analysis utilized the Gene Logic GeneExpress® Software System.

Statistical analysis

Student's *t*-test was performed as a test of significance with the use of Microsoft Excel 1997 (Microsoft Co., Redmond, Washington). *P*-values of < 0.01 were considered to indicate statistically significant differences.

Results

Ovarian carcinoma cell adhesion to ECM components is altered by glycosidase treatment

The effect of cell membrane glycosylation upon the ability of ovarian carcinoma cells to adhere to ECM proteins was measured in an *in vitro* adhesion assay (Figure 1). Pretreatment with chondroitinase ABC inhibited cell adhesion to fibronectin, type IV collagen, and laminin. This suggests that proteoglycans that contain chondroitin sulfate residues may augment ovarian carcinoma cell adhesion to ECM proteins. Hyaluronidase pretreatment augmented cell adhesion to fibronectin and laminin, suggesting that the presence of cell-surface hyaluronan may inhibit cell adhesion to fibronectin and laminin, but not type IV collagen. Neuraminidase treatment had no effect on cell adhesion to ECM proteins, suggesting that sialic acid residues may not affect ovarian carcinoma cell adhesion to ECM proteins.

The ability of glycosidase-treated ovarian carcinoma cells to adhere to the glycosaminoglycans chondroitin sulfate A or hyaluronan was also determined (Figure 2). Chondroitinase ABC pretreatment augmented cell adhesion to hyaluronan, which suggests that chondroitin sulfate proteoglycans may partially inhibit ovarian carcinoma cell adhesion to hyaluronan, which has been shown to coat mesothelial cells [9]. The other glycosidases had no effect on ovarian carcinoma adhesion to chondroitin sulfate A or hyaluronan.

To ensure that glycosidase treatment did not induce cell death, aliquots of each enzymatically treated cell population were stained with trypan blue dye following both enzymatic treatment and the completion of the assays. In all cases, the cells excluded trypan blue stain, indicating that alterations in cell function were not attributable to the induction of cell death (data not shown).

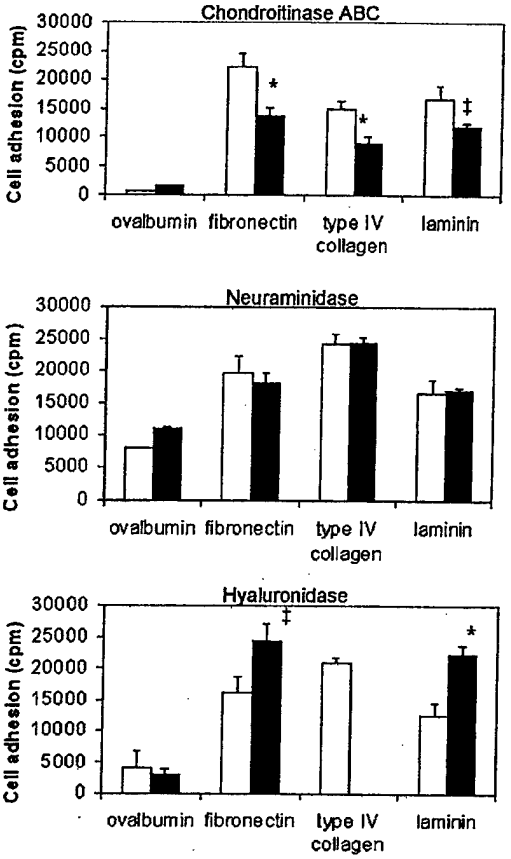

Figure 1. Ovarian carcinoma cell adhesion to ECM proteins is altered by glycosidase treatment. Untreated ovarian carcinoma cells (open bars) were incubated with glycosidases (solid bars) before their addition to the adhesion assays. Pretreatment with chondroitinase ABC inhibited cell adhesion to fibronectin, type IV collagen, and laminin, while hyaluronidase pretreatment augmented cell adhesion to fibronectin and laminin. Neuraminidase treatment had no effect on cell adhesion to ECM proteins. $*P < 0.001$ and $‡P < 0.01$.

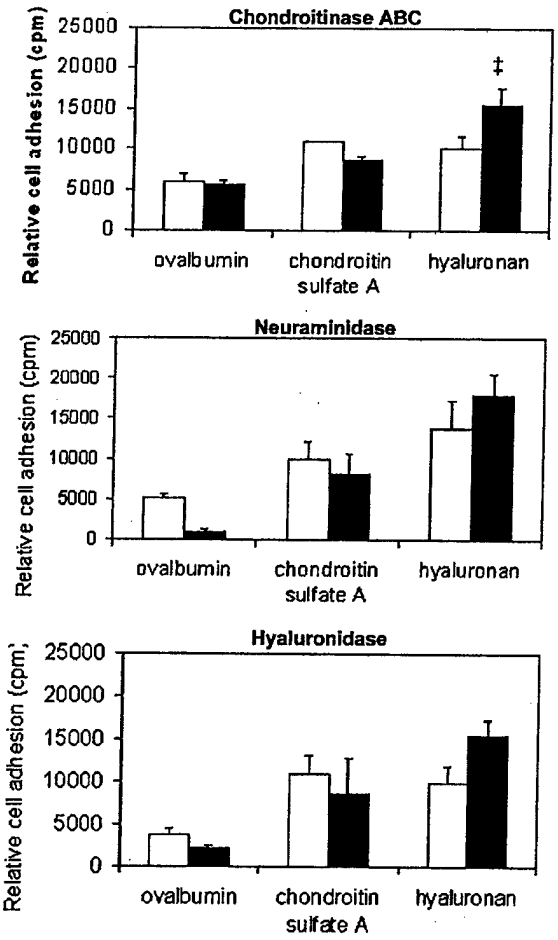

Figure 2. Ovarian carcinoma cell adhesion to hyaluronan is augmented by removal of chondroitin sulfate chains. Untreated ovarian carcinoma cells (open bars) were incubated with glycosidases (solid bars) before their addition to the adhesion assay. Chondroitinase ABC pretreatment augmented cell adhesion to hyaluronan. $‡P < 0.01$.

Ovarian carcinoma cell adhesion to mesothelial cells is partially mediated by chondroitin sulfate moieties

The role of cell membrane glycosylation on ovarian carcinoma cell adhesion to mesothelial cells was determined (Figure 3). The adhesion of ovarian carcinoma cells was inhibited by chondroitinase ABC pretreatment, but not by pretreatment with hyaluronidase or neuraminidase. This suggests that chondroitin sulfate proteoglycans may facilitate ovarian carcinoma cell adhesion to mesothelial cells.

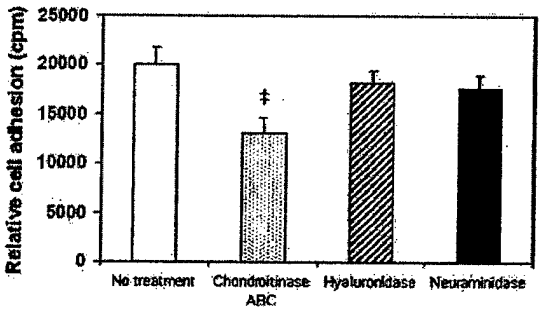

Figure 3. Ovarian carcinoma cell adhesion to mesothelial cells is inhibited by the removal of chondroitin sulfate chains. Ovarian carcinoma cells were untreated (open bar) or treated with chondroitinase ABC (dotted bar), hyaluronidase (striped bar), or neuraminidase (solid bar) before their addition to the adhesion assays. Adhesion of ovarian carcinoma cells was inhibited by chondroitinase ABC pretreatment, but not by pretreatment with hyaluronidase or neuraminidase. $‡P < 0.01$ compared to untreated controls.

Ovarian carcinoma cell migration toward ECM proteins is altered by glycosidase treatment

The role of cell membrane glycosylation on ovarian carcinoma cell migration toward fibronectin, type IV collagen, and laminin was determined (Figure 4). Ovarian carcinoma cell migration toward all three ECM proteins was increased by pretreatment with chondroitinase ABC. This suggests

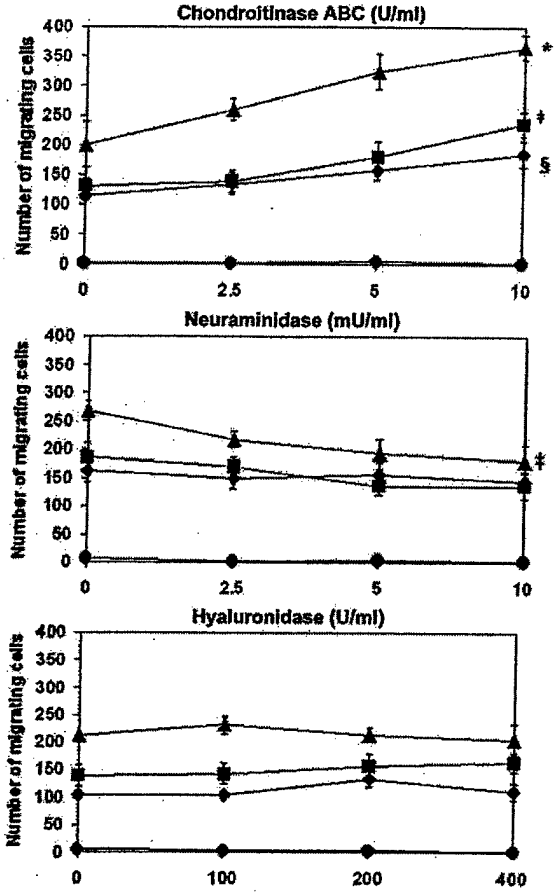

Figure 4. Ovarian carcinoma cell migration toward ECM proteins is altered by glycosidase treatment. Ovarian carcinoma cells were treated with chondroitinase ABC, neuraminidase, or hyaluronidase, then allowed to migrate toward ovalbumin (circles), fibronectin (triangles), type IV collagen (diamonds), or laminin (squares). Ovarian carcinoma cell migration toward fibronectin was increased by pretreatment with chondroitinase ABC and was inhibited by pretreatment with neuraminidase. Chondroitinase ABC pretreatment also resulted in increased cell migration toward type IV collagen and laminin. $*P < 0.001$, $\ddagger P < 0.01$, and $\S P < 0.05$.

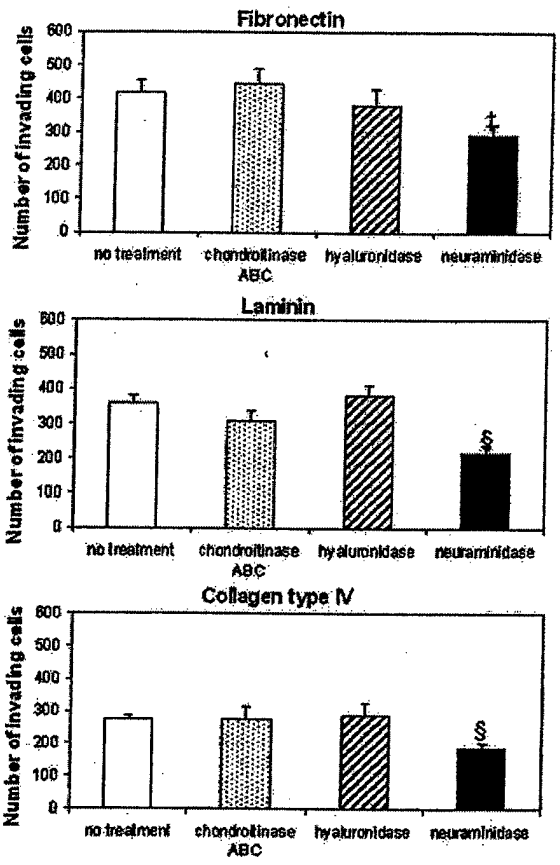

Figure 5. Ovarian carcinoma cell invasion through Matrigel is altered by glycosidase treatment. Ovarian carcinoma cells were untreated (open bars) or treated with chondroitinase ABC (dotted bars), hyaluronidase (striped bars), or neuraminidase (solid bars) before their addition to the invasion assays. Pretreatment with neuraminidase inhibited cell invasion through Matrigel toward fibronectin, laminin, and type IV collagen. Chondroitinase ABC and hyaluronidase treatment had no effect on cell invasion through Matrigel. $\ddagger P < 0.01$, and $\S P < 0.05$.

that the presence of chondroitin sulfate proteoglycans on the surface of ovarian carcinoma cells may impede cell migration toward ECM proteins, possibly by increasing their adhesion to ECM molecules (Figures 1 and 3). Neuraminidase pretreatment resulted in decreased cell migration toward fibronectin, but had no effect on cell migration toward type IV collagen and laminin. These results suggest that sialic acid-modified proteoglycans may specifically mediate cell migration toward fibronectin. Hyaluronidase pretreatment had no effect upon ovarian carcinoma cell migration toward ECM proteins.

Ovarian carcinoma cell invasion is altered by glycosidase treatment

Ovarian carcinoma cells were treated with glycosidases before their addition to the invasion assays. Pretreatment with neuraminidase inhibited cell invasion through Matrigel toward fibronectin, collagen type IV, and laminin (Figure 5). This suggests that sialic acid-modified glycoproteins may mediate ovarian carcinoma cell invasion. Chondroitinase ABC and hyaluronidase treatment had no effect on cell invasion through Matrigel.

Many proteoglycans are differentially expressed in ovarian carcinoma cells

The relative expression of proteoglycan gene transcripts in NIH:OVCAR5 cells are listed in Figure 6. Proteoglycan transcripts that were detected in high amounts in NIH:OVCAR5 cells included syndecan 4, decorin, perlecan, and bamacan. Also expressed, although in lower amounts, were transcripts of the proteoglycans CD44, glypican 1, syndecan 1, secretory granule proteoglycan (PG) 1, glypican 4, versican, and syndecan 2.

Table 1. Many proteoglycan genes are differentially expressed in ovarian carcinoma.

Gene expressed	Ovarian carcinoma tumor vs. normal ovary mean fold change	Secondary omental metastases vs. normal omenta mean fold change
Versican	4.9 ↑	2.7 ↑
Syndecan 1	2.6 ↑	4.4 ↑
Biglycan	2.3 ↑	4.4 ↑
Neuroglycan C	2.1 ↑	1.7 ↑
Glypican 4	NC	NC
CD44	NC	2.1 ↓
Perlecan	NC	1.9 ↓
Decorin	NC	NC
Glypican 3	4.2 ↓	6.4 ↓
Lumican	2.7 ↓	NC
Bamacan	NC	NC
Glypican 1	NC	NC
Secretory granule PG1	NC	2.2 ↓
Syndecan 2	*	*

The mean fold change ratio differences in proteoglycan gene expression were compared between 20 primary ovarian carcinoma tumors and 50 normal ovaries, and between 17 secondary omental metastases and 7 normal omenta. Unchanged tumor:normal mean fold changes are denoted as NC. *Because syndecan 2 gene expression was not detected in ovarian carcinoma tumors or omental metastases, the tumor:normal mean fold change could not be computed.

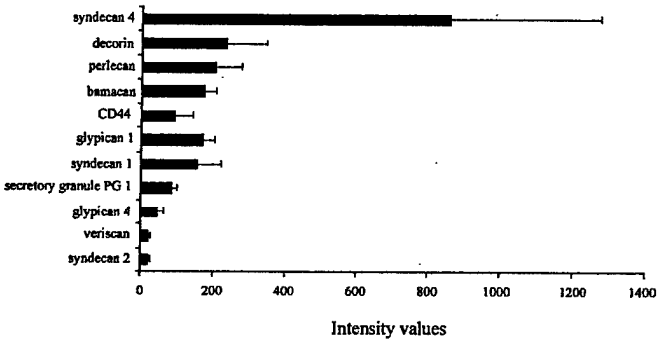

Figure 6. Gene expression of proteoglycans in ovarian carcinoma cells. Mean intensity values of proteoglycan transcripts that were present in NIH:OVCAR5 cells. For each transcript, the intensity values are expressed as the mean and standard deviation of quadruplicate samples, each performed in duplicate.

We also examined the gene expression of proteoglycan transcripts in relevant human samples: normal ovaries, primary ovarian carcinoma tumors, secondary ovarian carcinoma metastases found in the omentum, and normal omentum. Almost all of the proteoglycans detected in NIH:OVCAR5 cells were also expressed in both primary and secondary ovarian carcinoma tumor tissues (Table 1), except for syndecan 2 and syndecan 4. Syndecan 2, which was detected a very low levels in NIH:OVCAR5 cells, was expressed also at very low levels in normal ovaries and omenta; however, syndecan 2 was not detected in primary ovarian carcinoma or secondary omental metastatic tumor samples. Expression of the syndecan 4 transcript was detected at high levels by the Affymetrix U_133 gene chips used to screen NIH:OVCAR5 cells, but we were not able to quantitate the expression of syndecan 4 in the human tissues since this probes for this gene transcript were not present on the Affymetrix U_95 gene chips used to screen them.

The relative expression of some proteoglycan transcripts underwent significant alterations in primary ovarian tumors compared to normal ovarian tissue. Versican and neuroglycan C, which contain chondroitin sulfate modifications, and the heparan sulfate proteoglycan syndecan 1 and biglycan were significantly up-regulated in primary ovarian tumors, compared to normal ovaries (Table 1). The expression of glypican 3 decreased 4.2-fold and lumican expression decreased 2.7-fold. Although syndecan 2 transcript expression was absent from both primary ovarian carcinoma tumors and secondary omental metastases, it was detected in both normal ovaries and normal omenta, suggesting that the transformation of ovarian epithelial cells may result in termination of the expression of syndecan 2 gene products. The expression of all other proteoglycan transcripts listed in Table 1 were altered by 2-fold or less, as indicated by NC for 'no change'.

Alterations of the relative expression of proteoglycan transcripts in omental metastases and normal omenta were

Table 2. Effects of glycosidase treatment on ovarian carcinoma cell metastasis.

Function	Enzyme treatment	Fibronectin	Type IV collagen	Laminin	Hyaluronan	Mesothelial monolayer
Adhesion	Chondroitinase ABC	↓↓↓	↓↓↓	↓	↑	↓
Adhesion	Hyaluronidase	↑	–	↑↑↑	–	–
Adhesion	Neuraminidase	–	–	–	–	–
Migration	Chondroitinase ABC	↑↑↑	↑	↑↑		
Migration	Hyaluronidase	–	–	–		
Migration	Neuraminidase	↓↓	–	–		
Invasion	Chondroitinase ABC	–	–	–		
Invasion	Hyaluronidase	–	–	–		
Invasion	Neuraminidase	↓↓	↓↓↓	↓↓↓		

This table summarizes the changes observed in NIH:OVCAR5 cell adhesion, migration, and invasion toward fibronectin, type IV collagen, laminin, hyaluronan, and mesothelial cell monolayers after glycosidase treatment. Increased cellular function is denoted by upward arrows (↑) and decreased cellular function is denoted by downward arrows (↓). The arrows denote significant alterations in cellular function caused by pretreatment with the indicated glycosidases: one arrow ($P < 0.05$), two arrows ($P < 0.01$), three arrows ($P < 0.001$), and – (no effect).

also observed. Significant increases in the expression of syndecan 1, biglycan, versican, and neuroglycan C were observed in secondary omental tumors, compared to normal omentum tissues. In constrast, the expression of glypican 3 and secretory granule PG1 was significantly lower in the secondary omental metastases compared to the normal omenta (Table 1). As in normal ovaries and primary ovarian carcinoma tumors, the expression of syndecan 2 was low in normal omentum, but completely absent from secondary omental metastases. The alterations in gene expression of these proteoglycans may reflect the ECM rearrangement frequently observed in tumor cells. They may also indicate responses to tumor cells or may identify effectors of ovarian carcinoma metastatic behavior.

Discussion

In this study, we attempted to elucidate the role of cell membrane glycosylation in cellular functions that mediate ovarian carcinoma secondary tumor growth. The effects of glycosidase treatment upon the functional abilities of NIH:OVCAR5 cells to adhere to ECM components and mesothelial cell monolayers, migrate toward ECM proteins, and invade through Matrigel are summarized in Table 2. In short, glycosidase treatment alters ovarian carcinoma cell adhesion, migration, and invasion. This suggests that proteoglycans, or to be more precise carbohydrate modifications of proteoglycans, may contribute to the activation or suppression of these metastatic processes. Different carbohydrate moieties may mediate different cellular functions in ovarian carcinoma cells. Several proteoglycans and their glycosyl modifications may contribute to or inhibit the formation of secondary tumor growths in ovarian carcinoma.

Many studies specifically describe roles for the proteoglycan CD44, and its ligand hyaluronan, in ovarian carcinoma cell adhesion and migration. Cell-cell adhesion between ovarian carcinoma cells and mesothelial cells are mediated by CD44-hyaluronan interactions [5, 9]. The removal of cell membrane-associated carbohydrate residues resulted in altered cell adhesion to hyaluronan in some ovarian carcinoma cell lines [11]. CD44-hyaluronan interactions have been shown to mediate ovarian carcinoma cell migration via signal transduction through c-src kinase, Ras, and Rac 1 [22, 23]. Disruptions of the CD44-hyaluronan interactions altered the ability of ovarian carcinoma cells to migrate toward ECM proteins [6]. For these reasons, we considered the proteoglycan CD44 a likely candidate as a carbohydrate-mediated modifier of cell functions. However, in the NIH:OVCAR5 cell line, CD44 was not extensively modified with sialic acid or chondroitin sulfate groups, as determined by Western blot analysis (not shown). This suggests that other proteoglycans present in the NIH:OVCAR5 cells' ECM may be responsible for the altered cellular functions that we described here.

Proteoglycans are mediators of cell function in both normal and cancer cells. In normal cells, the chondroitin sulfate proteoglycan versican enhances cell proliferation, at least in part through binding to the EGF receptor [24]. Versican also inhibits cell adhesion in astrocytoma cells [25]. The chondroitin sulfate proteoglycan decorin can inhibit growth in ovarian carcinoma cells [16]. Syndecans, a family of heparan sulfate proteoglycans, mediate cell adhesion [26] and invasion [12] in myeloma cells. Syndecans also bind and modulate activity of fibroblast growth factor [27, 28] and promote oligomerization of bound ligands, which enhances activation of primary signaling receptors [29]. Overexpression of the chondroitin sulfate proteoglycan bamacan resulted in the transformation of normal mouse fibroblasts [30]. Ovarian carcinoma cells synthesize both chondroitin sulfate and heparan sulfate proteoglycans that mediate cell adhesion to fibronectin, type I collagen, and type III collagen [13]. Here we report that cell surface proteoglycans with chondroitin sulfate or sialic acid residues mediate the adhesion, migration, and invasion of ovarian carcinoma cells.

In particular, the loss of chondroitin sulfate residues resulted in decreased cell adhesion to the ECM proteins fibronectin, type IV collagen, and laminin and to mesothelial cell monolayers. Coupled with our observation that the re-

moval of chondroitin sulfate residues resulted in increased cell migration, our results suggest that chondroitin sulfate proteoglycans promote ovarian carcinoma cell adhesion toward mesothelial cells and their associated ECM proteins. This is consistent with reports that the chondroitin sulfate proteoglycan modulates the adhesive abilities of integrin $\alpha_4\beta_1$ [31] and matrix metalloproteinase-dependent invasion into type I collagen in melanoma cell lines [32]. Ovarian carcinoma cell adhesion to hyaluronan increased after the digestion of chondroitin sulfate residues. This suggests that some chondroitin sulfate proteoglycans may act as negative effectors of cell adhesion. We observed gene expression of versican, which contains chondroitin sulfate residues and a hyaluronan-binding domain [14], in the NIH:OVCAR5 cell line. Taken together, these results suggest that ovarian carcinoma cell adhesion may be inhibited by versican–hyaluronan interactions. We also report that versican expression is significantly up-regulated in primary and secondary ovarian carcinoma tumors, which suggests that ovarian carcinoma cell interactions with mesothelial cell hyaluronan may mediate secondary tumor growth. Further studies are required to determine the contributions of individual chondroitin sulfate proteoglycans that result in their net effect upon ovarian carcinoma cell adhesion and migration.

The removal of sialic acid residues from the surface of NIH:OVCAR5 cells resulted in decreased cell migration toward fibronectin and decreased invasion through Matrigel. Taken together, these results suggest that proteoglycans with sialic acid residues may promote a more invasive phenotype in ovarian carcinoma.

The removal of hyaluronan resulted in increased adhesion to ECM proteins and mesothelial cell monolayers, but did not affect cell migration or invasion. We have previously shown that the NIH:OVCAR5 cells have a hyaluronan-rich pericellular matrix that can be cleared by hyaluronidase treatment [5]. The clearance of hyaluronan from these tumor cells may unmask the integrins that are present on the cells' surfaces [6], thus facilitating the increased adhesion to ECM proteins and mesothelial cell monolayers that we observed. However, bovine testicular hyaluronidase can also cleave chondroitin sulfate residues. Our data suggests that the net increased cell adhesion that resulted from hyaluronan digestion was greater than the decreased cell adhesion that may have resulted from the concurrent removal of chondroitin sulfate residues, thus indicating that few chondroitin sulfate residues were cleaved during treatment with hyaluronidase.

To identify proteoglycans potentially responsible for the altered cellular functions that were reported here, gene expression analysis of the NIH:OVCAR5 cell line was performed. The expression of several proteoglycan transcripts, including syndecans, glypicans, decorin, perlecan, and bamacan was detected. We also screened patient samples for the expression of proteoglycan genes in primary ovarian carcinoma tumors and secondary omental metastases, a common site of metastasis in ovarian carcinoma. These values were compared to those of samples obtained from normal ovary and omental tissues. Except for syndecan 4, whose expression was not measured in the Affymetrix gene chips used to screen the human tissues, and syndecan 2, all of the proteoglycan transcripts detected in the NIH:OVCAR5 cell line were detected in primary ovarian carcinoma cell lines. These data suggest that this cell line expresses proteoglycan transcripts in a fashion similar to that of primary ovarian carcinoma tumors. Syndecan 2 gene expression was absent from primary and secondary ovarian carcinoma tumors, but was expressed at low levels in both normal ovaries and omenta.

In addition to their detection in NIH:OVCAR5 cells, versican and syndecan 1 gene expression values increased more than 2-fold in primary and secondary ovarian tumors compared to normal ovarian and omental tissues. These alterations in gene expression may indicate roles for these proteoglycans in ovarian carcinoma metastasis. In human ovarian tumors, we also observed significant decreases in the gene expression of glypican 3 and lumican, compared to normal ovaries. Glypican 3 expression was also significantly down-regulated in secondary omental metastases, suggesting that its loss may be a general feature of ovarian carcinoma. Interestingly, decreased lumican expression was noted only in primary ovarian carcinoma tumors, but not in secondary metastases. The loss of lumican expression in primary ovarian carcinoma tumors may reflect early-stage events in the development of the disease, rather than events associated with secondary tumor growth.

The gene expression of CD44 was unchanged in primary ovarian tumors, compared to normal ovaries, but glycosyl residues of CD44 have been implicated in tumor cell adhesion [11]. CD44 was immunoprecipitated from NIH:OVCAR5 cells incubated in base medium alone or glycosidase-digested cells and then subjected to Western blotting. In both cases, CD44 exhibited a relative mobility of approximately 90 kDa, which is consistent with the standard isoform of CD44 (not shown). The failure of all three glycosidase treatments to alter the relative mobility of CD44 suggests that the CD44 present on NIH:OVCAR5 cells was not extensively glycosylated with carbohydrate residues sensitive to these enzymes. This does not, however, preclude the possibility that CD44 on the surface of NIH:OVCAR5 cells may contain small amounts of sialic acid or chondroitin sulfate groups, below the detection limits of this assay.

We observed no significant change in the gene expression of other proteoglycans in ovarian carcinoma tumors compared to normal ovaries. These findings contradict another study that reported significantly decreased gene expression of decorin in ovarian carcinoma tumors, compared to the pooled brushings of ovary epithelial cells from patients without cancer [33]. However, alterations of gene expression observed in several proteoglycan transcripts suggest that the modulation of ovarian carcinoma metastasis is a complex phenomenon mediated by several proteoglycans. Here, we identify several proteoglycans that may be involved in secondary tumor growth. They may reflect alterations in tumor cell ECM or may mediate the formation of secondary tumor growths in ovarian carcinoma. Further study is required to determine whether alterations of the proteins encoded by

these transcripts are also altered in ovarian carcinoma tumors and cell lines.

Many of the cellular functions attributed to proteoglycans are due to post-translational modifications. Both syndecans and glypicans bind fibroblast growth factor via their heparan sulfate moieties [34, 35]. The ability of glypicans to target apical surfaces is partially dependent upon the extent of their glycosylation [36]. In healing wounds and several carcinomas, antigenic epitopes of decorin were masked by the addition of chondroitin sulfate chains [37]. Further studies are required to elucidate the roles of carbohydrate moieties in the cellular functions of proteoglycans.

In this study, we report that cell membrane glycosylation mediates cellular functions associated with ovarian carcinoma secondary tumor growth. Glycosidase treatment altered the functional abilities of NIH:OVCAR5 cells to adhere to ECM components and mesothelial cell monolayers, migrate toward ECM proteins, and invade through Matrigel. This suggests that the carbohydrate residues of several proteoglycans contribute to the activation or suppression of cell adhesion, migration, and invasion in ovarian carcinoma cells. Further study is required to identify the roles of individual proteoglycans that may participate in the formation of secondary tumor growths in ovarian carcinoma.

Acknowledgements

Supported by grants from the National Institute of Health/National Cancer Institute (CA0913825), Department of the Army (DA/DAMD17-99-1-9564), Minnesota Medical Foundation (SMF-2078-99), Graduate School Grant-in-Aid of Research (#18118), and the Biomedical Genomics Center, University of Minnesota. The content of the information presented in this article does not necessarily reflect the position of the United States Government.

We thank the staff of Gene Logic Inc., Gaithersburg, Maryland, for performing the gene expression experiments with the human tissue samples, the staff of the Biomedical Genomics Center, University of Minnesota, for performing gene expression experiments on NIH:OVCAR5 cells, and Diane Rauch and Sarah Bowell of the University of Minnesota Tissue Procurement Facility for assistance in collecting and processing the human tissue samples. We thank Dr James McCarthy for providing fibronectin, Dr Leo Furcht for providing laminin and the monoclonal antibody P5D2 against the $\beta 1$ integrin subunit, and Drs Thomas Hamilton and Judah Folkman for providing the NIH:OVCAR5 cell line.

References

1. Knox P, Wells P. Cell adhesion and proteoglycans I. The effect of exogenous proteoglycans on the attachment of chick embryo fibroblasts to tissue culture plastic and collagen. J Cell Sci 1979; 40: 77–88.
2. Baciu PC, Goetinck PF. Protein kinase C regulates the recruitment of syndecan-4 into focal contacts. Mol Biol Cell 1995; 6: 1503–13.
3. Dhodapkar MV, Abe E, Theus A et al. Syndecan-1 is a multifunctional regulator of myeloma pathobiology: Control of tumor cell survival, growth, and bone cell differentiation. Blood 1998; 91: 2679–88.
4. Cannistra SA, Abu-Jawdeh G, Niloff J et al. CD44 variant expression is a common feature of epithelial ovarian cancer: Lack of association with standard prognostic factors. J Clin Oncol 1995; 13: 1912–21.
5. Lessan K, Aguiar DJ, Oegema T et al. CD44 and $\beta 1$ integrin mediate ovarian carcinoma cell adhesion to peritoneal mesothelial cells. Am J Pathol 1999; 154: 1525–37.
6. Casey RC, Skubitz APN. CD44 and $\beta 1$ integrins mediate ovarian carcinoma cell migration toward extracellular matrix proteins. Clin Exp Metastasis 2000; 18: 67–75.
7. Aruffo A, Stamenkovic I, Melnick M et al. CD44 is the principal cell surface receptor for hyaluronate. Cell 1990; 61: 1303–13.
8. Jalkanen S, Jalkanen M. Lymphocyte CD44 binds the COOH-terminal heparin-binding domain of fibronectin. J Cell Biol 1992; 116: 817–25.
9. Gardner MJ, Catterall, JB, Jones LM et al. Human ovarian tumour cells can bind hyaluronic acid via membrane CD44: A possible step in peritoneal metastasis. Clin Exp Metastasis 1996; 14: 325–34.
10. Strobel T, Swanson L, Cannistra SA. *In vivo* inhibition of CD44 limits intra-abdominal spread of a human ovarian cancer xenograft in nude mice: A novel role for CD44 in the process of peritoneal implantation. Cancer Res 1997; 57: 1228–32.
11. Catterall JB, Jones LMH, Turner GA. Membrane glycosylation and CD44 content in the adhesion of human ovarian cancer cells to hyaluronan. Clin Exp Metastasis 1999; 17: 583–91.
12. Liebersbach BF, Sanderson RD. Expression of syndecan-1 inhibits cell invasion into type I collagen. J Biol Chem 1994; 269: 20013–19.
13. Kokenyesi R. Ovarian carcinoma cells synthesize both chondroitin sulfate and heparan sulfate cell surface proteoglycans that mediate cell adhesion to interstitial matrix. J Cell Biochem 2001; 83: 259–70.
14. LeBaron RG, Zimmermann DR, Ruoslahti E. Hyaluronate binding properties of versican. J Biol Chem 1992; 267: 10003–10.
15. Touab M, Villena J, Barranco C et al. Versican is differentially expressed in human melanoma and may play a role in tumor development. Am J Pathol 2002; 160: 549–57.
16. Nash MA, Loercher AE, Freedman RS. *In vitro* growth inhibition of ovarian cancer cells by decorin: Synergism of action between decorin and carboplatin. Cancer Res 1999; 59: 6192–6.
17. Molpus KL, Koelliker D, Atkins L et al. Characterization of a xenograft model of human ovarian carcinoma which produces intraperitoneal carcinomatosis and metastases in mice. Int J Cancer 1996; 68: 588–95.
18. Hamilton TC, Young RC, Ozols RF. Experimental model systems of ovarian cancer: Applications to the design and evaluation of new treatment approaches. Semin Oncol 1984; 11: 285–98.
19. McCarthy JB, Skubitz APN, Palm SL et al. Metastasis inhibition of different tumor types by purified laminin fragments and a heparin-binding fragment of fibronectin. J Natl Cancer Inst 1988; 80: 108–16.
20. Smith DE, Mosher DF, Johnson RB et al. Immunological identification of two sulfhydryl-containing fragments of human plasma fibronectin. J Biol Chem 1982; 257: 5831–8.
21. Pattaramalai S, Skubitz KM, Skubitz APN. A novel recognition site on laminin for $\alpha 3\beta 1$ integrin. Exp Cell Res 1996; 222: 281–90.
22. Bourguignon LYW, Zhu H, Shao L et al. CD44 interactions with c-Src kinase promotes cortactin-mediated cytoskeleton function and hyaluronic acid-dependent ovarian tumor cell migration. J Biol Chem 2001; 276: 7327–36.
23. Bourguignon LYW, Zhu H, Zhou B et al. Hyaluronan promotes CD44v3-Vav2 interaction with Grb2-p185HER2 and induces Rac1 and Ras signaling during ovarian tumor cell migration and growth. J Biol Chem 2001; 276: 48679–92.
24. Yang BL, Zhang Y, Cao L et al. Cell adhesion and proliferation mediated through the G1 domain of versican. J Cell Biochem 1999; 72: 210–20.
25. Ang LC, Zhang Y, Cao L et al. Versican enhances locomotion of astrocytoma cells and reduces cell adhesion through its G1 domain. J Neuropathol Exp Neurol 1999; 58: 597–605.
26. Ridley RC, Xiao H, Hata H et al. Expression of syndecan regulates human myeloma plasma cell adhesion to type I collagen. Blood 1993; 8: 767–74.
27. Feyzi E, Saldeen T, Larsson E et al. Age-dependent modulation of heparan sulfate structure and function. J Biol Chem 1998; 273: 13395–8.
28. Asundi VK, Carey DJ. Self-association of N-syndecan (syndecan-3) core protein is mediated by a novel structural motif in the transmem-

brane domain and ectodomain flanking region. J Biol Chem. 1995; 270: 26404–10.
29. Johnson GR, Wong L. Heparan sulfate is essential to amphiregulin-induced mitogenic signaling by the epidermal growth factor receptor. J Biol Chem 1994; 269: 27149–54.
30. Ghiselli G, Iozzo RV. Overexpression of bamacan/SMC3 causes transformation. J Biol Chem 2000; 275: 20235–8.
31. Iida J, Pei D, Kang T et al. Melanoma chondroitin sulfate proteoglycan regulates matrix metalloproteinase-dependent human melanoma invasion into type I collagen. J Biol Chem 2001; 276: 18786–94.
32. Iida J, Meijne AML, Oegema TR et al. A role of chondroitin sulfate proteoglycosaminoglycan binding site in $\alpha 4\beta 1$ integrin-mediated melanoma cell adhesion. J Biol Chem 1998; 273: 5955–62.
33. Shridhar V, Sen A, Chien J et al. Identification of underexpressed genes in early- and late-stage primary ovarian tumors by suppression subtraction hybridization. Cancer Res 2002; 62: 262–70.
34. Zhou FY, Owens R, Hermonen J et al. Sensitivity of cells for FGF-1 and FGF-2 is regulated by cell surface heparan sulfate proteoglycans. Eur J Cell Biol 1997; 73: 166–74.
35. Aviezer D, Levy E, Safran M et al. Differential structural requirements of heparin and heparan sulfate proteoglycans that promote binding of basic fibroblast growth factor to its receptor. J Biol Chem 1994; 269: 114–21.
36. Mertens G, Van der Schueren B, Van den Berghe H et al. Heparan sulfate expression in polarized epithelial cells: The apical sorting of glypican (GPI – anchored proteoglycan) is inversely related to its heparan sulfate content. J Cell Biol 1996; 132: 487–97.
37. Yeo TK, Brown L, Dvorak HF. Alterations in proteoglycan synthesis common to healing wounds and tumors. Am J Pathol 1991; 138: 1437–50.

Clinical & Experimental Metastasis **20:** 343–356, 2003.

Establishment of an *in vitro* assay to measure the invasion of ovarian carcinoma cells through mesothelial cell monolayers

Rachael C. Casey[1], Kimberly A. Koch[1], Theodore R. Oegema Jr.[2], Keith M. Skubitz[3], Stefan E. Pambuccian[1], Suzanne M. Grindle[4] & Amy P.N. Skubitz[1]

Department of [1]Laboratory Medicine and Pathology, [2]Orthopaedic Surgery, and [3]Medicine, and the [4]Cancer Center Informatics Center, University of Minnesota, Minneapolis, Minnesota, USA

Received 25 September 2002; accepted in revised form 4 December 2002

Key words: cell invasion, integrins, mesothelial cells, ovarian carcinoma

Abstract

Ovarian carcinoma is the leading cause of gynecological cancer deaths in the United States. Secondary tumor growths form by tumor cell invasion through the mesothelial lining of the peritoneal cavity and peritoneal organs. To study this interaction, we developed a dye-based *in vitro* model system in which mesothelial cells were grown as confluent monolayers, permeabilized, and then co-cultured with ovarian carcinoma cells for up to seven days. The mesothelial cells were then stained with trypan blue dye, which enabled the visualization of ovarian carcinoma cell invasion through the monolayers of mesothelial cells. Ovarian carcinoma cell invasion was inhibited for up to 7 days by the addition of GRGDSP peptides, a blocking monoclonal antibody against the $\beta 1$ integrin subunit, or blocking monoclonal antibodies against matrix metalloproteinases 2 and 9. Cell invasion was also inhibited by hyaluronan and GM6001, a chemical inhibitor of matrix metalloproteinases. Differential gene expression of matrix metalloproteinases, tissue inhibitors of matrix metalloproteinases, and disintegrins were observed in primary ovarian carcinoma tumors and secondary metastases, compared to normal ovaries. Taken together, these results suggest that complex interactions between integrins, disintegrins, matrix metalloproteinases, and tissue inhibitors of matrix metalloproteinases may mediate ovarian carcinoma cell invasion, and that the dye-based assay described herein is a suitable model system for its study.

Abbreviations: ADAM – a disintegrin and metalloproteinase; ADAMTS – a disintegrin and metalloproteinase with thrombospondin type I repeat; CMFDA – 5-chloromethylfluorescein diacetate; DMSO – dimethylsulfoxide; ECM – extracellular matrix; EHS – Engelbreth-Holm-Swarm; FBS – fetal bovine serum; IgG – immunoglobulin; mAb – monoclonal antibody; MMP – matrix metalloproteinase; PBS – phosphate buffered saline; TIMP – tissue inhibitor of metalloproteinase

Introduction

Ovarian cancer is the leading cause of gynecologic malignancy and the fifth leading cause of cancer death among women in the United States [1]. In ovarian carcinoma, cancer cells detach from the surface of the tumor into the peritoneal cavity. Subsequent peritoneal implants are characterized by the invasion of the tumor cells through the mesothelial cells that line the peritoneum and underlying organs. However, the mechanisms that contribute to ovarian carcinoma invasion are not well understood.

One technique for studying cancer cell invasion is by performing Matrigel invasion assays [2]. Matrigel is comprised of extracellular matrix (ECM) extracted from mouse Engelbreth–Holm–Swarm (EHS) sarcoma cells, and is believed to mimic the basement membrane through which tumor cells invade [3]. Several factors make this procedure a less than ideal method to study ovarian carcinoma cell invasion. Matrigel is murine in origin, not human. It is made by tumor cells, which synthesize and organize their ECMs differently than normal cells. Most importantly, the Matrigel invasion assay measures only cell-ECM interactions, and can not be used to examine cell-cell interactions between the tumor cells and target cells. Finally, Matrigel is synthesized by sarcoma cells, which are not typical targets of ovarian carcinoma metastasis. The Matrigel invasion assay provides only an approximation of the *in vivo* conditions found at sites of metastasis.

A second technique for studying cancer cell invasion was described by Niedbala et al. [4]. They developed an *in vitro* model system for studying the adhesion and invasion of ovarian carcinoma cells when co-cultured on mesothelial cells. In their model, bovine corneal endothelial cells were grown to confluence in order provide an ECM upon which the mesothelial cells were then grown. ^{51}Cr-radiolabeled ovarian carcinoma cells were then added to the wells and allowed to adhere and invade for up to eight days. A disad-

Correspondence to: Dr Amy P.N. Skubitz, Department of Laboratory Medicine and Pathology, University of Minnesota, MMC 609, 420 Delaware St. S.E., Minneapolis, MN 55455, USA. Tel: +1-612-625-5920; Fax: +1-612-625-1121; E-mail: skubi002@umn.edu

vantage of this model system is that it requires the use of bovine corneal endothelial cells for the establishment of a substratum on which the human mesothelial cells are grown. A second disadvantage is that this model system requires the use of radioactive material, which many research laboratories are trying to avoid. Finally, it is difficult to distinguish ovarian carcinoma cells from mesothelial cells when attempting to quantitate areas of invasion by the ovarian carcinoma cells.

Ovarian carcinoma metastasis is mediated by interactions between ovarian cancer cells and ECM components of the mesothelial cells at sites of secondary tumor growth. It has previously been shown that ovarian carcinoma cell adhesion and migration are mediated by interactions between $\beta 1$ integrins and fibronectin, collagens, and laminin [5–7] and interactions between CD44 and hyaluronan [5, 7–9]. Pretreatment of lung adenocarcinoma cells with blocking monoclonal antibodies (mAb) against $\beta 1$ integrins inhibited the formation of lung metastases in murine models [10]. Up-regulation of $\beta 1$ integrin expression promoted matrix metalloproteinase-dependent cell invasion in ovarian carcinoma cells [11]. Perturbation of CD44-hyaluronan interactions decreased the invasive ability of human breast cancer cells [12], inhibited murine mammary carcinoma cell growth [13], and induced apoptosis in mammary carcinoma cells [14]. The addition of hyaluronan into Matrigel resulted in increased glioma cell invasion in Matrigel invasion assays [15]. Together, these studies suggest that $\beta 1$ integrin- and CD44-mediated cell–ECM interactions may contribute to ovarian carcinoma cell invasion.

Cancer cell invasion is mediated by a complex balance between degradative enzymes, including matrix metalloproteinases (MMPs), tissue inhibitors of matrix metalloproteinases (TIMPs), and ADAMs (a disintegrin and metalloproteinase). MMPs are proteolytic enzymes that play an important role in cancer cell invasion through the degradation of ECM proteins, such as fibronectin and collagens [16, 17]. Increased activity of MMPs has been linked to the invasive potential of tumor cells [18, 19]. In ovarian carcinoma, increased secretion and activity of MMP 2, MMP 9, and MT1-MMP have been reported [20, 21]. However, the expression of TIMP 1 was shown not to be altered in ovarian carcinoma [22, 23]. These studies suggest that elevation of MMP secretion, relative to the concentrations of MMP inhibitors, can facilitate ovarian cancer cell invasion. The ADAMs are a recently discovered family of cell adhesion receptors, most of which are composed of pro- , metalloproteinase, disintegrin-like, cysteine-rich, EGF-like repeat, transmembrane and cytoplasmic tail domains [24, 25]. Type I and type II procollagens can be degraded by an ADAMTS (a disintegrin and metalloproteinase with thrombospondin type I repeat) [26]. ADAM 12 was detected immunohistochemically in breast, colon, and lung carcinomas, and overexpression of disintegrin domains of ADAM 12 and ADAM 15 promoted cell adhesion in melanoma cells [27]. Interactions between MMPs, TIMPs, and ADAMs are believed to regulate cancer cell invasion, but their particular interactions are not fully understood.

In this report, we set out to establish a new model system that would mimic the *in vivo* situation whereby ovarian carcinoma cells adhere, spread, migrate, and invade the mesothelial cell monolayer that lines the peritoneal cavity. In our first attempt to develop a model system, we used two different colored fluorescent dyes to label the cells, so that we could differentiate the red ovarian carcinoma cells from the green mesothelial cells during the assay. However, the cells did not retain the dyes for the entire length of the seven-day invasion assay. Since that technique did not prove to be ideal, we then developed a second *in vitro* model system that can be used to monitor the ability of ovarian carcinoma cells to invade through mesothelial cell monolayers for seven days or more. Our model system is a modification of an invasion assay described by Yu et al. [14], in which the invasive capacity of TA3/St murine mammary carcinoma cells was examined on monolayers of G8 mouse fetal myoblasts. Our model system is an attempt to improve upon the invasion assays that are currently described in the literature for ovarian carcinoma. This model system mimics *in vivo* conditions and does not use radiolabeled material. By use of this model system, it has been possible to identify adhesion molecules and proteinases that are involved in the invasion of ovarian carcinoma cells through mesothelial cell monolayers. In addition, gene expression analysis was performed to determine whether the expression of genes associated with cell invasion (such as MMPs, TIMPs, and ADAMS) were differentially expressed in ovarian carcinoma compared to normal ovaries. Our results suggest that complex cell-cell and cell-ECM interactions between the tumor cells and their target cells mediate ovarian carcinoma cell invasion, and that this assay may be a suitable model system for further study.

Materials and methods

Unless otherwise stated, all standard reagents and materials were obtained from Sigma Chemical Company (St. Louis, Missouri), all pictures were photographed with a Nikon Coolpix 950 camera, and all experiments were performed in triplicate and repeated a minimum of three times.

Cell culture

The human ovarian carcinoma cell line NIH:OVCAR5, which mimics the progression of ovarian carcinoma when injected into *in vivo* mouse models [28], was maintained in RPMI 1640 medium, 10% fetal bovine serum (FBS), 2 mM glutamine, 0.2 U/ml insulin, and 50 U/ml penicillin G/streptomycin (Life Technologies, Grand Island, New York). The ovarian carcinoma cell line NIH:OVCAR5 was originally established by Dr Thomas Hamilton (Fox Chase Cancer Center) [29] and obtained from Dr Judah Folkman, Harvard Medical School. The human peritoneal mesothelial cell line LP9 (Coriell Cell Repositories, Camden, New Jersey) was maintained in a medium containing a 1:1 ratio of M199 and MCDB 10 media, 15% FBS, 2 mM glutamine, 5 ng/ml epidermal growth factor, 400 ng/ml hydrocortisone, and 50 U/ml penicillin G/streptomycin. Both cell lines were

maintained in 75-mm^2 tissue culture flasks in a humidified incubator with 5% CO_2 at 37 °C.

Fluorescent dye-based model for cell invasion

A model system for monitoring the ability of NIH:OVCAR5 ovarian carcinoma cells to invade through live mesothelial cell monolayers was developed. In order to distinguish between the ovarian carcinoma cells and the mesothelial cells, the cell lines were labeled with stains that fluoresced at different wavelengths. LP9 mesothelial cells were grown to confluence in 24-well tissue culture plates (Becton Dickinson, Franklin Lakes, New Jersey) and rinsed twice with phosphate buffered saline (PBS). The mesothelial cells were labeled with 10 μg/ml 5-chloromethylfluorescein diacetate (CMFDA) (Molecular Probes, Inc., Eugene, Oregon), a green fluorescent stain, in PBS for 30 min at 37 °C, and then rinsed twice with PBS. The NIH:OVCAR5 cells were released from tissue culture flasks with 0.5% trypsin, 2 mM EDTA as described previously [30], and resuspended in PBS at a concentration of 10^6 cells/ml. The NIH:OVCAR5 cells were labeled with 10 μg/ml carboxy SNARF-1 (Molecular Probes, Inc.), a red fluorescent stain, in PBS for 30 min, and then rinsed twice with PBS. The NIH:OVCAR5 cells were added to the live mesothelial cell monolayers at a concentration of 10,000 cells/ml/well. The co-cultures were maintained in a 1:1 ratio of complete media for each cell type. At 24 h intervals, the wells were gently washed twice with PBS, and the cells were visualized with a Nikon Eclipse TE200 fluorescent microscope.

Trypan blue dye-based model for cell invasion

A second model system for quantitating the ability of NIH:OVCAR5 ovarian carcinoma cells to invade through monolayers of mesothelial cells was developed using a modification of the protocol described by Yu et al. [14]. LP9 cells (10,000 cells/well) were added to 24-well tissue culture plates and grown to confluence for 48 h in complete medium. The mesothelial cell monolayers were rinsed twice with 1 ml PBS, permeabilized with 250 μl dimethyl sulfoxide (DMSO) for 1 h at room temperature, rinsed twice with 1 ml PBS, and rinsed twice with RPMI 1640 media. Permeabilization with DMSO did not disrupt the confluency of the monolayers of mesothelial cells. Single cell suspensions of NIH:OVCAR5 cells were resuspended in complete cell culture media and added to the DMSO-treated mesothelial cell monolayers. At 24 h intervals for 7 days, the media was removed and replaced with fresh media. Alternatively, the wells were gently washed twice with 1 ml PBS, then 500 μl of 0.2% trypan blue solution (Sigma) was applied to each well for 15 min, and gently rinsed with 1 ml PBS. Since the mesothelial cells had been permeabilized with DMSO, they retained the trypan blue dye, while the live ovarian carcinoma cells did not retain the trypan blue dye. Thus, it was relatively easy to distinguish the two cell types, and quantitate the level of invasion during the course of the seven-day assay by use of a light microscope. The extent of invasion of the ovarian carcinoma cells into the mesothelial cell monolayers was quantified by measuring the size of the areas of the confluent monolayers of mesothelial cells that were displaced by the proliferating ovarian carcinoma cells. No invasion is represented as (-), 50–200 μm of invasion is represented as (+), 220–400 μm of invasion is represented as (++), and areas of invasion greater than 400 μm are represented as (+ + +).

Inhibition of ovarian carcinoma cell invasion through mesothelial cell monolayers

In order to identify the adhesion molecules or proteinases that may be involved in the invasion of the ovarian carcinoma cells through the mesothelial cell monolayers, invasion assays were performed as described above, except that the cells were incubated in the presence of a variety of potential inhibitors. Briefly, mesothelial cells were grown to confluence, permeabilized with DMSO, rinsed, and then the ovarian carcinoma cells were added to the wells. Following a one-hour incubation period at 37 °C, during which time the ovarian carcinoma cells were allowed to settle atop the mesothelial cell monolayers and commence adhesion to the mesothelial cells, the potential inhibitors were added. The potential inhibitors were tested at a range of concentrations, and included the following: 1, 10, and 25 mM GM6001, a chemical inhibitor of MMP-1, -2, -3, - 8, and -9 [31] (Chemicon International, Temecula, California); 1, 10, and 100 μg/ml GRGDSP or GRGESP peptides (Life Technologies); 5, 20, and 50 nM TIMP-1 (Chemicon); 5, 20, and 50 nM TIMP-2 (Chemicon); 10, 100, and 1000 μg/ml of human umbilical cord hyaluronan (Sigma); 10, 100, and 1000 μg/ml of chondroitin sulfate A (Sigma); 10, 100, and 1000 μg/ml of heparin; and 0.1 and 1 μg/ml of normal mouse immunoglobulin (IgG). The following mAbs were used at concentrations of 0.1 and 1 ug/ml: P5D2, which blocks the adhesive activity of human β1 integrin subunits (provided by Dr Leo Furcht, University of Minnesota); mAb 21C8, which stimulates the adhesive activity of human β1 integrin subunits (Chemicon); mAb IM7, which a blocks the hyaluronan-binding site of CD44 (Pharmingen, San Diego, California); a mAb against MMP-2 (Chemicon), and a mAb against MMP-9 (Chemicon). In addition, purified mAbs that block the adhesive activity of human integrin subunits α1 (mAb FB12), α2 (mAb P1E6), α3 (mAb P1B5), α4 (mAb P1H4), α5 (mAb P1D6), and α6 (mAb GoH3) were purchased from Chemicon and used at concentrations of 0.1 and 1 ug/ml. Each of the putative inhibitors was replenished daily by removing 500 ul of media and replacing it with 500 ul of fresh inhibitors in media.

ECM molecules

Type IV collagen, isolated from mouse EHS tumor, was purchased from Trevigen, Gaithersburg, Maryland. Mouse EHS laminin, prepared as previously described [32], was provided by Dr Leo Furcht, University of Minnesota. Human plasma fibronectin, purified as described [33], was provided by Dr James McCarthy, University of Minnesota. Ovalbu-

min was purchased from Sigma. Matrigel was purchased from Becton Dickinson, Bedford, Massachusetts.

Cell proliferation assay

96-well tissue culture plates were coated with 50 μg/ml of fibronectin, laminin, type IV collagen, or ovalbumin or with 1 mg/ml hyaluronan in PBS (100 μl/well) at 4 °C for 16 h. Nonspecific binding sites were blocked with 200 ul/well of 2 mg/ml ovalbumin in PBS at 4 °C for 1 h, and then rinsed twice with PBS. Single cell suspensions of NIH:OVCAR5 cells in complete medium were added at a concentration of 500 cells/200 μl/well and cultured for up to 7 days. At various time points, 2 mg/ml WST-1 (Boehringer-Mannheim Corporation, Indianapolis, Indiana) was added to each well and incubated for 2 h. The resulting formazan product was quantitated by a SpectaMax 250 scanning multi-well spectrophotometer (Molecular Devices Corporation, Sunnyvale, California) by measuring absorbance at 450 nm. These experiments were performed in quadruplicate.

Toxicity assay in the presence of 'inhibitors'

In order to determine whether the putative inhibitors of cell invasion were toxic to the ovarian carcinoma cells, and thus, were inhibiting the invasion of the ovarian carcinoma cells by killing them, we performed the following toxicity assay. Briefly, single cell suspensions of NIH:OVCAR5 cells in complete medium were added at a concentration of 500 cells/200 μl/well and cultured for up to 7 days in the presence of the inhibitors listed above. At various time points, 2 mg/ml WST-1 (Boehringer-Mannheim Corporation, Indianapolis, Indiana) was added to each well and quantitated as described above.

Gene expression analysis of human tissues

Humans tissue samples from 50 normal ovaries, 20 primary ovarian carcinomas, 17 secondary omental metastases, and 7 normal omenta were obtained from the Tissue Procurement Facility of the University of Minnesota Cancer Center. Samples were obtained using protocols approved by the University of Minnesota Institutional Review Board. All samples were snap frozen in liquid nitrogen within 30 min after resection from the patient. As a quality control measure, a pathologist examined an H&E stained slide of each tissue sample to confirm the pathologic nature of the sample. Each of the ovarian carcinoma samples was comprised almost entirely of tumor cells and none of the samples were necrotic.

The expression of genes associated with invasion in primary ovarian carcinomas, secondary omental metastases, normal ovaries, and normal omenta was studied. RNA was prepared from the tissue samples according to Affymetrix protocols and gene expression was determined at Gene Logic Inc. (Gaithersburg, Maryland) using Affymetrix GeneChip® U_95 arrays (Santa Clara, California) containing approximately 12,000 known genes and 48,000 ESTs. We limited our analysis to genes involved in cell invasion by performing a query of the human U95 chip annotation on the Affymetrix web site (www.affymetrix.com/analysis). We searched the text database for the words 'MMP', 'TIMP', and 'ADAM' and found 100 gene fragments. We excluded eleven of the gene fragments since they were ESTs or the gene name was not known, and another group of seven gene fragments were excluded since the gene names were not MMP, TIMP, or ADAM. Thus, of the 60,000 gene fragments present on the U95 chips, this study was limited to 82 gene fragments or 48 different genes. The gene expression values for these 82 gene fragments were then analyzed by the Gene Logic GeneExpress® Software System in order to identify those genes that were over- or under-expressed 2-fold or more in ovarian carcinoma samples compared to normal ovary samples or normal omentum samples. Genes associated with cell invasion were selected for further analysis only if their mean expression intensity values were greater than or equal to 100 for the tumor samples. Our final selection criteria was limiting our studies to only those gene fragments whose expression values were classified by the Gene Logic GeneExpress® Software System as being 'present', regardless of whether they were greater than or equal to 100. Clustering of the gene expression data was performed with Eisen Cluster and TreeView software (available at http://rana.lbl.gov/EisenSoftware.htm).

Results

Ovarian carcinoma cells invade through mesothelial cell monolayers

To determine the invasive ability of ovarian carcinoma cells, we developed an *in vitro* assay that we believe more closely mimics *in vivo* conditions than the commonly used Matrigel invasion assay [2]. Ovarian carcinoma differs from most other types of cancer in the means by which it spreads to secondary sites. Namely, most other types of cancer metastasize to secondary sites via the blood stream and thus, invade through the ECM that underlies endothelial cells lining blood vessels. In contrast, ovarian carcinoma cells spread to secondary sites by adhering to the mesothelial cells that line the organs of the peritoneal cavity. Thus, the focus of this study was on the interaction between ovarian carcinoma cells with mesothelial cells. In addition, we wanted to develop an *in vitro* invasion assay that would improve upon the model system developed by Niedbala et al. [4]. In particular, we wanted to quantitate the ability of ovarian carcinoma cells to invade through monolayers of mesothelial cells without using bovine corneal endothelial cells or radioactive material. We have previously shown that human LP9 mesothelial cells can synthesize the ECM molecules fibronectin, laminin, type I collagen, type III collagen, and type IV collagen within 24 h after plating [5]. Thus, we designed a model system that would allow mesothelial cells to grow to confluent monolayers by 48 h, and thus, obviate the need for bovine corneal endothelial cells.

Our initial strategy involved the use of fluorescently labeled co-cultures of live cells. In these initial assays,

Figure 1. Ovarian carcinoma cell invasion through live mesothelial cell monolayers. NIH:OVCAR5 ovarian carcinoma cells labeled with the red fluorescent stain SNARF-1 were allowed to invade through monolayers of live mesothelial cells labeled with the green fluorescent stain CMFDA. After three days, the wells were photographed under a phase objective to visualize the cocultures (A), or under fluorescent objectives to visualize the ovarian carcinoma cells (B), or the mesothelial cell monolayers (C). Arrows point to a cluster of NIH:OVCAR5 cells that have invaded through the mesothelial cell monolayer. Bar = 100 μm.

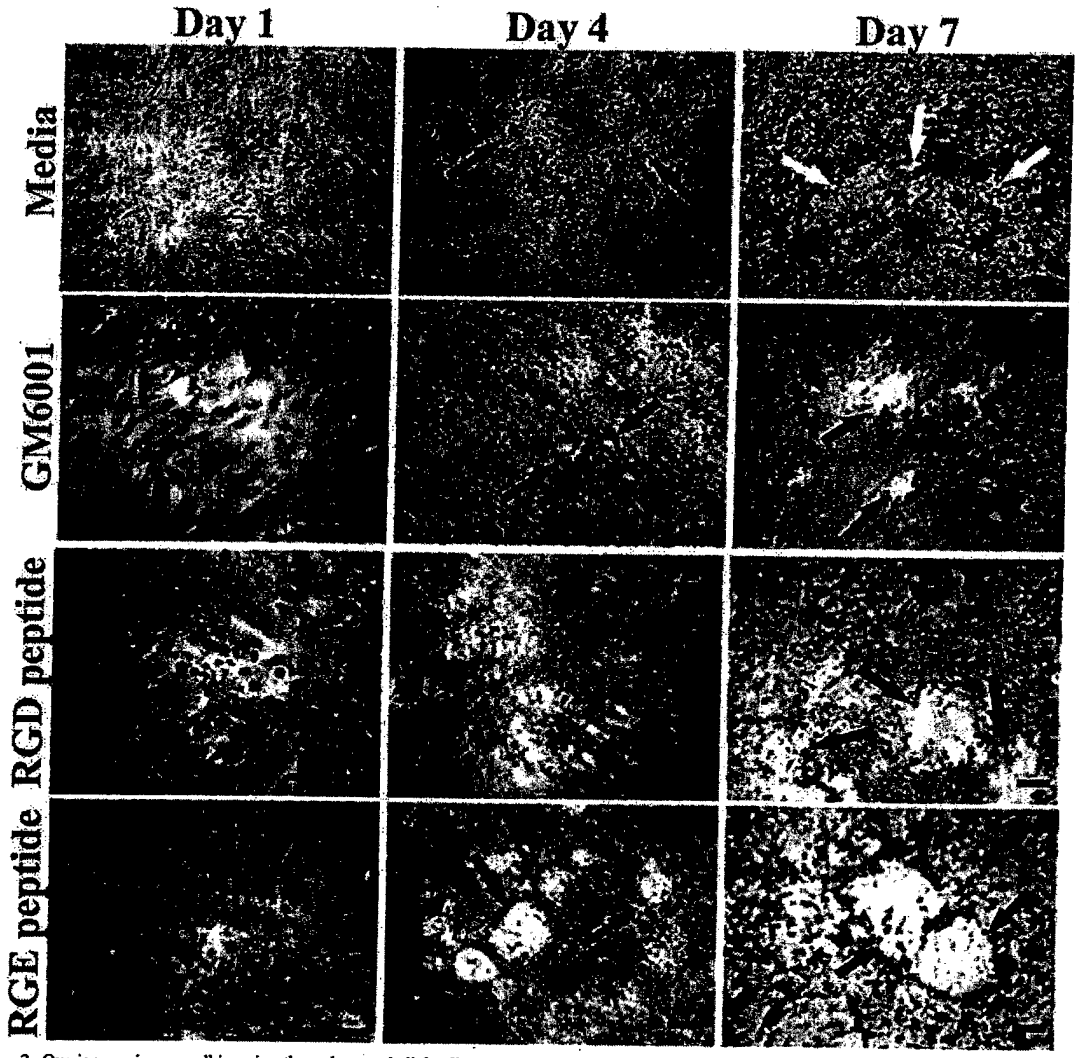

Figure 2. Ovarian carcinoma cell invasion through mesothelial cells monolayers is inhibited by an MMP inhibitor and GRGDSP peptide. NIH:OVCAR5 ovarian carcinoma cells were placed atop monolayers of DMSO-treated mesothelial cells in complete media alone or in the presence of 25 mM GM6001, 100 μg/ml GRGDSP peptide, or 100 μg/ml GRGESP peptide. In the presence of media or the GRGESP peptide, ovarian carcinoma cell invasion is observed at 4 and 7 days (arrows). In the presence of GM6001 or the GRGDSP peptide, cell invasion is completely inhibited for 4 days, and is still partly inhibited by 7 days (arrows). Bar = 200 μm.

the ovarian carcinoma cells and mesothelial cells were labeled with two different colored fluorescent dyes (Figure 1). At three days, the two cell types were indistinguishable from each other when viewed with a phase microscope (Figure 1A). When viewed with fluorescent filters, the NIH:OVCAR5 cells (Figure 1B) could be distinguished from the mesothelial cell monolayers (Figure 1C). One cluster of NIH:OVCAR5 cells, highlighted with arrows, was observed under phase and fluorescent filters (Figures 1A, 1B), and its absence was noted from the visualized mesothelial cell monolayer (Figure 1C). The ovarian carcinoma tumor cells had invaded through the mesothelial cell monolayer and adhered to the tissue culture plate, creating a focal point of invasion. For up to three days, the cells were easily visualized with the fluorescent microscope. However, the fluorescent dyes diluted to undetectable levels after approximately six to eight cell divisions and could not be used for longer time points. We therefore decided to try another approach for differentiating the two cell types.

In the second model system described herein, we used trypan blue dye to distinguish between the two cell types, based on a modification of a protocol described by Yu et al. [14]. In this model system, we used DMSO to permeabilize the confluent human mesothelial cell monolayers, and then the ovarian carcinoma cells were allowed to invade through monolayers of permeabilized mesothelial cells (Figure 2). At 24 h intervals, nonadherent ovarian carcinoma cells were gently rinsed away, and the cultures were subjected to trypan blue dye staining. The permeabilized mesothelial cells stained blue, since they were unable to exclude the trypan blue dye. In contrast, the live ovarian carcinoma cells remained unstained.

During the early phases of invasion, the ovarian carcinoma cells must adhere to the mesothelial cells. Adhesion and spreading may then occur, as well as proliferation and invasion. We were able to distinguish these various processes by vigilantly observing the ovarian carcinoma cells during the course of the weeklong assay. At the one-day time point, the ovarian carcinoma cells still remained round and appeared to have adhered to the surface of the mesothelial cell monolayers. However, there was no evidence of invasion of the mesothelial cell monolayers by the ovarian carcinoma cells. Within two to three days, the ovarian carcinoma cells had spread out on the surface of the mesothelial cells and were also beginning to show signs of proliferation. At the four-day time point, initial invasion by the ovarian carcinoma cells through the mesothelial cell monolayers was observed (Figure 2, arrows). The ovarian carcinoma cells had moved between the mesothelial cells that formed the monolayers, and had actually pushed the mesothelial cells aside. By microscopic examination, the ovarian carcinoma cells were no longer sitting atop the mesothelial cells, but were on the same plane of vision as the mesothelial cells. By seven days, the foci of invasion had increased in size (Figure 2, arrows), in some cases displacing the majority of the mesothelial cell monolayers in the well. The ovarian carcinoma cells appeared to act as a 'snow plow' and had virtually cleared off entire sections of the wells where the mesothelial cells had once been, leaving mounds or piles of mesothelial cells at the edges of these displaced areas. We did not observe mesothelial cells being exfoliated as a monolayer; rather we observed piles of displaced mesothelial cells at the perimeter of these areas where the ovarian carcinoma cells now were growing.

Ovarian carcinoma cell invasion through mesothelial cell monolayers is blocked by MMP inhibitors

Ovarian carcinoma cell invasion has been shown to be mediated, in part, by the induction of MMPs [11, 20, 21]. For this reason, we examined whether some potential inhibitors of MMP activity would alter the invasive capacity of ovarian carcinoma cells in our model system. We tested the following potential inhibitors: GM6001 which is a broad-spectrum MMP inhibitor; a mAb against MMP 2; a mAb against MMP 9; TIMP-1; and TIMP-2. Ovarian cancer cell invasion through mesothelial cell monolayers was dramatically inhibited by the addition of GM6001 (Table 1 and Figure 2). In the presence of 25 mM GM6001, ovarian carcinoma cell invasion was completely inhibited for up to 4 days. However, by seven days, some ovarian carcinoma cell invasion was observed in the presence of GM6001 (Table 1), but the areas of invasion were much smaller than those observed in the absence of the GM6001 (Figure 2, arrows). Furthermore, many ovarian carcinoma cells adhered to and spread upon the mesothelial cell monolayers, but did not invade. At lower concentrations of GM6001 (i.e., 1 mM and 10 mM), we did not observe significant inhibition of invasion (Table 1). Furthermore, when the ovarian carcinoma cells were grown in the presence of GM6001 for up to seven days, the rate of proliferation was not altered, indicating that GM6001 was not toxic at the range of concentrations tested (data not shown). The mAbs against MMP 2 and MMP 9 were able to almost completely inhibit the invasion of the ovarian carcinoma cells for up to four days (Table 1). However, by seven days, some invasion was observed, although not to the same extent as those ovarian carcinoma cells that were untreated. Similarly, TIMP-1 and TIMP-2 inhibited ovarian carcinoma cell invasion for up to 4 days when tested at 50 nM, while a lower concentration of 5 nM seemed to cause a minimal increase in invasion (Table 1). By 7 days, invasion was observed to be partially inhibited by 50 nM TIMP-2, while 50 nM TIMP-1 had no effect on ovarian carcinoma cell invasion (Table 1). These results suggest that ovarian carcinoma cell invasion through mesothelial cell monolayers requires some selective MMP activity.

Ovarian carcinoma cell invasion through mesothelial cell monolayers is mediated by integrins

We have previously shown that $\beta 1$ integrins mediate ovarian carcinoma cell adhesion [5, 6] and migration [7] to ECM components. To determine whether integrins affect ovarian carcinoma cell invasion through mesothelial cell monolayers, we performed the assays in the presence of exogenous GRGDSP peptide, a ligand bound by many integrins [34]. At 4 days, cell invasion was partially inhibited in the pres-

Table 1. Effect of metalloproteinases on the invasion of NIH:OVCAR5 ovarian carcinoma cells through monolayers of mesothelial cells.

Potential inhibitor	Concentration of inhibitor	Day 1	Day 4	Day 7
No treatment	–	–	+	+++
GM6001	1 mM	–	+	+++
	10 mM	–	+	++
	25 mM	–	–	+
mAb vs. MMP-2	0.1 μg/ml	–	+	++
	1 μg/ml	–	–	–
mAb vs. MMP-9	0.1 μg/ml	–	+	++
	1 μg/ml	–	–	+
TIMP-1	5 nM	–	++	+++
	20 nM	–	+	+++
	50 nM	–	–	+++
TIMP-2	5 nM	–	++	+++
	20 nM	–	+	+++
	50 nM	–	–	++

The invasion of the ovarian carcinoma cells into the mesothelial cell monolayers was quantified by measuring the size of the areas of the confluent monolayers of mesothelial cells that were displaced by the proliferating ovarian carcinoma cells. No invasion is represented as (–), 50–200 μm of invasion is represented as (+), 220–400 μm of invasion is represented as (++), and maximal levels of invasion greater than 400 μm are represented as (+++).

ence of 10–100 μg/ml GRGDSP peptide (Table 2, Figure 2), compared to cells incubated in the presence of GRGESP control peptide (Table 2, Figure 2, arrows). The addition of the GRGDSP peptide inhibited most ovarian carcinoma cell invasion (Figure 2), but it did not completely prevent tumor cells from adhering to the mesothelial cell monolayer. By 7 days, areas of invasion of the ovarian carcinoma cells into the mesothelial cell monolayers were observed when 100 μg/ml of the GRGDSP peptide was present (Table 2). However, these areas of invasion were much smaller than those observed in the presence of the GRGESP peptide at similar concentrations (Table 2, Figure 2). Furthermore, when the ovarian carcinoma cells were grown in the presence of the GRGDSP and GRGESP peptides for up to 7 days, the rate of proliferation was not altered, indicating that the GRGDSP and GRGESP peptides were not toxic at the range of concentrations tested (data not shown).

Further studies to determine the role of β1 integrins in mediating ovarian carcinoma cell invasion through mesothelial cell monolayers were performed in the presence of normal mouse IgG or mAbs against the binding sites of integrin subunits. A blocking mAb against the β1 integrin subunit completely inhibited ovarian carcinoma cell invasion up to four days; however by seven days some small areas of invasion were observed (Table 2, Figure 3). Furthermore, when the ovarian carcinoma cells were grown in the presence of the mAb against the β1 integrin subunit for up to seven days, the rate of proliferation was not altered, indicating that the mAb was not toxic at the range of concentrations tested (data not shown). A stimulating mAb against the β1 integrin subunit was able to inhibit cell invasion for up to 4 days when used at concentrations of 1 μg/ml. However, by seven days, the area of ovarian carcinoma cell invasion was almost the same as that observed in the presence of normal mouse IgG. Blocking mAbs against the alpha integrin subunits α1, α2, α3, α4, α5, and α6 were tested in this model system at 0.1 and 1 ug/ml. They had no inhibitory effect when compared to the normal mouse IgG controls (Table 2). Taken together, these data suggest that β1 integrins may mediate ovarian carcinoma cell invasion through mesothelial cell monolayers, although the alpha subunit(s) that participate in this invasion have not been defined.

Ovarian carcinoma cell invasion through mesothelial cell monolayers is partially mediated by glycosaminoglycans

We have previously shown that CD44 mediates ovarian carcinoma adhesion [5] and migration [7] to ECM components. To determine whether CD44 affects ovarian carcinoma cell invasion through mesothelial cell monolayers, we performed the assays in the presence of a blocking mAb against CD44 and various glycosaminoglycans. The mAb against CD44, when tested at concentrations of 0.1 and 1 μg/ml, did not inhibit ovarian carcinoma cell invasion at 4 days, and had only a minor inhibitory effect on cell invasion at 7 days (Table 3 and Figure 3, arrows) when compared to normal mouse IgG. The glycosaminoglycan hyaluronan, which serves as a ligand for CD44, inhibited ovarian carcinoma cell invasion up to day 4, at a concentration of 1000 μg/ml (Table 3). In the presence of 1000 μg/ml hyaluronan, the area of invasion increased from day 4 up to day 7 (Table 3). Even the lower concentrations of hyaluronan appeared to have a minor inhibitory effect on cell invasion at day 7. As controls, the glycosaminoglycans heparin and chondroitin sulfate A were tested and found to have no inhibitory effect on ovarian car-

Table 2. Effect of integrins on the invasion of NIH:OVCAR5 ovarian carcinoma cells through monolayers of mesothelial cells.

Potential inhibitor	Concentration of inhibitor	Day 1	Day 4	Day 7
No treatment	–	–	+	+++
GRGDSP peptide	1 μg/ml	–	+	+++
	10 μg/ml	–	–	+++
	100 μg/ml	–	–	+
GRGESP peptide	1 μg/ml	–	+	+++
	10 μg/ml	–	+	+++
	100 μg/ml	–	+	+++
Normal mouse IgG	0.1 μg/ml	–	+	+++
	1 μg/ml	–	+	+++
Blocking mAb vs. β1 integrin	0.1 μg/ml	–	–	+
	1 μg/ml	–	–	+
Stimulating mAb vs.β1 integrin	0.1 μg/ml	–	+	++
	1 μg/ml	–	–	++
mAb vs. α1 integrin	0.1 μg/ml	–	+	+++
	1 μg/ml	–	+	+++
mAb vs. α2 integrin	0.1 μg/ml	–	+	+++
	1 μg/ml	–	+	+++
mAb vs. α3 integrin	0.1 μg/ml	–	+	+++
	1 μg/ml	–	+	+++
mAb vs. α4 integrin	0.1 μg/ml	–	+	+++
	1 μg/ml	–	+	+++
mAb vs. α5 integrin	0.1 μg/ml	–	+	+++
	1 μg/ml	–	+	+++
mAb vs. α6 integrin	0.1 μg/ml	–	+	+++
	1 μg/ml	–	+	+++

The invasion of the ovarian carcinoma cells into the mesothelial cell monolayers was quantified as described in Table 1.

Table 3. Effect of glycosaminoglycans on the invasion of NIH:OVCAR5 ovarian carcinoma cells through monolayers of mesothelial cells.

Potential inhibitor	Concentration of inhibitor	Day 1	Day 4	Day 7
No treatment	–	–	+	+++
Normal mouse IgG	0.1 μg/ml	–	+	+++
	1 μg/ml	–	+	+++
mAb vs. CD44	0.1 μg/ml	–	+	+++
	1 μg/ml	–	+	++
Hyaluronan	10 μg/ml	–	+	++
	100 μg/ml	–	+	++
	1000 μg/ml	–	–	+
Chondroitin sulfate A	10 μg/ml	–	+	+++
	100 μg/ml	–	+	+++
	1000 μg/ml	–	++	+++
Heparin	10 μg/ml	–	++	+++
	100 μg/ml	–	++	+++
	1000 μg/ml	–	+	+++

The invasion of the ovarian carcinoma cells into the mesothelial cell monolayers was quantified as described in Table 1.

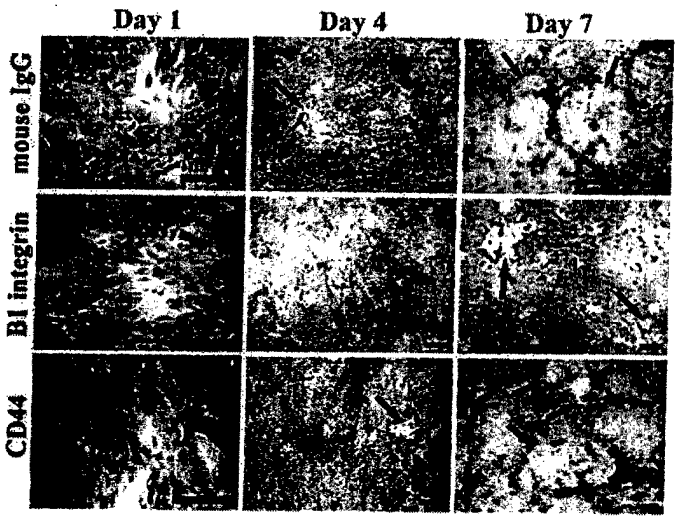

Figure 3. Ovarian carcinoma cell invasion through mesothelial cells monolayers is inhibited by monoclonal antibodies against the $\beta 1$ integrin subunit. NIH:OVCAR5 ovarian carcinoma cells were placed atop monolayers of DMSO-treated mesothelial cells in the presence of 1 μg/ml mouse IgG, blocking mAb against the $\beta 1$ integrin subunit, or blocking mAb against CD44. In the presence of mouse IgG or a blocking mAb against CD44, the NIH:OVCAR5 cells invaded through the mesothelial cell monolayers (arrows). In the presence of a blocking mAb against the $\beta 1$ integrin subunit, invasion through the mesothelial cell monolayer was almost completely inhibited on day 4, and still significantly inhibited on day 7. Bar = 200 μm.

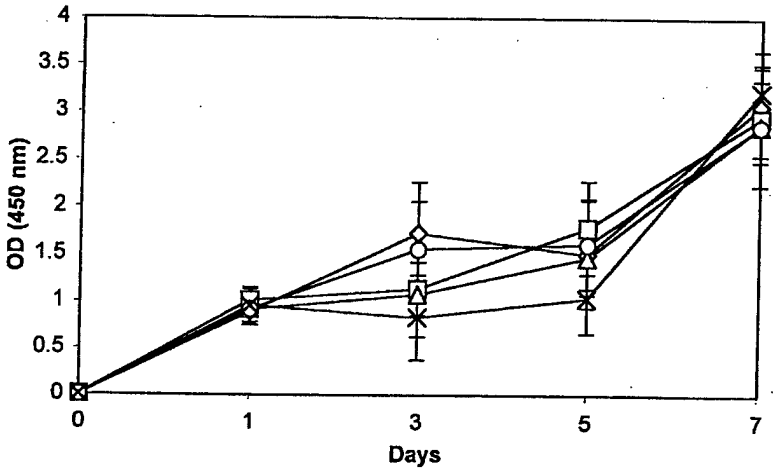

Figure 4. Ovarian carcinoma cell proliferation is not affected by the composition of the adhesive substrata. 96-well plates were coated with fibronectin (diamonds), type IV collagen (squares), laminin (triangles), hyaluronan (circles), or ovalbumin (crosses). NIH:OVCAR5 cells were added to ECM-coated wells at a concentration of 500 cells/well and incubated for up to 7 days. The levels of proliferation were quantitated as described in the 'Materials and methods' section. Data are expressed as mean ± SD.

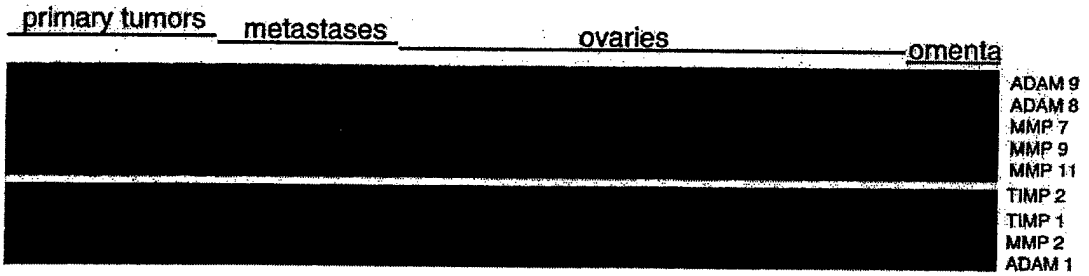

Figure 5. Differential gene expression between ovarian carcinomas and normal tissues. The expression values for gene fragments of MMPs, TIMPs, and ADAMs were analyzed by the Gene Logic GeneExpress® Software System for 20 primary ovarian carcinoma tumors ('primary tumors'), 17 secondary ovarian carcinoma tumors that had spread to the omentum ('metastases'), 50 normal ovaries ('ovaries'), and 7 normal omentum ('omenta'). The nine gene fragments listed in Table 4 were differentially expressed in the sample sets and the gene expression data was clustered with Eisen Cluster and TreeView software. Columns represent individual human tissue samples; rows represent individual genes. Each box represents the expression level of a single transcript in a single sample, with red and green indicating transcript levels above and below the mean for that gene across all samples, respectively.

cinoma cell invasion any time during the assay, even when tested at concentrations as high as 1000 μg/ml (Table 3). Furthermore, when the ovarian carcinoma cells were grown in the presence of hyaluronan, chondroitin sulfate A, or heparin for up to seven days, the rate of proliferation was not altered, indicating that these glycosaminoglycans were not toxic at the range of concentrations tested (data not shown). These results suggest that hyaluronan may play a role in ovarian carcinoma cell invasion.

The composition of the adhesive substratum does not affect the proliferative abilities of ovarian carcinoma cells

We were next interested in determining whether different ECM molecules on the surface of the wells affected the growth, and thus, the invasion, of the ovarian carcinoma cells. The first step in this model system requires growing the mesothelial cells to confluency in the wells. During this 48-h period, mesothelial cells have been shown to produce a variety of ECM molecules [5]. During the next seven days, while the ovarian carcinoma cells were co-cultured with the mesothelial cells, the mesothelial cells appeared to be pushed aside by the invading ovarian carcinoma cells. In addition, the ovarian carcinoma cells appeared to spread and/or proliferate on the cleared off areas of the wells. Thus, it is possible that the underlying ECM molecules that were secreted by the mesothelial cells may be promoting the proliferation and growth of the ovarian carcinoma cells. Earlier studies by Niedbala et al. [4] had postulated that such a scenario may be occurring. Thus, we wished to determine whether the ovarian carcinoma cells proliferate (and not just spread out) on a variety of ECM molecules that are synthesized by the mesothelial cells. To examine the effects of adhesive substrata on the proliferative ability of the ovarian carcinoma cells, NIH:OVCAR5 were cultured as monolayers in 96-well plates that were coated with different ECM components known to be secreted by mesothelial cells: fibronectin, laminin, type IV collagen, and hyaluronan (Figure 4) [5, 35]. The ovarian carcinoma cells proliferated rapidly within the first 24 h of the assay regardless of the ECM component on which they were growing. Moderate growth rates were observed between days 3 and 7 on each of the ECM molecules (Figure 4). Thus, we observed that the NIH:OVCAR5 cells proliferated equally well in the presence of any of the four ECM molecules we tested as adhesive substrata. Interestingly, none of the ECM molecules that we tested preferentially increased or decreased ovarian carcinoma cell proliferation.

Differential expression of genes associated with cell invasion in normal and malignant ovarian tissues

Since cancer cell invasion is thought to be mediated by a complex interaction between MMPs, ADAMs, and TIMPs, we decided to determine whether these genes are differentially expressed in ovarian carcinoma tissues, compared to normal ovaries. Gene Logic Inc. quantitated the expression levels of 12,000 known genes and 48,000 ESTs using Affymetrix GeneChip® U_95 arrays on RNA samples obtained from 20 primary ovarian carcinoma tumors, 17 secondary omental metastases, 50 normal ovaries, and 7 normal omenta. We limited our analysis to the 82 gene fragments or 48 different genes that contained the word 'MMP', 'TIMP', or 'ADAM'. The gene expression values for these 82 gene fragments were then analyzed by the Gene Logic GeneExpress® Software System in order to identify those genes that were over- or under-expressed 2-fold or more in ovarian carcinoma samples compared to normal ovary samples or normal omentum samples. Genes associated with cell invasion were selected for further analysis only if their mean expression intensity values were greater than or equal to 100 for the tumor samples and were classified as 'present' by the Gene Logic GeneExpress® Software System.

By performing gene expression analysis, we analyzed 94 different tissue samples for their expression levels of 82 gene fragments related to cell invasion. This process led us to generate almost 8,000 data points. Eisen Cluster analysis (Figure 5) allows for a visual depiction of the range of fluorescent values for the various samples. For example, 75% (15/20) of the primary ovarian carcinoma samples and 82% (14/17) of the secondary omental metastases samples expressed high levels of MMP 7; indicated by the boxes that are shades of red. In contrast, only 4% (2/50) of the normal ovary samples express low levels of MMP 7; shown by the two boxes that are faintly red. The intensity of color depicts the level of expression of each gene.

Nine genes appeared to be differentially expressed between the cancerous tissues and the normal tissue counterparts. The fluorescent intensity values for these nine genes are shown in Figure 5. ADAM 8, ADAM 9, MMP 7, MMP 9, and MMP 11 were highly expressed in both primary ovarian carcinomas and secondary omental metastases, compared to normal ovaries and omenta (Figure 5). Comparison of the expression values assigned to these gene transcripts confirmed significant mean fold increases of these transcripts in tumor samples compared to normal tissues (Table 4). The tissue distribution of MMP 7 gene expression was found to show the most marked change among the gene fragments we studied. Expression of MMP 7 was 90-fold higher in primary ovarian carcinoma tissues compared to normal ovaries, 97-fold higher in secondary ovarian carcinoma tumors compared to normal ovaries, and 37-fold higher in secondary ovarian carcinoma tumors compared to normal omentum (Table 4). In addition, the expression of MMP 9 transcripts increased over 5-fold, while the expression of ADAM 8, ADAM 9, and MMP 11 transcripts increased over 2-fold (Table 4). In contrast, the expression of gene transcripts of TIMP 2, TIMP 1, MMP 2, and ADAMTS 1, was down-regulated 2.0 to 4.4-fold in tumor tissues compared to normal samples (Figure 5 and Table 4).

Discussion

Currently, cancer cell invasion is most commonly measured by the ability of the cells to invade through Matrigel [2], a mixture of matrix components synthesized by mouse EHS tumors that approximates the basement membrane ECM

through which cancer cells invade [3]. While the Matrigel invasion assay provides an ECM through which cancer cells can invade, there are several caveats to this procedure. Matrigel is a mixture of ECM components synthesized by mouse sarcoma cells, which is a less than ideal milieu to examine metastasis in human ovarian carcinoma cells. More importantly, this assay measures interactions between tumor cells and ECM components, but not cell–cell interactions between tumor cells and target cells. Ovarian carcinoma differs from most other types of cancer in the means by which it spreads to secondary sites. Namely, most other types of cancer metastasize to secondary sites via the blood stream and thus, invade through the ECM that underlies endothelial cells lining blood vessels. In contrast, ovarian carcinoma cells spread to secondary sites by adhering to the mesothelial cells that line the organs of the peritoneal cavity. Thus, the focus of this study was on the interaction between ovarian carcinoma cells with mesothelial cells.

Niedbala et al. [4] described a model system for studying the interaction of radiolabeled ovarian carcinoma cells with: (i) monolayers of mesothelial cells grown on bovine corneal endothelial cell ECM, (ii) ECM alone, or (iii) plastic. After a 72 h incubation, Niedbala et al. [4] observed a retraction of the mesothelial cell monolayers in the presence of the ovarian carcinoma cells. Our model system was similar to that of Niedbala et al. [4]; however, we permeabilized the mesothelial cell monolayers with DMSO prior to the addition of the ovarian carcinoma cells, based on the work of Yu et al. [14]. In addition, we did not precoat the wells with ECM components prior to the addition of the mesothelial cells. Interestingly, the retraction described by Niedbala et al. [4] seems to be similar to what we observed after 72 h of coculture. Namely, the mesothelial cells appeared to be pushed aside by the invading ovarian carcinoma cells, similar to how a snowplow pushes snow into piles. Then, as days passed, the areas cleared away by the invasive ovarian carcinoma cells became occupied by more spreading and proliferating ovarian carcinoma cells. In this study, we have extended the descriptive experiments of others in an effort to identify the cell surface molecules that may play a role in this cell–cell interaction and invasion process.

The *in vitro* cell-based ovarian carcinoma cell invasion assay described herein has several advantages over other invasion assays. First, the *in vitro* invasion model described herein is comprised of cells and ECM components of human origin, derived from human mesothelial cells, unlike Matrigel, which is murine in origin, or bovine corneal endothelial cells used by Niedbala et al. [4]. We have previously published that the human mesothelial cell line LP9 forms a confluent monolayer in tissue culture-treated plastic wells within 48 h [5]. We have shown that during a 48-h period, this mesothelial cell line secretes the ECM molecules: fibronectin, laminin, type I collagen, type IV collagen, and hyaluronan [5]. Since the mesothelial cells secrete an abundance of ECM molecules during the 48-h period prior to the start of the invasion assay, we did not find it necessary to precoat the wells with ECM molecules from other sources. Furthermore, since these human mesothelial cells did not detach from the plastic wells during the course of the seven-day invasion assay, it was not necessary to treat the mesothelial cells with a harsh fixative that could have altered the cell surface adhesion molecules. Matrigel is not completely characterized, and may contain murine-specific components that may alter the function of human cells. Interestingly, others have shown that the addition of exogenous hyaluronan to Matrigel alters glioma cell invasion [15], suggesting that the precise composition of the invasive matrix is critical in the accurate assessment of tumor cell invasion. Second, unlike the Matrigel invasion assay, this *in vitro* invasion model is a cell-based assay that allows interactions to occur between tumor cells and permeabilized target mesothelial cells. Although not as ideal as live mesothelial cells, the use of the permeabilized mesothelial cells as an invasive matrix more closely approximates *in vivo* conditions than the mixture of ECM components that comprise Matrigel. Thus, our *in vitro* invasion model may provide a more accurate gauge of metastatic events. Third, our *in vitro* model facilitates interactions between ovarian carcinoma cells and mesothelial cells, their most likely *in vivo* targets of metastasis, providing a more optimal environment in which to study ovarian carcinoma cell invasion. Furthermore, this model could easily be adapted to measure the invasive capacities of other types of tumor cells.

We initially attempted to perform invasion assays using live mesothelial cell monolayers. Ovarian carcinoma cells and mesothelial cells were labeled with different fluorescent dyes prior to their use in the assay. However, the fluorescent dyes diluted to undetectable levels after approximately six to eight cell divisions, rendering this assay unsuitable within a few days. For this reason, we permeabilized the mesothelial cell monolayers for use as a matrix of invasion. The permeabilized mesothelial cells were not able to exclude trypan blue dye, and thus they stained blue, while the ovarian carcinoma cells did not retain the dye and remained clear. Thus, it was quite easy to distinguish between the mesothelial cells

Table 4. Genes associated with cell invasion are differentially expressed in ovarian carcinoma.

Gene	1° tumor: normal ovary	2° tumor: normal ovary	2° tumor: normal omentum
MMP 7	90.1 ↑	97.0 ↑	37.4 ↑
MMP 9	5.7 ↑	9.5 ↑	–
MMP 11	2.3 ↑	4.6 ↑	7.9 ↑
ADAM 8	2.3 ↑	2.0 ↑	–
ADAM 9	–	2.0 ↑	–
TIMP 1	–	–	3.3 ↓
ADAMTS 1	3.9 ↓	4.1 ↓	4.4 ↓
TIMP 2	2.2 ↓	–	–
MMP 2	2.0 ↓	–	–

The mean fold change ratio differences in gene expression were compared between 20 primary ovarian carcinoma tumors and 50 normal ovaries, and between 17 secondary omental metastases and 7 normal omenta. In those cases where the ratio of mean fold change between tumor:normal tissue was less than 2.0, then the ratio is denoted as –.

and the ovarian carcinoma cells without using fluorescent dyes or radioactive material.

The invasive process was easily visualized in this cell-based model. Ovarian carcinoma cells readily adhered to, spread upon, and invaded through the mesothelial cell monolayers. After the formation of invasive foci, the cancer cells proliferated and displaced the mesothelial cells. Interestingly, the mesothelial cells did not stimulate contact inhibition in the invading ovarian carcinoma cells. It is still possible, however, that mesothelial cells may provide an inhibitory effect upon ovarian carcinoma cell invasion or proliferation *in vivo*.

The pericellular matrices that coat mesothelial cell monolayers is comprised of numerous ECM components, including glycoproteins and proteoglycans [5, 9]. To determine whether adhesion to a particular substrata may affect ovarian carcinoma cell proliferation, the cells were cultured in 96-well plates coated with fibronectin, type IV collagen, laminin, or hyaluronan, the major components of mesothelial cell ECM [5, 9]. The ovarian carcinoma cells adhered to all of the substrata and grew to confluence. The composition of the adhesive substrata failed to affect the cells' ability to proliferate, which suggests that the general phenomenon of cell adhesion mediates ovarian carcinoma cell proliferation, rather than adhesion to a particular substratum. Further studies are required to determine the role of the mesothelial cells as positive or negative effectors of secondary tumor growth in ovarian cancer.

In the assays whereby we attempted to inhibit the invasion of the ovarian carcinoma cells into the mesothelial cell monolayers, we allowed the ovarian carcinoma cells to settle onto the mesothelial cell monolayers for 1 h prior to the addition of the potential inhibitors. This time point was selected so as to ensure that when we added the potential 'inhibitors of invasion' to the assay, there would be no concern that the 'inhibitors of invasion' may be inhibiting cell adhesion instead. We have previously published that ovarian carcinoma cells adhere very rapidly to mesothelial cell monolayers [5]; over 60% of the ovarian carcinoma cells adhere within 30 min and over 90% adhere within 45–60 min. Therefore, we added our 'inhibitors' 1 h after the ovarian carcinoma cells were added to the wells, so that the initial stages of adhesion would not be affected. Furthermore, this assay was designed to more closely mimic the *in vivo* situation, whereby the patient's ovarian carcinoma cells are already present in their peritoneal cavity, and may have already adhered to the surface of the mesothelial cells. Thus, we were testing 'inhibitors' to see if they can disrupt the invasion, not the adhesion of ovarian carcinoma cells.

Ovarian carcinoma cell invasion was partially inhibited by the addition of GM6001, a potent chemical inhibitor of MMP-1, -2, -3, -8, and -9. The presence of this inhibitor slowed cell invasion, although the phenomenon was not completely halted at seven days. Perhaps other degradative enzymes accumulated at sufficient concentrations to overcome the inhibitory effect of GM6001. GM6001 did not negatively affect ovarian carcinoma cell adhesion to the mesothelial cell monolayers, or subsequent spreading of the adherent ovarian carcinoma cells. Furthermore, GM6001 was not toxic to the ovarian carcinoma cells at the concentrations tested. In order to determine which of the various MMPs may be affected by GM6001 in this model system, we also tested mAbs against MMP 2 and MMP 9. Both of these mAbs were able to partially inhibit the invasion of the ovarian carcinoma cells, indicating that these MMPs may be involved in ovarian carcinoma cell invasion. When TIMP-1 and TIMP-2 were tested in this model system, they served as effect inhibitors of invasion up to day 4 of the assay, but were not effective by day 7. Again, it is possible that other proteolytic enzymes that are not affected by TIMP-1 and TIMP-2 may be involved in this invasive process. Future studies are planned to pinpoint the exact proteases that play a role in the invasion of ovarian carcinoma cells through mesothelial cell monolayers, including other classes of proteases, using this model system.

We have previously shown that the $\beta 1$ integrins play a major role in the adhesion of ovarian carcinoma cells to mesothelial cell monolayers [5]. In addition, we have also shown that the $\beta 1$ integrins play a major role in ovarian carcinoma cell migration toward ECM components [7]. In this study, we observed that ovarian carcinoma cell invasion through mesothelial cell monolayers was inhibited by the addition of the GRGDSP peptide or a blocking mAb against the $\beta 1$ integrin subunits. In addition, the ovarian carcinoma cells remained more rounded up in the presence of the GRGDSP peptide or the blocking mAb against the $\beta 1$ integrin subunit. However, cell invasion was not altered by the addition of the control GRGESP peptide or by blocking mAbs against the various alpha integrin subunits. It is not too surprising that none of the mAbs against the alpha integrin subunits had an effect on invasion, since these same mAbs (although functionally active) were not able to inhibit the short-term adhesion of ovarian carcinoma cells to mesothelial cell monolayers [5]. It is likely that each individual alpha subunit plays a role in the adhesion and invasion process. However, since there are multiple alpha subunits that complex with the $\beta 1$ integrin subunit, we were not able to completely block this interaction. We have previously shown that this mAb against the $\beta 1$ integrin subunit is extremely powerful in its ability to inhibit the adhesive and migratory activity of the $\beta 1$ integrin subunit [5–7], perhaps since it can simultaneously block all of the alpha subunits with which it complexes (i.e., $\alpha 1$, $\alpha 2$, $\alpha 3$, $\alpha 4$, $\alpha 5$, and $\alpha 6$) as well. Interestingly, the stimulatory mAb against the $\beta 1$ integrin subunit served to partially inhibit the invasion of the ovarian carcinoma cells. In addition, this stimulatory mAb increased the area of spreading of the ovarian carcinoma cells on the mesothelial cell monolayer.

CD44 has been shown to mediate ovarian carcinoma cell adhesion to ECM components and to mesothelial cells [5, 8, 9]. We therefore had expected that the mAb against CD44 would also affect cell invasion. Interestingly, we observed that the mAb against CD44 only caused a minimal inhibition of cell invasion at day 7. One possible explanation for this lack of activity could be attributed to the treatment of the mesothelial cells with DMSO prior to the addition of

the ovarian carcinoma cells. Thus, one could argue that permeabilization of the mesothelial cells had altered the CD44, such that the mAb against CD44 was no longer able to adhere to the cells. However, previous studies by Yu et al. [14] had shown that CD44 on the surface of murine mammary carcinoma cells was still functionally active following treatment with DMSO. In order to rule out the possibility that permeabilization of the mesothelial cells had altered the CD44 in our model system, we performed immunohistochemistry on the permeabilized cells. We found that the mAb against CD44 bound to the permeabilized cells and stained positively by immunohistochemistry; thus, treatment with DMSO does not alter CD44 in these cells. Interestingly, high concentrations of exogenous hyaluronan inhibited the invasive ability of the ovarian carcinoma cells, while chondroitin sulfate A and heparin had no effect. This suggests that ovarian carcinoma cell invasion through mesothelial cell monolayers may be partially mediated by hyaluronan, while the role of CD44 in this process is not clear.

Because tumor cell invasion has been attributed to alterations in the net expression of MMPs, TIMPs, and ADAMs, the expression of these gene transcripts was examined in ovarian carcinoma tumors, secondary metastases, normal ovaries, and normal omenta. Several genes associated with cell invasion were differentially expressed. In primary ovarian carcinoma tumors and secondary omental metastases, the level of expression of ADAM 8, ADAM 9, MMP 7 (also known as uterine matrilysin), MMP 9 (also known as gelatinase B, 92 kD gelatinase, and 92 kD type IV collagenase), and MMP 11 (also known as stromelysin 3) transcripts was much greater than that of normal ovaries and omenta. High levels of gene expression of TIMP 1, TIMP 2, MMP 2 (also known as gelatinase A, 72 kD gelatinase, and 72 kD type IV collagenase), and ADAMTS 1 were observed in samples obtained from normal ovaries and omenta compared to ovarian carcinoma samples. TIMPs complex with and inactivate MMPs. Although relatively high levels of MMP 2 were also detected in normal tissues, the simultaneous expression of the TIMPs suggest that the MMP may be present in an inactive state, or that the TIMPs are present in adequate amounts to inhibit MMP activity.

In ovarian carcinoma, increased secretion and activity of MMP 2 and TIMP 1, but not TIMP 2 has been reported [20–23]. Increased expression of MMP 7 mRNA has also been observed in ovarian cancers [36, 37]. Our gene expression experiments indicated that MMP 7 RNA levels in ovarian carcinoma tissue samples were 90-fold greater than the levels in normal ovary tissues. The ADAMs are a recently discovered family of cell adhesion receptors, most of which are composed of pro-, metalloproteinase, disintegrin-like, cysteine-rich, EGF-like repeat, transmembrane and cytoplasmic tail domains [24, 25]. Type I and type II procollagens can be degraded by an ADAMTS [26], which may augment cancer cell invasion. Since it is not known whether the collagenase activity of ADAMTS is susceptible to effectors of MMP activity, such as GM6001, members of the ADAM family may provide an alternate degradative pathway that contributes to cancer cell invasion. Upregulation of ADAM 12 and ADAM 15 domains in melanoma cells resulted in enhanced cell adhesion [27]. Cell migration in fibroblast cells was increased by the binding of an ADAM 9 fusion protein via integrin $\alpha 6\beta 1$ [38]. The role of ADAMs in cancer metastasis is not well understood, but their ability to affect cellular functions suggests that they may contribute to cancer cell invasion. MMPs, TIMPs, and ADAMs are believed to regulate cancer cell invasion, but their particular interactions are not fully understood. More comprehensive gene expression experiments are planned in the future in order to determine those genes that are differentially expressed among ovarian carcinoma cells that are adherent to plastic vs. ECM vs. mesothelial cell monolayers. These gene expression experiments may provide insight into the complex process of ovarian carcinoma cell invasion.

In summary, in this study we report the development of an *in vitro* dye-based model system to study ovarian carcinoma cell invasion. The primary advantage this model system has over the commonly used Matrigel invasion assay lies in its similarity to *in vivo* conditions found in ovarian carcinoma. The use of mesothelial cell monolayers as an invasive matrix enables one to study cell–cell interactions that are not available in Matrigel assays. In addition, this model system uses only human ECM molecules and non-radioactive means to quantitate cell invasion. Using this model system, $\beta 1$ integrin subunits, MMPs, and hyaluronan were found to be involved in mediating ovarian carcinoma cell invasion. Furthermore, our gene expression analysis supports the results we obtained with the model system; revealing differential expression of MMP, TIMP, and ADAM genes in ovarian carcinoma tumors. Taken together, the invasion model system and the differential gene expression results may help elucidate the events that regulate ovarian carcinoma cell invasion and metastasis.

Acknowledgements

We thank Diane Trussoni Rauch and Sarah Bowell of the University of Minnesota Cancer Center's Tissue Procurement Facility for assistance in collecting and processing the human tissue samples. We thank the staff of Gene Logic Inc., Gaithersburg, Maryland, for performing the gene expression experiments with the human tissue samples. We thank Drs Thomas Hamilton and Judah Folkman for providing the NIH:OVCAR5 cell line, Dr James McCarthy for providing fibronectin, and Dr Leo Furcht for providing laminin and the mAb P5D2 against the $\beta 1$ integrin subunit.

Supported by grants from the National Institute of Health/National Cancer Institute (CA0913825), Department of the Army (DA/DAMD17-99-1-9564), and the Minnesota Medical Foundation (SMF-2078-99). The content of the information presented in this manuscript does not necessarily reflect the position of the United States Government.

References

1. Jemal A, Thomas A, Murray T et al. Cancer statistics, 2002. CA Cancer J Clin 2002; 52: 23–47.
2. Hendrix MJ, Seftor EA, Seftor RE et al. A simple quantitative assay for studying the invasive potential of high and low human metastatic variants. Cancer Lett 1987; 38: 137–47.
3. Kleinman HK, McGarvey ML, Liotta LA et al. Isolation and characterization of type IV procollagen, laminin, and heparan sulfate proteoglycan from the EHS sarcoma. Biochem 1982: 21: 6188–93.
4. Niedbala MJ, Crickard K, Bernacki RJ. Interactions of human ovarian tumor cells with human mesothelial cells grown on extracellular matrix. Exp Cell Res 1985; 160: 499–513.
5. Lessan K, Aguiar DJ, Oegema T et al. CD44 and $\beta 1$ integrins mediate ovarian carcinoma cell adhesion to peritoneal mesothelial cells. Am J Pathol 1999; 154: 1525–37.
6. Casey RC, Burleson KM, Skubitz KM et al. $\beta 1$ integrins regulate the formation and adhesion of ovarian carcinoma multicellular spheroids. Am J Pathol 2001; 159: 2071–80.
7. Casey RC, Skubitz APN. CD44 and $\beta 1$ integrins mediate ovarian carcinoma cell migration toward extracellular matrix proteins. Clin Exp Metastasis 2000; 18: 67–75.
8. Cannistra SA, Kansas GF, Niloff J et al. Binding of ovarian cancer cells to peritoneal mesothelium *in vitro* is partly mediated by CD44H. Cancer Res 1993; 53: 3830–8.
9. Gardner MJ, Catterall JB, Jones LM et al. Human ovarian tumour cells can bind hyaluronic acid via membrane CD44: A possible step in peritoneal metastasis. Clin Exp Metastasis 1996; 14: 325–34.
10. Takenaka K, Shibuya M, Takeda Y et al. Altered expression and function of beta 1 integrins in a highly metastatic human lung adenocarcinoma cell line. Int J Oncol 2000; 17: 1187–94.
11. Fishman DA, Liu Y, Ellerbroek SM et al. Lysophosphatidic acid promotes metalloproteinase (MMP) activation and MMP-dependent invasion in ovarian cancer cells. Cancer Res 2001; 61: 3194–9.
12. Herrera-Gayol A, Jothy S. CD44 modulates Hs578T human breast cancer cell adhesion, migration, and invasiveness. Exp Mol Pathol 1999; 66: 99–108.
13. Peterson RM, Yu Q, Stamenkovic I et al. Perturbation of hyaluronan interactions by soluble CD44 inhibits growth of murine mammary carcinoma cells in ascites. Am J Pathol 2000; 156: 2159–67.
14. Yu Q, Toole BP, Stamenkovic I. Induction of apoptosis of metastatic mammary carcinoma cells *in vivo* by disruption of tumor cell surface CD44 function. J Exp Med 1997; 186: 1985–96.
15. Radotra B, McCormick D. Glioma invasion *in vitro* is mediated by CD44-hyaluronan interactions. J Pathol 1997; 181: 434–8.
16. Mignatti P, Rifkin DB. Biology and biochemistry of proteinases in tumor invasion. Physiol Rev 1993; 73: 161–95.
17. Liotta LA, Stetler-Stevenson WG. Metalloproteinases and cancer invasion. Semin Cancer Biol 1990; 1: 99–106.
18. Davies B, Brown PD, East N et al. A synthetic matrix metalloproteinase inhibitor decreases tumor burden and prolongs survival of mice hearing human ovarian carcinoma xenografts. Cancer Res 1993; 53: 2087–91.
19. Gilles C, Polette M, Piette J et al. High level of MT-MMP expression is associated with invasiveness of cervical cancer cells. Int J Cancer 1996; 65: 209–13.
20. Moser TL, Young TN, Rodriguez GC et al. Secretion of extracellular matrix-degrading proteinases is increased in epithelial ovarian carcinoma. Int J Cancer 1994; 56: 552–9.
21. Sakata K, Shigemasa K, Nagai N et al. Expression of matrix metalloproteinases (MMP-2, MMP-9, MT1-MMP) and their inhibitors (TIMP-1, TIMP-2) in common epithelial tumors of the ovary. Int J Oncol 2000; 17: 673–81.
22. Naylor MS, Stamp GW, Davies BD et al. Expression and activity of MMPs and their regulators in ovarian cancer. Int J Cancer 1994; 58: 50–6.
23. Hoyhtya M, Fridman R, Komarek D. et al. Immunohistochemical localization of matrix metalloproteinase 2 and its specific inhibitor TIMP-2 in neoplastic tissues with monoclonal antibodies. Int J Cancer 1994; 56: 500–5.
24. Wolfsberg TG, Straight PD, Gerena RL et al. ADAM, a widely distributed and developmentally regulated gene family encoding membrane proteins with a disintegrin and metalloprotease domain. Dev Biol 1995; 169: 378–83.
25. Huovila APJ, Almeida EA, White JM. ADAMS and cell fusion. Curr Opin Cell Biol 1996; 8: 692–9.
26. Colige A, Li SW, Sieron AL et al. cDNA cloning and expression of bovine procollagen I N-proteinase: A new member of the superfamily of zinc-metalloproteinases with binding sites for cells and other matrix components. Proc Natl Acad Sci USA 1997; 94: 2374–9.
27. Iba KR, Albrechtsen BJ, Gilpin F et al. Cysteine-rich domain of ADAM 12 (meltrin alpha) supports tumor cell adhesion. Am J Pathol 1999; 154: 1489–501.
28. Molpus KL, Koelliker D, Atkins L et al. Characterization of a xenograft model of human ovarian carcinoma which produces intraperitoneal carcinomatosis and metastases in mice. Int J Cancer 1996, 68: 588–95.
29. Hamilton TC, Young RC, Ozols RF. Experimental model systems of ovarian cancer: Applications to the design and evaluation of new treatment approaches. Semin Oncol 1984; 11: 285–98.
30. Pattaramalai S, Skubitz KM, Skubitz APN. A novel recognition site on laminin for $\alpha 3\beta 1$ integrin. Exp Cell Res 1996; 222: 281–90.
31. Galardy RE, Grobelny D, Foellmer HG et al. Inhibition of angiogenesis by the matrix metalloprotease inhibitor N-[2R-2-(hydroxamidocarbonymethyl)-4-methylpentanoyl)]- L-tryptophan methylamide. Cancer Res 1994; 54: 4715–8.
32. McCarthy JB, Skubitz APN, Palm SL et al. Metastasis inhibition of different tumor types by purified laminin fragments and a heparin-binding fragment of fibronectin. J Natl Cancer Inst 1988; 80: 180–16.
33. Smith DE, Mosher DF, Johnson RB et al. Immunological identification of two sulfhydryl-containing fragments of human plasma fibronectin. J Biol Chem 1982; 257: 5831–8.
34. Pierschbacher MD, Ruoslahti E. Variants of the cell recognition site of fibronectin that retain attachment-promoting activity. Proc Natl Acad Sci USA 1984; 81: 5985–8.
35. Jones LM, Gardner MJ, Catterall JB et al. Hyaluronic acid secretion by mesothelial cells: A natural barrier to ovarian cancer cell adhesion. Clin Exp Metastasis 1995; 13: 373–80.
36. Tanimoto H, Underwood LJ, Shigemasa K et al. The matrix metalloproteinase pump-1 (MMP-7, matrilysin): A candidate marker/target for ovarian cancer detection and treatment. Tumour Biol 1999; 20: 88–98.
37. Zhai Y, Wu R, Schwartz DR et al. Role of beta-catenin/T-cell factor-regulated genes in ovarian endometrioid adenocarcinomas. Am J Pathol 2002; 160: 1229–38.
38. Nath D, Slocombe PM, Webster A et al. Meltrin gamma (ADAM-9) mediates cellular adhesion through $\alpha 6\beta 1$ integrin, leading to a marked induction of fibroblast cell motility. J Cell Sci 2000; 113: 2319–28.

Gene Expression in Ovarian Carcinoma: Identification of β8 integrin, Claudin-4, and S100A1 as Potential Biomarkers

Kathleen Hibbs,* Keith M. Skubitz,† Stefan E. Pambuccian,* Rachael C. Casey,* Kathryn M. Burleson,* Theodore R. Oegema Jr.,‡ Jeannine J. Thiele,§ Suzanne M. Grindle,¥ Robin L. Bliss,¥ and Amy P.N. Skubitz*

From the Departments of Laboratory Medicine and Pathology,* Medicine,† and Orthopaedic Surgery,‡ College of Biological Sciences,§ and the Cancer Center,¥ University of Minnesota, Minneapolis, Minnesota

Number of text pages: 27; **Number of tables:** 4; **Number of figures:** 5

Running head: Novel biomarkers of ovarian carcinoma

Sources of support: Supported by grants from the Department of the Army (DA/DAMD17-99-1-9564), National Institute of Health/National Cancer Institute (CA0913825), and Minnesota Medical Foundation (SMF-2078-99). The content of the information presented in this manuscript does not necessarily reflect the position of the United States Government.

Correspondence and reprint requests to: Amy P.N. Skubitz, Ph.D., Department of Laboratory Medicine and Pathology, University of Minnesota, MMC 609, 420 Delaware St. S.E., Minneapolis, MN 55455. Phone: (612) 625-5920; Fax: (612) 625-1121; email: skubi002@umn.edu

This work was presented, in part, at the Rivkin Foundation's "Fourth Biennial Ovarian Carcinoma Research Symposium: Integration of Research and Treatment" held September 19-20, 2002 in Seattle, WA. Portions of this manuscript were submitted as a thesis in partial fulfillment of the requirements for the degree of Master of Science [K.H.] and a Master of Science joint degree in Law, Health, and the Life Sciences [J.J.T].

ABSTRACT

Ovarian cancer remains the fifth leading cause of cancer death for women in the United States. In this study, the gene expression of 20 ovarian carcinomas, 17 ovarian carcinomas metastatic to the omentum, and 50 normal ovaries was determined by Gene Logic Inc. using Affymetrix GeneChip® HU_95 arrays containing approximately 12,000 known genes. Differences in gene expression were quantified as fold changes in gene expression in ovarian carcinomas compared to normal ovaries and ovarian carcinoma metastases. Genes up-regulated in ovarian carcinoma tissue samples compared to over 300 other normal and diseased tissue samples were identified. Seven genes were selected for further screening by immunohistochemistry to determine the presence and localization of the proteins. These seven genes were: the β8 integrin subunit, bone morphogenetic protein-7, claudin-4, collagen type IX α2, cellular retinoic acid binding protein-1, forkhead box J1, and S100 calcium binding protein A1. Statistical analyses showed that the β8 integrin subunit, claudin-4, and S100A1 provided the best distinction between ovarian carcinoma and normal ovary tissues, and may serve as the best candidate tumor markers among the seven genes studied. These results suggest that further exploration into other up-regulated genes may identify novel diagnostic, therapeutic, and/or prognostic biomarkers in ovarian carcinoma.

INTRODUCTION

Ovarian cancer is the leading cause of gynecological malignancy in North American women. Each year in the U.S., approximately 24,000 new cases of ovarian cancer are diagnosed and 14,000 deaths are attributed to this disease (1). Contributing to the poor prognosis is the lack of symptoms in the early stages of the disease. Over 75% of diagnoses are made in stage III and IV, after distant metastasis has occurred. The five-year survival rate for women diagnosed with late-stage disease is 25%, compared to over 90% for women diagnosed with stage I of the disease (1).

CA-125 is a glycoprotein antigen that is elevated in the serum of a majority of women with late-stage disease (2). However, it is elevated in only half of patients with stage I disease, and thus has limited use in the early detection of ovarian cancer (2). In addition, CA-125 can also be elevated in patients with other types of cancer as well as non-malignant conditions. Many groups have attempted to develop biomarkers for ovarian carcinoma to be used individually or in conjunction with CA-125 in order to improve the sensitivity and specificity of diagnostic tests. Such markers include: oncofetal antigens, mucin-associated antigens, enzymes, co-enzymes, enzyme inhibitors, receptors, cytokines, hormones, lipids, sialylated lipids, other proteins, and peptides (3). However, none of these markers, except possibly lysophosphatidic acid, has been shown to be consistently more sensitive than CA-125 (3).

In recent years, large-scale gene expression analyses have been performed to identify differentially expressed genes in ovarian carcinoma (4-22). A common goal of these studies was to identify potential tumor markers for the diagnosis of early-stage ovarian cancer, as well as to utilize these markers as targets for improved therapy and treatment of the disease during all stages. These earlier studies compared the gene expression profiles of tissues or cell lines derived from ovarian cancer samples, normal ovaries, other normal samples, and other types of

tumors (4-22). A major problem in identifying genes up-regulated in ovarian carcinoma is that normal ovary epithelial cells are very difficult to obtain in large enough numbers to perform gene microarray experiments. Although some groups have used the cells which are on the surface of normal ovaries, it is still controversial whether these cells truly serve as the normal counterpart for ovarian epithelial tumors (23). The cumulative results of these gene expression studies reveal over 150 potentially up-regulated genes that are associated with ovarian cancer. However, only a small portion of the genes reported as up-regulated in ovarian carcinoma were further validated by a second technique such as immunohistochemical analysis or RT-PCR. A number of the genes that show promise as biomarkers based on their secondary validation include: ApoJ, claudin-3, claudin-4, COL3A1, HE4, CD24, LU, progesterone binding protein, mucin 1, ryudocan, E16, osteoblast specific factor-2, prostatin, and secretory protein P1.B (4-12,24). Finally, proteomics and two-dimensional electrophoresis protein analysis are also being used in an attempt to identify protein patterns that are unique to ovarian cancer (25,26).

In this study we sought to improve upon earlier studies by comparing the gene expression of ovarian carcinoma tissue samples to more than 300 other tissue samples. By examining a large number of other types of tissues, it was possible to identify genes relatively specific to ovarian carcinoma, without relying entirely upon the gene expression profile of normal ovary epithelial cells. Seven known genes that were over-expressed in ovarian carcinoma tissues were selected for further analysis: bone morphogenetic protein-7 (BMP-7), the β8 integrin subunit, claudin-4, cellular retinoic acid binding protein-1 (CRABP1), collagen type IX α2 (COL IX α2), forkhead box J1 (FOX J1), and S100A1. In order to verify the corresponding protein expression of these seven genes, immunohistochemical staining was performed on normal ovaries, ovarian carcinoma tissues, and ovarian carcinoma tumors metastatic to the omentum. Statistical analyses

were conducted to determine how well the expression of each gene/protein distinguishes ovarian carcinoma from normal ovarian tissues.

MATERIALS AND METHODS

Tissue Samples. Tissues were obtained from the University of Minnesota Cancer Center's Tissue Procurement Facility upon approval by the University of Minnesota Institutional Review Board (Protocol #9608E11625). Tissue Procurement Facility employees obtained signed consent from each patient, allowing procurement of excess waste tissue and access to medical records (Protocol #9602M10848). Bulk tumor and normal tissues were identified, dissected, and snap frozen in liquid nitrogen within 15-30 min of resection from the patient. Tissue sections were made from each sample, stained with hematoxylin and eosin, and examined by a pathologist by light microscopy to confirm the pathologic state of each sample. Later, a second pathologist confirmed the diagnosis of each sample, documented the percent tumor (typically 100%), and documented any necrosis (typically none).

Tissue samples from 50 normal ovaries (women ranging in age from 32 to 79 with a mean age of 51.0 years), 20 serous papillary ovarian carcinoma tumors (age range of 29 to 79 with a mean age of 57.6 years), 17 metastases of serous papillary ovarian carcinoma to the omentum (age range of 29 to 79 years with a mean age of 59.7 years), and 20 other sets of tissue samples were provided to Gene Logic Inc. (Gaithersburg, MD) for microarray analysis as part of a collaboration with the University of Minnesota. The majority of ovarian tumor samples were classified as stage 3 tumors, while the tumor grade varied among the samples. None of the patients had been treated with chemotherapy prior to surgical resection of the tissue. The 20 other tissue sets which encompassed 304 different tissue samples were: 12 normal adipose tissue, 7 normal cervix, 24 normal colon, 11 normal kidney, 12 normal liver, 24 normal lung, 7 normal

omentum, 12 normal skeletal muscle, 9 normal skin, 8 normal small intestine, 55 normal thymus, 43 normal myometrium, 11 normal tonsil, 11 tonsils with lymphoid hyperplasia, 7 colon adenocarcinoma, 7 lung adenocarcinoma, 8 kidney cell carcinoma, 9 squamous carcinoma of the lung, 8 gall bladder with chronic inflammation, and 19 leiomyoma. Upon receipt of the tissue samples at Gene Logic Inc., a third pathologist examined the hematoxylin and eosin stained slides to verify the diagnosis.

A portion of the ovarian tissues were embedded in O.C.T. by the Tissue Procurement Facility and provided to us for the purpose of immunohistochemical analysis; specifically, 10 normal ovaries, 10 ovarian carcinoma tissues, and 10 ovarian tumors metastatic to the omentum. Fifteen additional tissues (5 each of normal ovaries, ovarian carcinoma tumors, and ovarian carcinoma tumors metastatic to the omentum) were also embedded in O.C.T. by the Tissue Procurement Facility and provided to us for the purpose of immunohistochemical analysis. These 15 additional tissues were not among the tissues analyzed by Gene Logic Inc.

Gene Expression Analysis. All tissue samples underwent stringent quality control measures in order to verify the integrity of the RNA prior to use in gene array experiments. Namely, RNA was isolated, the quantity was determined spectrophotometrically, and the quality was assessed on agarose gels. Tissue samples were not used if the RNA yield was low or RNA degradation was evident. Gene expression was determined by Gene Logic Inc. using Affymetrix HU_95 arrays containing approximately 12,000 known genes and 48,000 EST's as we have previously described (27,28). Briefly, RNA was obtained from 20 serous ovarian carcinoma tissues, 17 ovarian carcinoma tumors metastatic to the omentum, 50 normal ovaries, and 304 other tissue samples. Gene expression analysis was performed with the Gene Logic GeneExpress® Software System using the Gene Logic normalization algorithm. Sample sets were created in which each

sample set contained gene expression data from all of the tissues of a particular organ or tissue type. Gene signature analyses were then performed, and genes were defined as being "present" in a sample set if over 75% of the samples expressed the gene above background levels.

Fold change analyses were performed in which the ratio of the geometric means of the expression intensities for each gene fragment was computed, and the ratio was reported in terms of the fold change (up or down). Confidence intervals and p values on the fold change were also calculated using a two-sided Welch modified two-sample t-test. Differences were considered significant if the p value was ≤ 0.05. Gene fragments that were most discriminatory between sample sets were also identified by Contrast Analysis™ using the Gene Logic GeneExpress® Software System. A subset of gene fragments was then further analyzed by performing e-Northerns™ using the Gene Logic GeneExpress® Software System. The e-Northerns™ provide a visual display of the gene expression values for each of the 391 tissue samples belonging to a sample set.

Hierarchical cluster analyses were performed using Eisen Cluster Software (29). Data were normalized and the genes were clustered using the complete linkage clustering algorithm. Graphical displays of the gene expression data were obtained by using Tree View Software (available at http://rana.lbl.gov/EisenSoftware.htm).

Antibodies. Primary antibodies were used at the following concentrations: 1 μg/ml purified mouse IgG (mIgG) was used as a negative control (Sigma, St. Louis, MO); 1 μg/ml monoclonal antibody (mAb) P5D2 against the β1 integrin subunit was used as a positive control (provided by Dr. Leo Furcht, University of Minnesota); 5 μg/ml purified mouse mAb against the β8 integrin subunit (provided by Dr. Stephen Nishimura, University of California San Francisco, CA); 5 μg/ml purified rabbit polyclonal antibody (Aby) against bone morphogenetic protein-7

(Biotrend, Cologne, Germany); 1 μg/ml purified mouse mAb against claudin-4 (Zymed Laboratories, San Francisco, CA); a dilution of 1:250 of mouse mAb against cellular retinoic acid binding protein-1 (Affinity BioReagents, Golden, CO); a dilution of 1:1000 of rabbit polyclonal Aby against collagen type IX α2 (Calbiochem, San Diego, CA); a ready-to-use solution of unknown concentration of purified mouse mAb against hepatocyte nuclear factor-3/forkhead box J1 (Lab Vision, Fremont, CA); and a dilution of 1:50 of purified rabbit polyclonal Aby against S100A1 (Dako, Carpinteria, CA). Secondary antibodies used in the immunohistochemical staining procedure were purified, biotinylated anti-mouse or anti-rabbit IgG (Vector Laboratories, Burlingame, CA).

Immunohistochemical Staining. Immunohistochemistry was performed as we have previously described (30,31) with minor modifications. Glass slides were incubated in a 0.01% poly-L-lysine solution (Sigma, St. Louis, MO) for 5 min at room temperature to enhance stabilization of tissues onto the slides. O.C.T.-embedded tissues were cut on a cryostat into 5-μm sections, affixed onto poly-L-lysine-coated glass slides, and submerged in acetone for 10 min at room temperature to fix the tissues onto the slides. Slides were then rinsed in an excess of phosphate buffered saline, pH 7.4 (PBS) and blocked for 1 h in PBS containing 3% ovalbumin and 1% normal goat serum (Pierce, Rockford, IL). Slides were rinsed again in excess PBS and incubated with 250 μl of the primary Aby in PBS containing 3% ovalbumin and 1% normal goat serum for 1 h at room temperature.

The slides were again rinsed in excess PBS, followed by the addition of 250 μl of 0.03% H_2O_2 in PBS for 10 min at room temperature to quench endogenous peroxidase. Following another rinse in excess PBS, the slides were incubated for 1 h at room temperature in 250 μl of a 1:500 dilution of the anti-mouse or anti-rabbit biotinylated secondary Aby to visualize the

primary antibodies. After rinsing in excess PBS, the slides were incubated with 250 µl of Vectastain ABC solution (Vector Laboratories) for 1 h at room temperature. Following another rinse in excess PBS, the slides were incubated in 250 µl of DAB (3,3' –diaminobenzidine) solution (Vector Laboratories) for 5-8 min at room temperature. After rinsing with tap water, the slides were incubated in Hematoxylin Counterstain Solution (Vector Laboratories) for approximately 2-3 min. Upon drying at room temperature for 20 min, glass coverslips were applied to the slides using Cytoseal aqueous mounting media (Richard-Allan Scientific, Kalamazoo, MI).

Quantitation of Tissue Staining Intensity. Upon completion of immunohistochemical staining of the tissue samples, a pathologist examined the tissue slides in a blinded manner and documented the intensity and localization of staining. The classifications of intensity were based on a five-point scale: (+++) indicated maximum positive staining, (++) indicated moderate positive staining, (+) indicated weak but positive staining, (+/-) indicated faint or questionable staining, and (-) indicated a complete lack of staining. All staining was compared to the positive control, the β1 integrin subunit, which received a score of (+++).

Statistical Analysis. To determine which gene markers were best for distinguishing ovarian carcinoma tissue from normal ovarian tissue, the specificity, sensitivity, and Youden's misclassification index were calculated for each gene marker via pairwise tissue comparisons. Linear and logistic regression analyses were used to evaluate associations between patient demographic characteristics (age, alcohol use, smoking history, and tumor grade) and gene frequencies or staining classification.

RESULTS

Gene Expression Analysis. RNA was prepared and gene expression was performed on all samples using Affymetrix HU_95 arrays. Gene signature analyses were performed in order to identify genes that were expressed ("present") in over 75% of the samples in each sample set. Using a threshold of 75%, 11,679 gene fragments were present in the set of 50 normal ovary samples; 12,651 gene fragments were present in the sample set of 20 serous papillary ovarian carcinomas; and 15,294 gene fragments were present in the sample set of 17 serous papillary ovarian carcinomas metastatic to the omentum. The dependence of the number of gene fragments present in all of the samples of a sample set is shown as a function of the number of samples analyzed in Fig. 1. The number of gene fragments defined as present in all of the samples in each sample set did not vary greatly, provided that eight or more samples of the set were included in the analysis (Fig. 1).

Fold Differences. The relative intensity of gene expression in the ovarian carcinomas compared to the normal ovary samples was determined (Table 1). One hundred thirty-seven gene fragments were expressed at ≥10-fold different levels in the ovarian carcinoma sample set compared with the set of normal ovaries (Table 1). An additional 427 gene fragments were expressed at ≥5-fold to 10-fold different levels between the two sample sets, and a total of 4322 gene fragments were expressed at ≥2-fold different levels between the two sample sets (Table 1).

The relative intensity of gene expression in the ovarian carcinoma samples compared to the omental metastatic samples was also determined (Table 1). Only three gene fragments were expressed at ≥10-fold different levels in the ovarian carcinoma set compared with the set of omental metastases (Table 1). Also, a total of 624 gene fragments were expressed at ≥2-fold

different levels between the two sample sets (Table 1). These results suggest that the ovarian carcinoma samples are much more similar to each other than to the normal ovary samples.

Contrast Analysis™ and e-Northerns™. The 4322 gene fragments that were expressed greater than 2-fold more in ovarian carcinomas compared to normal ovaries were analyzed by Contrast Analysis™ using the Gene Logic GeneExpress® Software System to identify those gene fragments that were the most discriminatory between ovarian carcinoma and normal ovaries. The 400 gene fragments that were more highly expressed in the ovarian carcinoma samples and most discriminatory between the two sample sets were then further analyzed by performing e-Northerns™ using the Gene Logic GeneExpress® Software System. The e-Northern™ analysis provides a graphic representation of the level of gene expression values for each sample in the sets of normal ovaries, ovarian carcinomas, metastases of ovarian carcinoma to the omentum, and 304 other tissue samples from 20 different sites.

Forty known genes were preferentially up-regulated in ovarian carcinomas compared to all of the other tissue types examined (Table 2). The gene products of these 40 genes spanned a large spectrum of functional activity, including: 9 enzymes, 6 cell adhesion molecules/receptors, 6 transcription factors, 5 cell signaling proteins, 3 ligand-binding proteins, 3 cell cycle/cell proliferation proteins, 3 ion transport proteins, 2 cytokines, 2 tumor antigens, and 1 scavenger receptor (Table 2). As a testament to the validity of our approach and selection criteria, 14 of the 40 genes listed in Table 2 that we found to be specifically upregulated in ovarian carcinoma had previously been shown by others using gene array technology to be upregulated in ovarian carcinoma (4-10,13,22,32). To date, only 6 of these 14 genes have been validated by a second technique. An additional 7 of the 40 genes listed in Table 2 have been previously shown by other techniques to be up-regulated in ovarian carcinoma. Furthermore, 10 of the 40 genes have

not been previously implicated in ovarian carcinoma, but have been implicated in other types of cancer. Thus, 9 of the 40 genes listed in Table 2 have not previously been identified as being up-regulated in ovarian carcinoma or any other type of cancer.

Another set of 26 known genes was up-regulated in the ovarian carcinoma samples compared to normal ovaries (Table 3). However, by e-Northern™ analysis, we found that these 26 genes were also expressed by one or more other types of tissue. These 26 genes included a variety of proteins, including: 5 cell adhesion molecules/receptors, 4 transcription factors, 3 cell cycle/cell proliferation proteins, 3 accessory proteins, 3 ion transport proteins, 2 enzymes, 2 cell signaling proteins, 1 tumor antigen, 1 ligand-binding protein, 1 histone, and 1 unknown. Again, as a testament to the validity of our approach and selection criteria, 4 of the 26 genes listed in Table 3 that we found to be upregulated in ovarian carcinoma had previously been shown by others using gene array technology to be upregulated in ovarian carcinoma (6,12,13,19,22). To date, only 2 of these 4 genes have been validated by a second technique. An additional 3 of the 26 genes listed in Table 3 have been previously shown by other techniques to be up-regulated in ovarian carcinoma. Furthermore, 9 of the 26 genes have not been previously implicated in ovarian carcinoma, but have been implicated in other types of cancer. Thus, 10 of the 26 genes have not previously been identified as being up-regulated in ovarian carcinoma or any other type of cancer. Although these 26 genes may play important roles in the development of ovarian carcinoma, they are not as specific to ovarian carcinoma as the genes listed in Table 2.

Clustering. The Eisen clustering software, Cluster, was used as another means of displaying the gene expression data for the set of 40 known genes preferentially expressed by the ovarian carcinoma sample set (Table 2). By this technique, the ovarian carcinoma samples had intensely positive gene expression values (shown in red in Fig. 2). The gene expression values for the

normal ovary samples as well as all the other tissue sample sets (shown in green or black in Fig. 2) were much less intense and very distinct from the ovarian carcinoma samples. The differences in intensity of the squares in Fig. 2 are indicative of the biological heterogeneity that exists among ovarian carcinomas.

Criteria for Selecting a Subset of Genes for Protein Analysis. To determine whether the differentially expressed gene fragments that were unique to ovarian carcinoma corresponded to protein expression, a subset of the genes listed in Tables 2 and 3 were selected for analysis of their protein counterparts via immunohistochemistry. The following criteria were used to select the genes. First, the genes must be up-regulated at least 2-fold or greater in ovarian carcinoma tissues compared to normal ovary tissues. Second, the genes should either be completely absent or expressed at significantly lower levels in normal ovarian tissues. Third, increased expression of the genes should be solely characteristic of ovarian carcinoma, and minimal expression should be detected in any other tissues in the body. Fourth, the genes should be present in the vast majority of ovarian carcinoma samples. Finally, genes were selected if antibodies against their corresponding proteins were available. Based on these selection criteria, seven genes were chosen for further analysis: the β8 integrin subunit, bone morphogenetic protein-7 (BMP-7), cellular retinoic acid binding protein-1 (CRABP-1), claudin-4, collagen type IX α2 (COL IX α2), forkhead box J1 (FOX J1), and S100 calcium binding protein A1 (S100A1). Only one of these seven genes, claudin-4, has been previously characterized for both gene and protein expression in ovarian cancer (6,13).

Tissue Distribution of the Differentially Expressed Genes by e-Northerns™. We compared the expression of the seven selected genes in ovarian tissues and other tissues. e-Northerns™

were generated using the Gene Logic GeneExpress® Software System to display the gene expression values for each sample in the sets of normal ovaries, ovarian carcinomas, ovarian carcinomas metastatic to the omentum, and 304 other tissue samples from 20 different sites. The percentage of samples expressing detectable levels of each gene fragment is shown as a bar graph on the left side and the intensity of gene expression in each sample of the set is indicated on the right side of Figure 3.

A representative portion of an e-Northern™ of a β8 integrin subunit gene fragments is shown in Fig. 3. 60% of the ovarian carcinoma tissues and 82% of the omental metastatic tissues expressed detectable levels of this gene fragment, while none of the normal ovaries expressed it. The β8 integrin gene fragment was not significantly expressed in over 90% of the 304 other tissues examined. Notably, 3 of the 8 kidney cell carcinoma tissues and 3 of the 9 squamous cell lung carcinomas expressed low levels of the β8 integrin subunit; the intensity of expression was less than that in the ovarian carcinoma tissue samples.

A representative portion of an e-Northern™ of a BMP-7 gene fragment is shown in Fig. 3. 60% of the ovarian carcinoma tissues and 82% of the omental metastatic tissues expressed measurable levels of this gene fragment, while only 4% of the normal ovary tissues expressed this BMP-7 gene fragment. Several other tissues also expressed this gene fragment, but in general, fewer than 20% of the samples in each tissue type expressed detectable levels. An exception to this finding was that 88% of skin tissue samples expressed the BMP-7 gene fragment, although at much lower intensities than the ovarian carcinoma tissues. The intensity of gene expression in the majority of the other tissues was considerably lower compared to the ovarian carcinoma tissues. An exception to this finding involved high BMP-7 intensities in 2 of the 24 normal lungs and 3 of the 9 squamous cell lung carcinoma tissues.

An e-Northern™ of the claudin-4 gene fragment revealed that 100% of the ovarian carcinoma tissues and 94% of the omental metastatic tissues expressed detectable levels of this gene fragment, while only 6% of the normal ovary tissues expressed measurable levels (Fig. 3). The majority of other tissue types also expressed this gene fragment, and the intensity of expression varied across all tissue types.

An e-Northern™ of the COL IX α2 gene fragment shows that 30% of ovarian carcinoma tissues and 41% of omental metastatic tissues expressed measurable levels of the gene fragment, while none of the normal ovaries expressed detectable levels of the COL IX α2 gene fragment (Fig. 3). This COL IX α2 gene fragment was minimally expressed in a few of the other tissues, including 1 of the 7 colon adenocarcinomas, 3 of the 24 normal lungs, 1 of the 12 normal skeletal muscles, and 1 of the 43 normal myometrium. Notably, over 95% of the other tissues did not express detectable levels of the COL IX α2 gene fragment.

A representative e-Northern™ of a CRABP-1 gene fragment indicates that 50% of the ovarian carcinoma tissues and 41% of the omental metastatic tissues expressed measurable levels of this gene fragment, while only 2% of the normal ovary tissues expressed the CRABP-1 gene fragment (Fig. 3). 55% of the skin tissues expressed the CRABP-1 gene fragment. Otherwise, only five other tissue samples minimally expressed this gene fragment, including one chronically inflamed gall bladder tissue, one normal kidney, one normal tonsil, and two leiomyoma tissues. Therefore, compared to the ovarian carcinoma tissues, >90% of the other tissues did not express this CRABP-1 gene fragment.

An e-Northern™ of the FOX J1 gene fragment shows that 85% of ovarian tissues and 52% of omental metastatic tissues expressed detectable levels of this gene fragment, while only 4% of the normal ovary tissues expressed measurable levels of the FOX J1 gene fragment (Fig. 3). Some of the other tissue types also expressed FOX J1; notably normal lung, lung

adenocarcinoma, and normal cervix. However, fewer of the samples within these tissue sets expressed the gene, and the gene was expressed at a lower intensity compared to the ovarian carcinoma tissues. Thus, 90% of the other tissue samples did not express detectable levels of the FOX J1 gene fragment.

An e-Northern™ of the S100A1 gene fragment revealed that 95% of the ovarian carcinoma tissues and 100% of the omental metastatic tissues expressed this gene fragment, while only one of the 50 normal ovary tissues expressed the S100A1 gene fragment (Fig. 3). The S100A1 gene fragment was also expressed in 71% of adipose tissues, 80% of kidney carcinoma tissues, 68% of normal kidney tissues, 93% of skeletal muscle tissues, and 44% of skin tissues. All of these tissues, except the skeletal muscle tissues, expressed the gene fragment at much lower intensities compared to the ovarian carcinoma tissues, while over 80% of the other tissue samples did not express the S100A1 gene fragment at all.

Immunohistochemical Staining of the Differentially Expressed Gene Products. The protein expression of the 7 differentially expressed genes was analyzed by immunohistochemistry in 45 ovarian tissues. Gene expression data was available from Gene Logic Inc. for 30 of the 45 ovarian tissues screened, including: 10 normal ovaries, 10 ovarian carcinoma tissues, and 10 ovarian carcinoma tumors metastatic to the omentum. The remaining 15 tissues that were analyzed by immunohistochemistry were: 5 normal ovaries, 5 ovarian carcinoma tumors, and 5 ovarian carcinoma tumors metastatic to the omentum.

Monoclonal and polyclonal antibodies against the seven proteins were used, as well as the normal mouse IgG (negative control) and a mAb against the β1 integrin subunit (positive control). The β1 integrin subunit was used as a positive control because it is a cell adhesion molecule known to be ubiquitously expressed on the surface of most cells except hematopoietic

cells. The β1 integrin subunit was expressed in normal ovary (Fig. 4A), ovarian carcinoma (Fig. 4B), and ovarian carcinoma metastatic to the omentum (Fig. 4C). All three tissue types exhibited a strong, membranous staining pattern for β1 integrin. As expected, normal mouse IgG did not stain normal ovary (Fig. 4D), ovarian carcinoma (Fig. 4E), or ovarian carcinoma metastatic to the omentum (Fig. 4F).

The β8 integrin subunit has been previously described as a cell surface molecule (33). In this study, the β8 integrin subunit was observed as a strong membranous staining pattern in the ovarian tumors (Figs. 4H and 4I), but was not detected in normal ovaries (Fig. 4G). The vast majority of ovarian tumors examined exhibited a membranous staining pattern for the β8 integrin subunit, while the majority of normal ovaries did not express the β8 integrin protein.

The second protein we studied was BMP-7, a cytokine that was expected to be localized in the cytoplasm and in the ECM upon secretion (34). Interestingly, BMP-7 staining was variable across all ovarian tumors studied. The protein was detected in the tumor cells in some ovarian carcinoma tissues and in the surrounding stroma in other ovarian carcinoma tissues. Fig. 4 shows BMP-7 expression in the stroma of one ovarian tumor (Fig. 4K) and BMP-7 expression in patches of tumor cells in one omental metastatic tumor (Fig. 4L). In the majority of cases, normal ovaries did not express BMP-7 (Fig. 4J).

The third protein of interest, claudin-4, is a tight junction protein located on the cell surface (35). Claudin-4 was detected on the cell surface in all ovarian tumor tissues examined. Fig. 4 shows a strong membranous staining pattern for claudin-4 in both the ovarian tumor (Fig. 4N) and the metastatic omental tumor (Fig. 4O). Claudin-4 was not detected in normal ovaries (Fig. 4M).

The fourth protein whose localization we examined, COL IX α2, is an adhesion molecule found in the ECM (36). The COL IX α2 protein was observed as an intercellular epitope in most

ovarian tumors (Figs. 5B and 5C), but was also detected in the cytoplasm in some cases. Also, COL IX α2 was frequently expressed in the stromal tissue surrounding the ovarian tumor nests, as well as in the stroma of normal ovaries (Fig. 5A). This high background staining pattern may be attributable to non-specific staining of the Aby against COL IX α2 used in the immunohistochemical analyses.

The fifth protein we studied was CRABP-1, a transport protein found in the cytoplasm (37). CRABP-1 expression was variable across all tissues examined, and it was localized to the cell membrane in some tissues and in the cytoplasm in other tissues. Representative examples show a membranous staining pattern for CRABP-1 in the ovarian tumor (Fig. 5E), a cytoplasmic staining pattern for CRABP-1 in the omental metastatic tumor (Fig. 5F), and no detection of CRABP-1 in the normal ovary (Fig. 5D).

The sixth protein we selected was FOX J1, a transcription factor with expected localization to the nucleus and possibly the cytoplasm (38). Interestingly, only a few of the ovarian tumor samples demonstrated a nuclear FOX J1 staining pattern (Figs. 5H and 5I). Instead, most tumor samples examined exhibited cytoplasmic and membranous staining patterns for FOX J1. In addition, over half of the normal ovary samples exhibited some degree of FOX J1 expression, as shown in Fig. 5G where a normal ovary exhibits slight nuclear staining of FOX J1 in the surface epithelium. This high background staining observed for FOX J1 may be in part attributable to non-specific staining of the anti-FOX J1 antibody used in the immunohistochemical analyses.

Our final protein of interest was S100A1, a protein involved in the cell cycle and localized to the cytoplasm (39). Most of the ovarian tumor tissues examined exhibited either a cytoplasmic or membranous S100A1 staining pattern. Fig. 5K shows an ovarian tumor with both cytoplasmic and membranous staining for S100A1, while Fig. 5L shows an omental metastatic

tumor with cytoplasmic staining for S100A1. The majority of normal ovaries examined did not express the S100A1 protein. An example of a normal ovary with S100A1 expression in the cytoplasm of the surface epithelial cells is shown in Fig. 5J.

In summary, the majority of ovarian tumor tissues exhibited positive staining for the β8 integrin subunit, claudin-4, COL IX α2, FOX J1, and S100A1, and negative staining for BMP-7 and CRABP-1. The majority of the normal ovary tissues exhibited negative staining for the β8 integrin subunit, BMP-7, claudin-4, CRABP-1, and S100A1, and positive staining for COL IX α2 and FOX J1.

Statistical analysis. Linear and logistic regression analyses were performed in order to assess whether associations exist between gene and protein expression of the seven genes and various patient characteristics such as age, alcohol use, smoking status, and tumor grade. The results of these analyses indicated no evidence of such associations.

In order to determine which of the seven gene markers were the strongest candidates for distinguishing normal ovarian tissue from ovarian carcinoma tissue, the specificity, sensitivity, and Youden's misclassification index were calculated via pairwise tissue comparisons. For the purpose of these statistical measures, tissue staining intensities were classified as either positive (+, ++, +++) or negative (-, +/-). Youden's misclassification index (J), which is based on the specificity and sensitivity, indicates the overall probability that the protein classifications correctly distinguish each tissue being compared. Genes with a J value of 0.5 or greater were considered to be predictive of disease state.

The results of the comparison between normal ovary and ovarian carcinoma tissues are shown in Table 4. The β8 integrin subunit, claudin-4, and S100A1 all had a J value greater than 0.5 and are thus considered to be the best markers for distinguishing ovarian tumor tissue from

normal ovary tissue. We then compared the immunohistochemistry results obtained for normal ovary tissues and ovarian tumors metastatic to the omentum. Again, the β8 integrin subunit, claudin-4, and S100A1 all had a J value greater than 0.5 in this comparison and were thus considered to be the best markers for distinguishing metastatic ovarian tumor tissue from normal ovary tissue (Table 4). Finally, a comparison was made between ovarian tumor tissues and metastatic ovarian tumor tissues; none of the seven genes were able to distinguish between them (Table 4). This result is not surprising since both types of ovarian carcinoma tissues exhibited similar gene expression profiles, as evidenced by the fold-change analysis (Table 1).

DISCUSSION

In this study, 66 genes were identified by microarray technology to be differentially expressed by ovarian carcinoma tissue samples compared with normal ovarian tissue samples. Nineteen of the 66 genes were reported here for the first time to be upregulated in cancerous tissues. Twenty-eight of the 66 genes had been previously reported to be upregulated in ovarian carcinoma by gene array technology or other techniques, while an additional 19 of the 66 genes had previously been reported to be upregulated in other types of cancer. The 66 genes identified in this study included a variety of proteins, including 11 cell adhesion molecules/receptors, 11 enzymes, 10 transcription factors, 7 cell signaling proteins, 6 cell cycle/cell proliferation proteins, 6 ion transport proteins, 4 ligand-binding proteins, 3 accessory proteins, 3 tumor antigens, 2 cytokines, 1 scavenger receptor, 1 histone, and 1 unknown. Interestingly, the cellular localization of the gene products of these 66 genes was rather equally divided between the membrane, nucleus, and secretory (~30% in each group) while fewer of the gene products were localized to the cytoplasm (~15%).

The design of the current study has several advantages in identifying potential ovarian carcinoma tumor markers compared to many of the earlier ovarian cancer gene expression studies. First, a relatively large number of ovarian tissues were utilized for the microarray analyses (50 normal ovaries, 20 serous papillary ovarian tumors, and 17 ovarian tumors metastatic to the omentum). By analyzing a large number of tissues, a more accurate picture of ovarian carcinoma gene profiles can be obtained. Earlier studies utilized fewer ovarian carcinoma tissues or cell lines in their large-scale analyses; the resulting gene expression profiles may have been skewed due to the expression of genes that were altered during the perpetuation of the cell lines (10,20,21).

A second advantage of this study was that protein expression was verified by using a relatively large number of ovarian tissues samples (15 normal ovaries, 15 ovarian carcinoma tumors, and 15 ovarian carcinomas metastatic to the omentum). In one earlier study, validation by immunohistochemistry was performed upon 13 ovarian tumors, but no normal ovary tissues were similarly screened (6).

A third advantage of this study is that 304 tissue samples from 20 other sites were analyzed, including: lung adenocarcinoma, kidney carcinoma, squamous cell carcinoma of the lung, and colon adenocarcinoma. By comparison, in one earlier study, only 7 tissue samples from other sites were included in the cDNA hybridization analysis (9). However, the majority of previously published ovarian carcinoma gene expression studies did not analyze any other type of tissue except for ovarian tissues and/or cell lines (14-18). Others have noted that a key step in determining the diagnostic potential of gene expression profiling is to compare the gene expression of a variety of tumors derived from many different organs (40).

One potential shortcoming of gene expression studies on ovarian carcinoma, the present study included, is the limited quantity of normal ovarian surface epithelium available for

microarray and immunohistochemical analysis. Although controversial, it is widely accepted that epithelial ovarian carcinomas arise from the thin layer of epithelial cells surrounding the ovary (23). Not surprisingly, it is difficult to obtain sufficient quantities of surface epithelial cells for further analysis. Therefore, the surface epithelial cells represented a very low percentage of the total normal ovary cells that are included in the microarray analysis. Some groups have circumvented this problem by enriching for the surface ovarian epithelial cells by creating a short-term ovarian surface epithelium cell culture (6,10,11). However, the development and maintenance of a cell line may alter the gene expression pattern. For this reason, in this study we used over 300 other tissues in order to determine the specificity of the up-regulated genes to ovarian carcinoma, and we verified our findings by immunohistochemistry. Therefore, it was possible for us to assess the protein expression in the normal ovarian surface epithelial cells.

Seven genes selected for further analysis were: the β8 integrin subunit, BMP-7, claudin-4, COL IX α2, CRABP-1, FOX J1, and S100A1. Immunohistochemical staining of 45 ovarian tissues for the presence and localization of the proteins corresponding to each of the genes, followed by statistical analysis, revealed that the β8 integrin subunit, claudin-4, and S100A1 are the most promising candidate ovarian carcinoma tumor markers.

The β8 integrin subunit is a member of the family of integrins that mediates cell-cell and cell-ECM interactions (41). The β8 integrin subunit protein has been reported in mice and rat neural synapses, suggesting its potential role in synaptic function (41). A recent study by Mu and colleagues revealed that the β8 integrin subunit binds the cytokine TGF-β, leading to changes in cell growth and matrix production, and thus regulating epithelial cell homeostasis (42). Another study revealed that the αVβ8 integrin may complex with the ECM components laminin and fibronectin, and that these interactions may play a role in human glial cell invasion

(43). Our study is the first to report and validate the expression of the β8 integrin subunit mRNA and protein in ovarian carcinoma. Another study reported up-regulation of β8 integrin subunit mRNA in highly differentiated serous ovarian adenocarcinomas compared to benign serous adenocarcinomas, but this was not verified by a second technique (7). It is possible that over-expression of the β8 integrin subunit in ovarian carcinoma may enhance tumor cell adhesion and stabilize contacts between the epithelial tumor cells, thus enabling further progression of the disease.

Claudin-4, a member of the claudin family of tight junction proteins (35), also showed promise as a candidate biomarker of ovarian carcinoma. Over-expression of claudin-4 mRNA has been demonstrated in several types of cancer including pancreatic (44) and prostate cancer (45). In addition, claudin-4 has recently been reported to be over-expressed in ovarian carcinoma by two other groups (6,13). Based on its role as a tight junction protein, it is possible that over-expression of claudin-4 in ovarian tumor cells may enhance and stabilize tumor cell connections, and could contribute to increased growth at secondary sites.

S100A1 is one of 19 members that make up the S100 protein family (46). S100 proteins are localized in the cytoplasm of a variety of cells, and are involved in cell cycle progression and differentiation (46). Several studies have shown that the S100A1 protein is highly expressed in the heart, and that the protein plays a key role in a variety of myocardial functions (47,48). S100A1 proteins are also involved in the assembly and disassembly of microtubules and intermediate filaments (49). Several members of the S100 protein family have been shown to promote invasion and metastasis of many human cancers (46). S100A1, S100A2, and S100B proteins have been detected in epithelial skin tumors (50). Expression of S100A4 has been demonstrated in many different human cancers, including pancreatic cancer, gastric adenocarcinoma, breast carcinomas, and colorectal cancer (46,51). A yeast two-hybrid system

has demonstrated a strong interaction between S100A4 and S100A1, suggesting that S100A1 may mediate the metastatic capabilities of S100A4 (51). In addition, the S100A2 gene was reported and confirmed to be up-regulated in ovarian carcinoma tissues (5). Our study confirms that of Su et al (22) to report S100A1 mRNA is over-expressed in ovarian carcinoma tissues. However, our study is the first to show that S100A1 protein expression is upregulated in ovarian carcinoma tissues compared to normal ovaries. Our statistical analyses revealed that S100A1 protein expression could be used to distinguish ovarian carcinoma tissues from normal ovary tissues.

A fourth protein that we studied, BMP-7, is a member of the TGF-β cytokine family (34). Bone morphogenetic proteins are involved in tissue differentiation, development, and remodeling (53). BMP-7 is expressed in articular cartilage (54), where it induces cartilage and bone formation (55). BMP-7 is also expressed in the kidney and may induce kidney epithelial cell differentiation (56,57). Several bone morphogenetic proteins have been implicated in various forms of cancer. BMP-4 mRNA was over-expressed in poorly differentiated gastric cancer cell lines (58), and BMP-4, -5, and -6 mRNA were over-expressed in colon cancer cells (59,60). BMP-7 mRNA has been shown to be up-regulated in osteosarcoma and in some breast and prostate tumors (61-63). However, the exact role of bone morphogenetic proteins in various cancers has yet to be elucidated. This study is the first to report that BMP-7 mRNA is up-regulated in ovarian carcinoma tissue samples, but we were unable to verify the presence of the corresponding protein by immunohistochemistry. Among the few ovarian carcinoma tissues in which the BMP-7 protein was detected, it was occasionally found in the stromal cells surrounding the tumor nests. A possible explanation for this finding is that ovarian carcinoma tumor cells may induce the expression of various factors in the surrounding stromal cells, thus forcing the stromal cells to participate in tumor invasion and metastasis (64).

Another protein that we observed to be up-regulated in ovarian carcinoma was COL IX α2, one of three different alpha chains that combine to form the heterotrimer type IX collagen (36). Type IX collagen is an ECM protein and is a major component of hyaline cartilage. Type IX collagen forms cross-links between type II collagen and other type IX collagen molecules (65). Several studies have identified COL IX α2 mutations that give rise to multiple epiphyseal dysplasia (66). Collagens type I, III, and IV have all been implicated in ovarian cancer (67-69). Interestingly, one study postulated that type IV collagen and BMP-2 may play a role in ovarian cancer (70). The accelerated synthesis and breakdown of type I and type III collagen was shown to be characteristic of ovarian cancer (68). Moser et al. reported that ovarian epithelial carcinoma cells exhibit preferential adhesion to type I collagen, and that this interaction may stimulate the production of other factors that promote the dissemination of ovarian cancer (71). Perhaps in similar fashion, COL IX α2 may interact with ovarian carcinoma cells in such a way to promote ovarian tumorigenesis. Alternatively, changes in expression of the COL IX α2 protein may lead to the disruption of the ECM, enabling enhanced tumor cell migration and invasion. Although this study is the first to report the up-regulation of COL IX α2 mRNA in ovarian carcinoma compared to normal ovaries, attempts to confirm this specificity by immunohistochemistry were not possible due to a high degree of non-specific staining. Due to a lack of additional commercially available antibodies against COL IX α2 or COL IX, it was not possible to verify our gene expression data. Clearly, additional studies are necessary in assessing the role of COL IX α2 in ovarian carcinoma.

CRABP-1, a carrier protein known to mediate the transport and biological activity of retinoic acid (37), also showed some promise as an ovarian carcinoma marker. Recent studies have revealed CRABP-1 mRNA expression in mouse cerebellum and rat lung (72,73), and CRAPB-1 protein expression in chick retina (74). However, few studies have examined

CRABP-1 expression in normal human tissues. The expression of cellular retinoic acid binding proteins has been evaluated in several human cancers. One study reported that changes in CRABP-2 gene expression affected retinoic acid-mediated target gene response, resulting in phenotypic alterations in various squamous carcinoma cells (75). Other studies have detected CRABP-1 protein in human cervical carcinoma tissues (76) and large bowel cancer (77). Ono and colleagues reported the presence of the CRABP-1 gene in ovarian carcinoma tissues, but this finding was not confirmed by a second method (12). In our study, we only detected the CRABP-1 protein in a few of the ovarian carcinoma tissues by immunohistochemistry. It is possible that the CRABP-1 mRNA may not be translated into a protein product. Alternatively, if the cells have a high protein turnover rate, then the protein product may not be detected despite its continual production. Whether CRABP-1 plays a role in ovarian carcinoma remains to be determined.

We also studied FOX J1, a transcription factor that belongs to the winged helix/forkhead gene family (38). Members of this family are thought to be involved in cell-specific differentiation (38). FOX J1 is present in ciliated cells of the human lung, oviduct, testis, and brain cortex, suggesting a possible role for FOX J1 in regulating axonemal structural proteins (38). FOX J1 may also play a role in the determination of left-right asymmetry (78), ciliated cell development (78), liver metabolism in humans (79), lung morphogenesis (80), and lung epithelial cell differentiation in mice (80). Other studies have demonstrated the expression of FOX J1 in lung epithelial cells (80) and hepatocellular carcinoma (79,81). This study is the first to report the over-expression of FOX J1 mRNA in ovarian carcinoma compared with normal ovaries. Interestingly, FOX J1 was the only gene of the seven we studied that was found to be significantly up-regulated (over three-fold) in ovarian carcinoma compared to ovarian carcinoma metastatic to the omentum. Contrary to the RNA expression data, immunohistochemical

analysis revealed that the FOX J1 protein was found in the majority of the ovarian tissues examined, including a majority of the normal ovaries, suggesting non-specific staining. Due to the lack of an additional commercially available Aby against FOX J1, we were not able to further test this finding.

The results of this study emphasize the usefulness of microarray analysis in elucidating the genetic profiles of ovarian carcinoma. By comparing the gene expression profiles of ovarian carcinoma tissues to those of a variety of other normal and malignant tissues, genes that are unique and specific to ovarian carcinoma may be identified. These genes may be further analyzed in subsequent studies in an attempt to obtain new and biologically relevant information about the molecular mechanisms involved in ovarian carcinogenesis. In addition, some of the proteins whose presence was confirmed in ovarian carcinoma samples may be studied as potential ovarian carcinoma tumor markers, and may contribute to the diagnosis and/or treatment of ovarian carcinoma. Further studies are needed to assess the ability of the β8 integrin subunit, claudin-4, and S100A1 as tumor markers to be utilized alone, or in combination with other markers such as CA-125, in the detection and treatment of patients with ovarian carcinoma.

ACKNOWLEDGEMENTS

We thank Diane Rauch and Sarah Bowell of the University of Minnesota Cancer Center's Tissue Procurement Facility for assistance in collecting and processing the human tissue samples. We thank the staff of Gene Logic Inc., Gaithersburg, MD, for performing the gene expression experiments with the human tissue samples. We thank Dr. Stephen Nishimura, University of California San Francisco, CA for generously providing the mAb against the β8 integrin subunit. We thank Dr. Leo Furcht for providing the mAb P5D2 against the β1 integrin subunit.

REFERENCES

1. Ahmedin J, Murray T, Samuels A, Ghafoor A, Ward E, Thun MJ: Cancer Statistics, 2003. CA Cancer J Clin 2003, 53:5-26
2. Verheijen RHM, von Mensdorff-Pouilly S, van Kamp GJ, Kenemans P: CA 125: fundamental and clinical aspects. Cancer Bio 1999, 9:117-124
3. Bast RC Jr., Urban N, Shridhar V, Smith D, Zhang Z, Skates S, Lu K, Liu J, Fishman D, Mills G: Early detection of ovarian cancer: promise and reality. In Ovarian Cancer volume (ed. MS Stack and DA Fishman) of Cancer Treatment and Research (ST Rosen, series editor) Boston, Kluwer Academic Publishers, 2002, pp. 61-97
4. Welsh JB, Zarrinkar PP, Sapinoso LM, Kern SG, Behling CA, Monk BJ, Lockhart DJ, Burger RA, Hampton GM: Analysis of gene expression profiles in normal and neoplastic ovarian tissue samples identifies candidate molecular markers of epithelial ovarian cancer. Proc Nat Acad Sci 2001, 98(3):1176-1181
5. Hough CD, Cho KR, Zonderman AB, Schwartz DR, Morin PJ: Coordinately up-regulated genes in ovarian cancer. Cancer Res 2001, 61:3869-3876
6. Hough CD, Sherman-Baust CA, Pizer ES, Montz FJ, Im DD, Rosenshein NB, Cho KR, Riggins GJ, Morin PJ: Large-scale serial analysis of gene expression reveals genes differentially expressed in ovarian cancer. Cancer Res 2000, 60:6281-6287
7. Tapper J, Kettunen E, El-Rifai W, Seppala M, Andersson L, Knuutila S: Changes in gene expression during progression of ovarian carcinoma. Cancer Genetics and Cytogenetics, 2001, 128:1-6
8. Wang K, Gan L, Jeffery E, Gayle M, Gown AM, Skelly M, Nelson PS, Ng WV, Schummer M, Hood L, Mulligan J: Monitoring gene expression profile changes in ovarian carcinomas using cDNA microarray. Gene 1999, 229: 101-108

9. Schummer M, Ng WV, Bumgarner RE, Nelson PS, Schummer B, Bednarski DW, Hassell L, Baldwin RL, Karlan BY, Hood L: Comparative hybridization of an array of 21,500 ovarian cDNA's for the discovery of genes overexpressed in ovarian carcinomas. Gene 1999, 238:375-385

10. Ismail RS, Baldwin RL, Fang J, Browning D, Karlan BY, Gasson JC, Chang DD: Differential gene expression between normal and tumor-derived ovarian epithelial cells. Cancer Res 2000, 60:6744-6749

11. Mok SC, Chao J, Skates S, Wong K, Yiu GK, Muto MG, Berkowitz RS, Cramer DW: Prostatin, a potential serum marker for ovarian cancer: Identification through microarray technology. J Nat Cancer Inst 2001, 93(19):1458-1464

12. Ono K, Tanaka T, Tsunoda T, Kitahara O, Kihara C, Okamoto A, Ochiai K, Takagi T, Nakamura Y: Identification by cDNA microarray of genes involved in ovarian carcinogenesis. Cancer Res 2000, 60: 5007-5011

13. Shridhar V, Lee J, Pandita A, Iturria S, Avula R, Staub J, Morrissey M, Calhoun E, Sen A, Kalli K, Keeney G, Roche P, Cliby W, Lu K, Schmandt R, Mills GB, Bast RC Jr., James D, Couch FJ, Hartmann LC, Lillie J, Smith DL: Genetic analysis of early- versus late-stage ovarian tumors. Cancer Res 2001, 61:5895-5904

14. Bayani J, Brenton JD, Macgregor PF, Beheshti B, Albert M, Nallainathan D, Karaskova J, Rosen B, Murphy J, Laframboise S, Zanke B, Squire JA: Parallel analysis of sporadic primary ovarian carcinomas by spectral karyotyping, comparative genomic hybridization, and expression microarrays. Cancer Res 2002, 62:3466-3476

15. Martoglio A, Tom BDM, Starkey M, Corps AN, Charnock-Jones DS, Smith SK: Changes in tumorigenesis and angiogenesis-related gene transcript abundance profiles in ovarian cancer detected by tailored high density cDNA arrays. Molecul Med 2000, 6(9):750-765

16. Suzuki S, Moore DH, Ginzinger DG, Godfrey TE, Barclay J, Powell B, Pinkel D, Zaloudek C, Lu K, Mills G, Berchuck A, Gray JW: An approach to analysis of large-scale correlations between genome changes and clinical endpoints in ovarian cancer. Cancer Res 2000, 60:5382-5385

17. Van Niekerk CC, Boerman OC, Ramaekers FCS, Poels LG: Marker profile of different phases in the transition of normal human ovarian epithelium to ovarian carcinomas. Am J Pathol 1991, 138(2):455-463

18. Van Niekerk CC, Ramaekers FCS, Hanselaar GJM, Aldeweireldt J, Poels LG: Changes in expression of differentiation markers between normal ovarian cells and derived tumors. Am J Pathol 1993, 142(1): 157-177

19. Shvartsman HS, Lu KH, Lee J, Lillie J, Deavers MT, Clifford SL, Wolf J, Mills GB, Bast RC, Gershenson DM, Schmandt RE: Over-expression of NES-1 in epithelial ovarian carcinoma. Society of Gynecology 32nd Annual Meeting, Abstract p. 103.

20. Tonin PN, Hudsno TJ, Rodier F, Bossolasco M, Lee PD, Novak J, Mandreson EN, Provencher D, Mes-Masson A: Microarray analysis of gene expression mirrors the biology of ovarian cancer model. Oncogene 2001, 20:6617-6626

21. Wong KK, Cheng RS, Mok SC: Identification of differentially expressed genes from ovarian cancer cells by MICROMAX cDNA microarray system. Biotechniques 2001, 30:670-675

22. Su AI, Welsh JB, Sapinoso LM, Kern SG, Dimitrov P, Lapp H, Schultz PG, Powell SM, Moskaluk CA, Frierson HF Jr., Hampton GM: Molecular classification of human carcinomas by use of gene expression signatures. Cancer Res 2001, 61(20):7388-7393

23. Dubeau L: The cell of origin of ovarian epithelial tumors and the ovarian surface epithelium dogma: Does the emperor have no clothes? Gynecol Oncol 1999, 72:437-442

24. Feng H, Ghazizadeh M, Konishi H, Araki T: Expression of MUC1 and MUC2 mucin gene products in human ovarian carcinomas. Jpn J Clin Oncol 2002, 32(12): 525-529

25. Alaiya AA, Franzen B, Hagman A, Silfversward C, Moberger B, Linder S, Auer G: Classification of human ovarian tumors using multivariate data analysis of polypeptide expression patterns. Int J Cancer 2000, 86:731-736

26. Petricoin EF, Ardekani AM, Hitt BA, Levine PJ, Fusaro VA, Steinberg SM, Mills GB, Simone C, Fishman DA, Kohn EC, Liotta LA: Use of proteomic patterns in serum to identify ovarian cancer. The Lancet 2002, 359:572-577

27. Skubitz KM, Skubitz APN: Differential gene expression in renal-cell cancer. J Lab Clin Med 2002, 140: 52-64

28. Skubitz KM, Skubitz APN: Differential gene expression in uterine leiomyoma. J Lab Clin Med 2003, 141:297-308

29. Eisen MB, Spellman PT, Brown PO, Botstein D: Cluster analysis and display of genome-wide expression patterns. Proc Nat Acad Sci 1998, 95:14863-14868

30. Skubitz APN, Bast RC, Jr., Wayner EA, Letourneau PC, Wilke MS: Expression of α6 and β4 integrins in serous ovarian carcinoma correlates with expression of the basement membrane protein laminin. Amer J Pathol 1996, 148(5):1445-1461

31. Casey RC, Burleson KM, Skubitz KM, Pambuccian SE, Oegema TR Jr., Ruff LE, Skubitz APN: β1-integrins regulate the formation and adhesion of ovarian carcinoma multicellular spheroids. Amer J Pathol 2001, 159:2071-2080

32. Galmozzi E, Tomassetti A, Sforzini S, Mangiarotti F, Mazzi M, Nachmanoff K, Elwood PC, Canevari S: Exon 3 of the α folate receptor gene contains a 5' splice site which confers enhanced ovarian carcinoma specific expression. FEBS Letters 2001, 502:31-34

33. Moyle M, Napier MA, McLean JW: Cloning and expression of a divergent integrin subunit β8. J Biol Chem 1991, 266(29):19650-19658

34. Ozkaynak E, Rueger DC, Drier EA, Corbett C, Ridge RJ, Sampath TK, Oppermann H: OP-1 cDNA encodes an osteogenic protein in the TGF-beta family. EMBO J 1990, 9:2085-2093

35. Morita K, Furuse M, Fujimoto K, Tsukita S: Claudin multigene family encoding four-transmembrane domain protein components of tight junction strands. Proc Nat Acad Sci 1999, 96:511-516

36. Perala M, Hanninen M, Hastbacka J, Elima K, Vuorio E: Molecular cloning of the human alpha-2 (IX) collagen cDNA and assignment of the human COL9A2 gene to chromosome 1. FEBS Lett 1993, 319:177-180

37. Cornic M, Guidez F, Delva L, Agadir A, Degos L, Chomienne C: Mechanism of action of retinoids in a new therapeutic approach to acute promyelocytic leukemia. Bulletin du Cancer 1992, 79(7):697-704

38. Murphy DB, Seeman S, Wiese S, Kirschner R, Grzeschik KH, Thies U: The human hepatocyte nuclear factor 3/fork head gene FKHL13: genomic structure and pattern of expression. Genomics 1997, 40:462-469

39. Schafer BW, Wicki R, Engelkamp D, Mattei M-G, Heizmann CW: Isolation of a YAC clone covering a cluster of nine S100 genes on human chromosome 1q21: rationale for a new nomenclature of the S100 calcium-binding protein family. Genomics 1995, 25:638-643

40. Giordano TJ, Shedden KA, Schwartz DR, Kuick R, Taylor JMG, Lee N, Misek DE, Greenson JK, Kardia SLR, Beer DG, Rennert G, Cho KR, Gruber SB, Fearon ER, Hanash S: Organ-specific molecular classification of primary lung, colon, and ovarian adenocarcinomas using gene expression profiles. Am J Pathol 2001, 159(4):1231-1238

41. Nishimura SL, Boylen KP, Einheber S, Milner TA, Ramos DM, Pytela R: Synaptic and glial localization of the integrin αvβ8 in mouse and rat brain. Brain Res 1998, 791:271-282

42. Mu D, Cambier S, Fjellbirkeland L, Baron JL, Munger JS, Kawakatsu H, Sheppard D, Broaddus VC, Nishimura SL: The integrin αvβ8 mediates epithelial homeostasis through MT1-MMP-dependent activation of TGF-β1. J Cell Biol 2002, 157(3):493-507

43. Belot N, Rorive S, Doyen I, LeFranc F, Bruyneel E, Dedecker R, Micik S, Brotchi J, Decaestecker C, Salmon I, Kiss R, Camby I: Molecular characterization of cell substratum attachments in human glial tumors relates to prognostic features. GLIA 2001, 36:375-390

44. Terris B, Blaveri E, Crnogorac-Jurcevic T, Jones M, Missiaglia E, Ruszniewski P, Sauvanet A, Lemoine NR: Characterization of gene expression profiles in intraductal papillary-mucinous tumors of the pancreas. Am J Pathol 2002, 160(5):1745-1754

45. Long H, Crean CD, Lee WH, Cummings OW, Gabig TG: Expression of Clostridium perfringens enterotoxin receptors claudin-3 and claudin-4 in prostate cancer epithelium. Cancer Res 2001, 61(21):7878-7881

46. Mazzucchelli L: Protein S100A4: Too long overlooked by pathologists? Am J Pathol 2002, 160(1):7-13

47. Brett W, Mandinova A, Remppis A, Sauder U, Ruter F, Heizmann CW, Aebi U, Zerkowski HR: Translocation of S100A1(1) calcium binding protein during heart surgery. Biochem Biophys Res Comm 2001, 284(3):698-703

48. Most P, Bernotat J, Ehlermann P, Pleger ST, Reppel M, Borries M, Niroomand F, Pieske B, Janssen PML, Eschenhagen T, Karczewski P, Smith GL, Koch WJ, Katus HA, Remppis A: S100A1: a regulator of myocardial contractility. Proc Nat Acad Sci 2001, 98:13889-13894

49. Sorci G, Agneletti AL, Donato R: Effects of S100A1 and S100B on microtubule stability. An in vitro study using triton-cytoskeletons from astrocyte and myoblast cell lines. Neuroscience 2000, 99(4):773-783

50. Shrestha P, Muramatsu Y, Kudeken W, Mori M, Takai Y, I1g, EC, Schafer BW, Heizmann CW: Localization of Ca(2+)-binding S100 proteins in epithelial tumours of the skin. Virchows Archiv 1998, 432(1):53-59

51. Rosty C, Ueki T, Argani P, Jansen M, Yeo CJ, Cameron JL, Hruban RH, Goggins M: Overexpression of S100A4 in pancreatic ductal adenocarcinomas is associated with poor differentiation and DNA hypomethylation. Am J Pathol 2002, 160(1):45-50

52. Wang G, Rudland PS, Whites MR, Barraclough R: Interaction in vivo and in vitro of the metastatic-inducing S100 protein, S100A4 (p9Ka) with S100A1. J Biol Chem 2000, 275(15):11141-11146

53. Yamamoto T, Saatcioglu F, Matsuda T: Cross-talk between bone morphogenic proteins and estrogen receptor signaling. Endocrinol 2002, 143(7):2635-2642

54. Rajshankar D, McCulloch CA, Tenenbaum HC, Lekic PC: Osteogenic inhibition by rat periodontal ligament cells: modulation of bone morphogenic protein-7 activity in vivo. Cell & Tissue Res 1998, 294(3):475-483

55. Hidaka C, Quitoriano M, Warren RF, Crystal RG: Enhanced matrix synthesis and in vitro formation of cartilage-like tissue by genetically modified chondrocytes expressing BMP-7. J Orthopaedic Res 2001, 19(5):751-758

56. Simon M, Maresh JG, Harris SE, Hernandez JD, Arar M, Olson MS, Abboud HE: Expression of bone morphogenetic protein-7 mRNA in normal and ischemic adult rat kidney. Am J Physio 1999, 276(3 pt 2):F382-F389

57. Ishibashi K, Sasaki S, Akiba T, Marumo F: Expression of bone morphogenic protein 7 mRNA in MDCK cells. Biochem Biophys Res Comm 1993, 193(1):235-239

58. Katoh M, Terada M: Overexpression of bone morphogenic protein (BMP)-4 mRNA in gastric cancer cell lines of poorly differentiated type. J Gastroenterology 1996, 31:137-139

59. Kim JS, Crooks H, Dracheva T, Nishanian TG, Singh B, Jen J, Waldman T: Oncogenic beta-catenin is required for bone morphogenetic protein 4 expression in human cancer cells. Cancer Res 2002, 62(10):2744-2748

60. Imai N, Iwai A, Hatakeyama S, Masuzaki K, Kitagawa Y, Kato S, Hokari R, Kawaguchi A, Nagao S, Miyahara T, Itoh K, Miura S: Expression of bone morphogenetic proteins in colon carcinoma with heterotopic ossification. Pathol Int 2001, 51(8):643-648

61. Sulzbacher I, Birner P, Trieb K, Pichlbauer E, Lang S: The expression of bone morphogenetic proteins in osteosarcoma and its relevance as a prognostic parameter. J Clinical Pathol 2002, 55(5):381-385

62. Weber KL, Bolander ME, Rock MG, Pritchard D, Sarkar G: Evidence for the upregulation of osteogenic protein-1 mRNA expression in musculoskeletal neoplasms. J Orthopaedic Res 1998, 16(1):8-14

63. Lin DL, Tarnowski CP, Zhang J, Dai J, Rohn E, Patel AH, Morris MD, Keller ET: Bone metastatic LNCaP-derivative C4-2B prostate cancer cell line mineralizes in vitro. Prostate 2001, 47(3):212-21

64. Weber BL: Cancer genomics. Cancer Cell 2002, 1:37-47

65. Diab M, Wu JJ, Eyre DR: Collagen type IX from human cartilage: a structural profile of intermolecular cross-linking sites. Biochem J 1996, 314(Pt 1): 327-332

66. Holden P, Canty EG, Mortier GR, Zabel B, Spranger J, Carr A, Grant ME, Loughlin JA, Briggs MD: Identification of novel pro-alpha-2(IX) collagen gene mutations in two families

with distinctive oligo-epiphyseal forms of multiple epiphyseal dysplasia. Am J Human Genet 1999, 65: 31-38

67. Wolanska M, Sobolewski K, Drozdzewicz M: Extracellular matrix components in ovarian tumors. Ginekologia Polska 1999, 70(4):179-185

68. Santala M, Risteli J, Risteli L, Puistola U, Kacinski BM, Stanley ER, Kauppila A: Synthesis and breakdown of fibrillar collagens: concomitant phenomena in ovarian cancer. Brit J Cancer 1998, 77(11):1825-1831

69. Zhu GG, Risteli J, Puistola U, Kauppila A, Ristela L: Progressive ovarian carcinoma induces synthesis of type I and type III procollagens in the tumor tissue and peritoneal cavity. Cancer Res 1993, 53(20):5028-5032

70. Kiyozuka Y, Nakagawa H, Senzaki H, Uemura Y, Adachi S, Teramoto Y, Matsuyama T, Bessho K, Tsubura A: Bone morphogenetic protein-2 and type IV collagen expression in psammoma body forming ovarian cancer. Anticancer Res 2001, 21(3B):1723-1730

71. Moser TL, Pizzo SV, Bafetti LM, Fishman DA, Stack MS: Evidence for preferential adhesion of ovarian epithelial carcinoma cells to type I collagen mediated by the alpha2beta1 integrin. Int J Cancer 1996, 67(5):695-701

72. Parenti R, Wassef M, Cicirata F: Expression of CRABP I mRNA in fastigial cells of the developing cerebellum. Eur J Neurosci 2002, 15(1):211-215

73. Whitney D, Massaro GD, Massaro D, Clerch LB: Gene expression of cellular retinoid-binding proteins: modulation by retinoic acid and dexamethasone in postnatal rat lung. Ped Res 1999, 45(1):2-7

74. Mey J, McCaffery P, Klemeit M: Sources and sink of retinoic acid in the embryonic chick retina: distribution of aldehyde dehydrogenase activities, CRABP-I, and sites of retinoic acid inactivation. Brain Res Dev Brain Res 2001, 127(2):135-148

75. Vo HP, Crowe DL: Transcriptional regulation of retinoic acid responsive genes by cellular retinoic acid binding protein-II modulates RA mediated tumor cell proliferation and invasion. Anticancer Res 1998, 18(1A):217-224

76. Hillemanns P, Tannous-Khuri L, Koulos JP, Talmage D, Wright TC Jr.: Localization of cellular retinoid-binding proteins in human cervical intraepithelial neoplasia and invasive carcinoma. Am J Pathol 1992, 141(4): 973-980

77. Di Fronzo G, Cappelletti V, Miodini P, Bertario L, Ravasi G: Role of cellular retinoic acid binding protein (cRABP) in patients with large bowel cancer. Cancer Detect Prevent 1987, 10(5-6):327-333

78. Chen J, Knowles HJ, Hebert JL, Hackett BP: Mutation of the mouse hepatocyte nuclear factor/forkhead homologue 4 gene results in an absence of cilia and random left-right asymmetry. J Clinical Invest 1998, 102:1077-1082

79. Naiki T, Nagaki M, Shidoji Y, Kojima H, Imose M, Kato T, Ohishi N, Yagi K, Moriwaki H: Analysis of gene expression profile induced by hepatocyte nuclear factor 4 alpha in hepatoma cells using an oligonucleotide microarray. J Biol Chem 2002, 277:14011-14019

80. Tichelaar JW, Lim L, Costa RH, Whitsett JA: HNF-3/forkhead homologue-4 influences lung morphogenesis and respiratory epithelial cell differentiation in vivo. Develop Biol 1999, 213(2):405-417

81. Xu L, Hui L, Wang S, Gong J, Jin Y, Wang Y, Ji Y, Wu X, Han Z, Hu G: Expression profiling suggested a regulatory role of liver-enriched transcription factors in human hepatocellular carcinoma. Cancer Res 2001, 61(7):3176-3181

FIGURE LEGENDS

Figure 1. Dependence of the number of gene fragments present in all samples on the number of samples analyzed. The number of fragments present in all samples of a sample set is shown as a function of the number of samples. Normal ovaries (top panel), ovarian carcinoma (middle panel), and ovarian carcinoma metastatic to the omentum (bottom panel).

Figure 2. Differentially expressed genes in ovarian carcinoma, normal ovaries, and 20 other tissues. Eisen Cluster software was used to graphically display the intensity of gene expression values for each of the 40 genes listed in Table 2 for the 391 different tissue samples. The color of each square represents the ratio of the gene expression in the indicated sample relative to the average signal of expression of all genes examined. Red indicates gene expression above the median; black, equal to the median; and green, below the median. The intensity of the color reflects the magnitude of divergence from the median. Columns represent individual cDNA's for the 40 genes listed in Table 2, and rows represent the indicated tissue samples, as described in the Material and Methods section.

Figure 3. e-Northern™ analysis of differentially expressed gene fragments in human tissues. The expression of each indicated gene fragment was examined in 20 ovarian carcinomas, 17 ovarian carcinomas metastatic to the omentum, and 50 normal ovaries. The bar graph on the left depicts the percentage of samples that express detectable levels of the indicated gene fragment. The intensity of gene expression in each sample is plotted as average expression value on a linear scale on the right; median +/- 2 SD of expression values are shown.

Figure 4. Immunohistochemical staining of differentially expressed gene products. Normal ovaries (A,D,G,J,M), ovarian carcinoma (B,E,H,K,N), and ovarian carcinoma metastatic to the omentum (C,F,I,L,O) tissues were stained with a mAb against the β1 integrin subunit (A-C), normal mouse IgG (D-F), and antibodies against: the β8 integrin subunit (G-I), BMP-7 (J-L), and claudin-4 (M-O). 60x magnification.

Figure 5. Immunohistochemical staining of differentially expressed gene products. Normal ovaries (A,D,G,J), ovarian carcinoma (B,E,H,K), and ovarian carcinoma metastatic to the omentum (C,F,I,L) tissues were stained with antibodies against: COL IX α2 (A-C), CRABP-1 (D-F), FOX J1 (G-I), and S100A1 (J-L). 60x magnification.

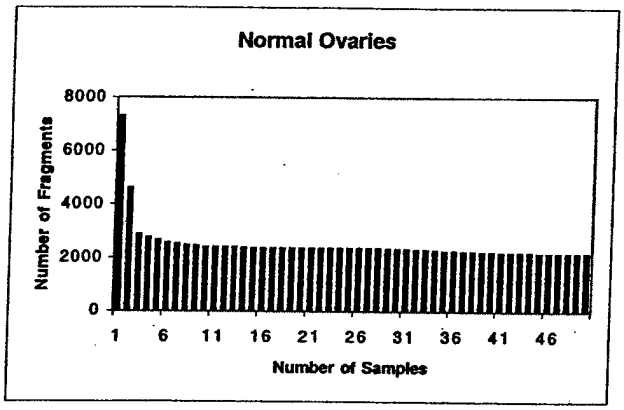
Normal Ovaries
Number of Fragments
8000
6000
4000
2000
0
1
6
11
16
21
26
31
36
41
46
Number of Samples

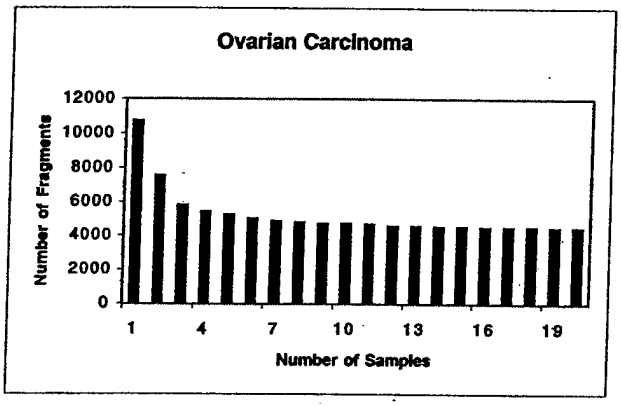
Ovarian Carcinoma
Number of Fragments
12000
10000
8000
6000
4000
2000
0
1
4
7
10
13
16
19
Number of Samples

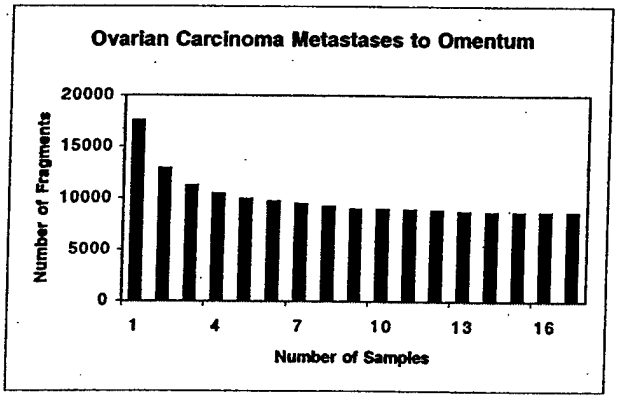
Ovarian Carcinoma Metastases to Omentum
Number of Fragments
20000
15000
10000
5000
0
1
4
7
10
13
16
Number of Samples

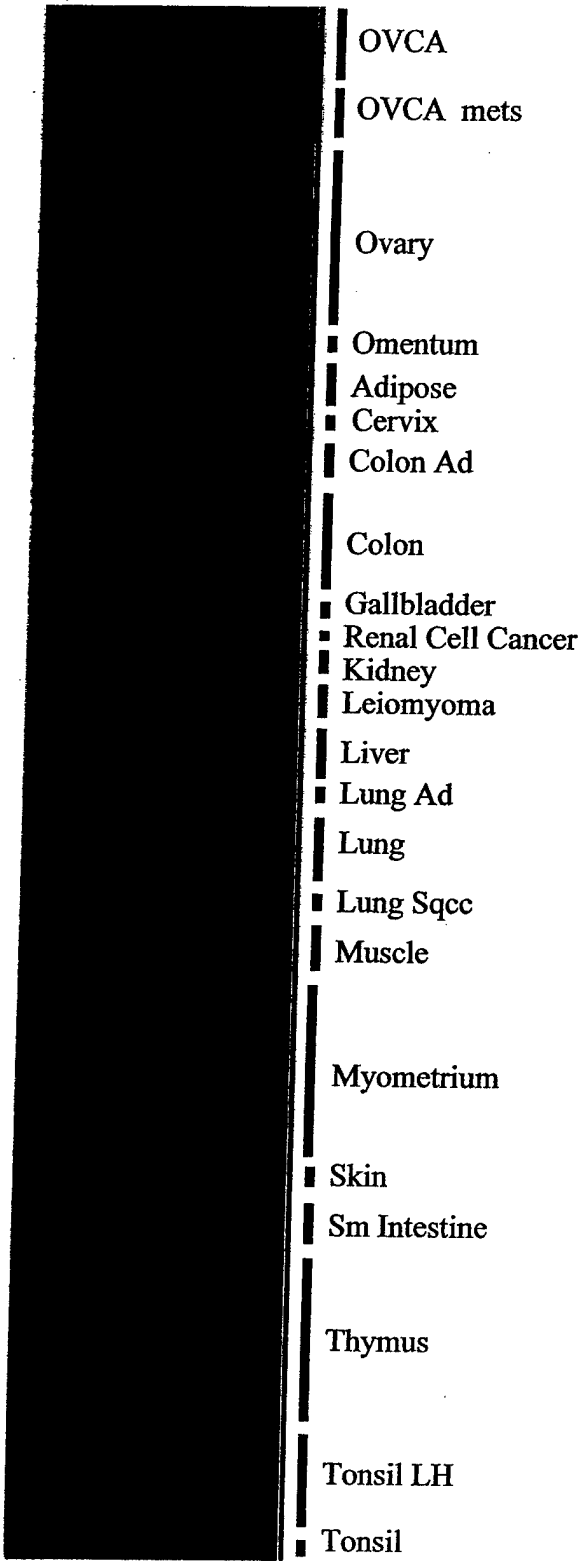
OVCA
OVCA mets
Ovary
Omentum
Adipose
Cervix
Colon Ad
Colon
Gallbladder
Renal Cell Cancer
Kidney
Leiomyoma
Liver
Lung Ad
Lung
Lung Sqcc
Muscle
Myometrium
Skin
Sm Intestine
Thymus
Tonsil LH
Tonsil

β8 Integrin

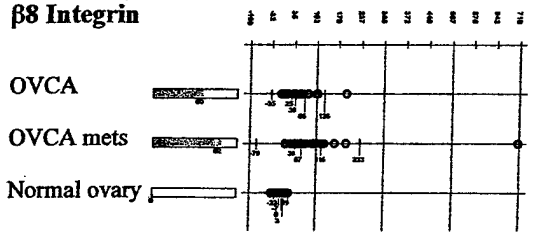

CRABP-1

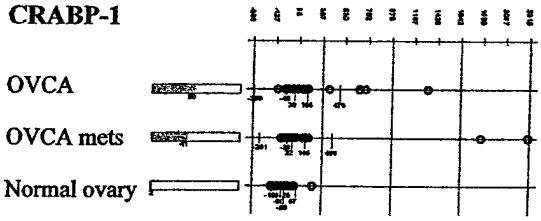

BMP-7

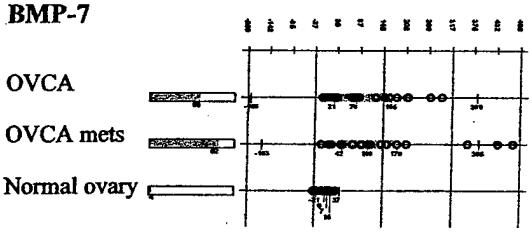

FOX J1

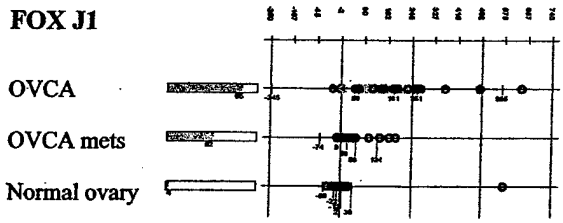

Claudin 4

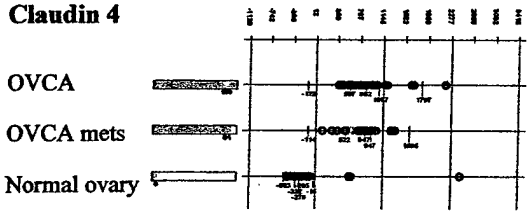

S100A1

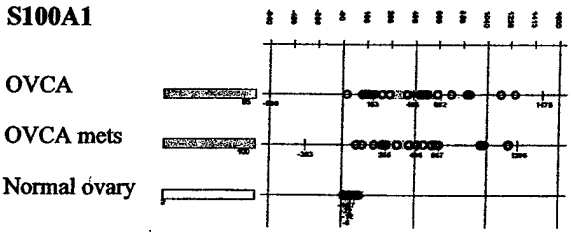

COL IX α2

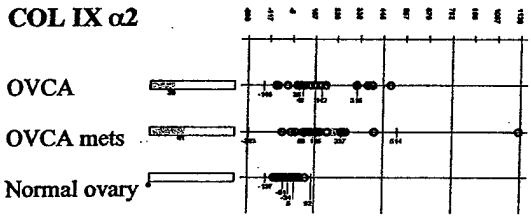

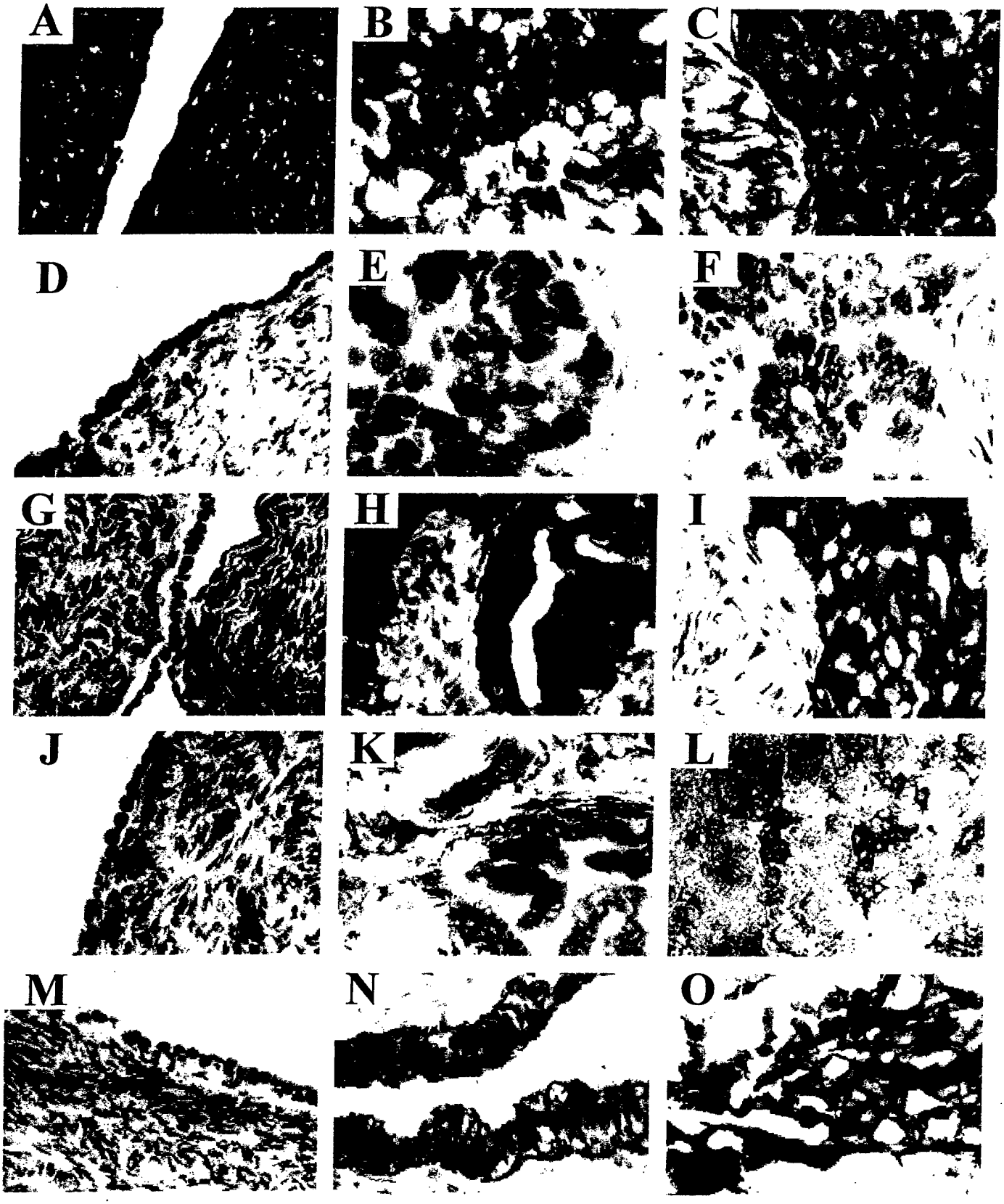
A
B
C
D
E
F
G
H
I
J
K
L
M
N
O

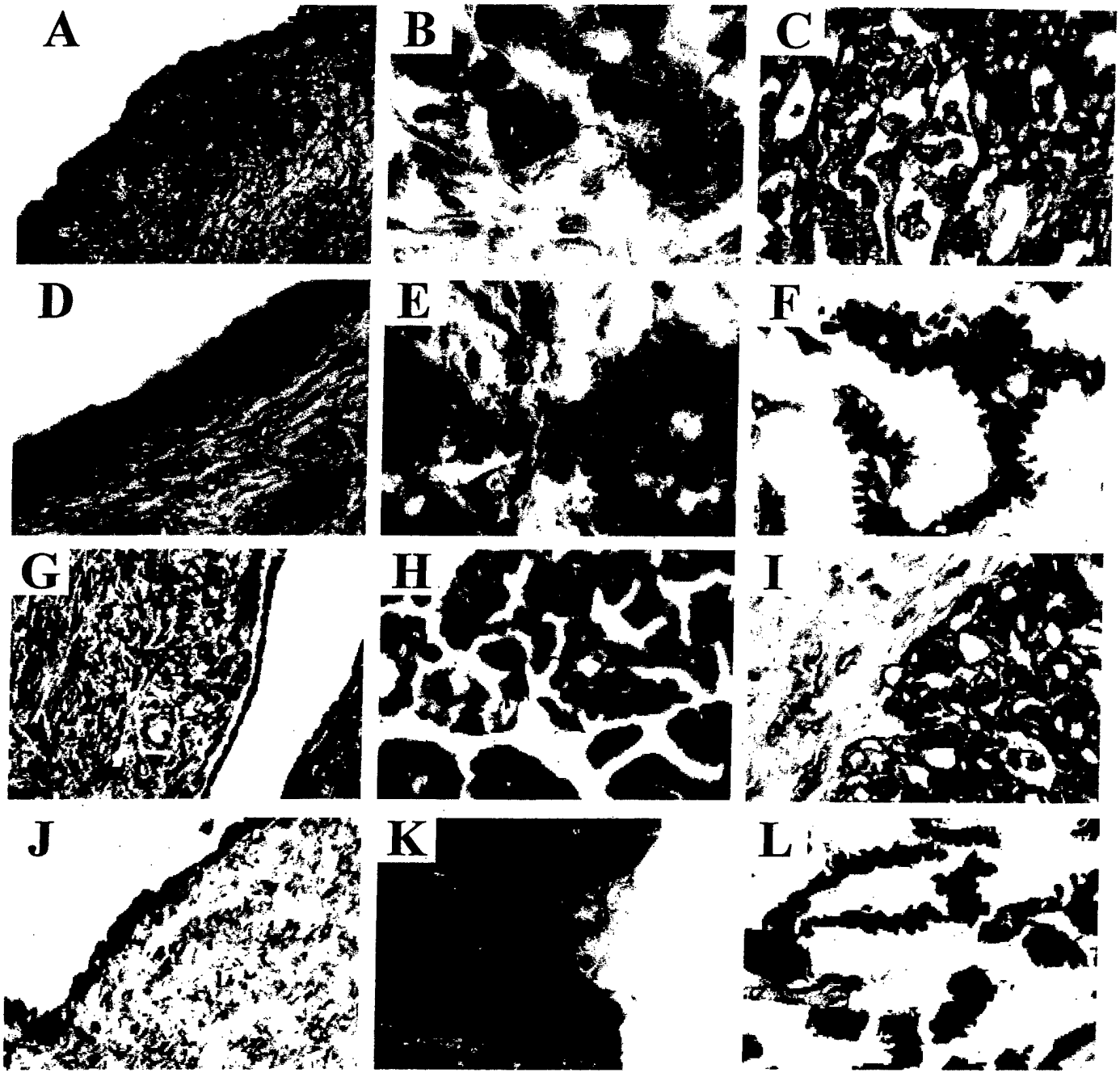
A
B
C
D
E
F
G
H
I
J
K
L

Table 1 *Fold change analysis of gene expression*

Fold Change Range[c]	Fold change of ovarian carcinoma vs. normal ovary[a]			Fold change of ovarian carcinoma vs. ovarian carcinoma metastases to the omentum[b]		
	Up in ovarian carcinoma	Down in ovarian carcinoma	Total gene fragments changed	Up in ovarian carcinoma	Down in ovarian carcinoma	Total gene fragments changed
Over 100	1	0	1	0	0	0
10 to 100	90	46	136	0	3	3
5 to 10	210	217	427	1	10	11
4 to 5	155	170	325	3	14	17
3 to 4	401	347	748	19	45	64
2 to 3	1499	1186	2685	136	393	529
1 to 2	23592	21348	44940	17378	27365	44743
Unchanged	-	-	923	-	-	1336

[a]A fold change analysis of gene expression in the set of 20 papillary serous ovarian carcinoma tissues compared with that in the set of 50 normal ovary tissues.

[b]A fold change analysis of gene expression in the set of 20 papillary serous ovarian carcinoma tissues compared with that in the set of 17 papillary serous ovarian carcinoma that had metastasized to the omentum.

[c]The number of gene fragments in each indicated range of fold change.

Table 2: Genes specifically upregulated in ovarian carcinoma tissue samples

Known Gene Symbol	Known Gene Name	Function	Previously referenced as upregulated in ovarian carcinoma		Previously referenced as expressed in other types of cancers
			Determined by gene arrays	Determined by another technique (eg. IH, PCR)	
ALDH3B2	aldehyde dehydrogenase 3 family, member B2	enzyme, metabolism	-	-	-
BHLHB3	basic helix-loop-helix domain containing, class B, 3	cell signaling, differentiation	-	-	*
BMP7	bone morphogenetic protein 7 (osteogenic protein 1)	cytokine	-	-	*
CAPS	calcyphosine	ion transport, Ca2+	-	-	-
CCNA1	cyclin A1	cell cycle	-	-	*
CCNE1	cyclin E1	cell cycle	-	*	*
CDH6	cadherin 6, type 2, K-cadherin (fetal kidney)	cell-cell adhesion receptor	*	*	*
CDKN2A	cyclin-dependent kinase inhibitor 2A (melanoma, p16, inhibits CDK4)	cell cycle	-	*	*
COL9A2	collagen, type IX, alpha 2	cell adhesion, ECM	-	-	*
CP	ceruloplasmin (ferroxidase)	ligand-binding protein, copper	*	*	*
DAG1	dystroglycan 1 (dystrophin-associated glycoprotein 1)	cell-ECM adhesion receptor	-	-	*
EGFL6	EGF-like-domain, multiple 6	cytokine	-	-	*
EYA2	eyes absent homolog 2 (Drosophila)	transcriptional co-activator	*	-	-
FOLR1	folate receptor 1 (adult)	cell signaling, receptor, transporter	*	*	-
FOXJ1	forkhead box J1	transcriptional activator	-	-	*
HOXD1	homeo box D1	transcription factor	-	-	*
HTR3A	5-hydroxytryptamine (serotonin) receptor 3A	ion transport, cations	-	-	-
ITGB8	integrin, beta 8 subunit	cell-ECM adhesion receptor	*	-	-
KLK5	kallikrein 5	protease, serine	-	*	*
KLK6	kallikrein 6 (neurosin, zyme)	protease, serine	*	*	*
KLK7	kallikrein 7 (chymotryptic, stratum corneum)	protease, serine	-	*	-
KLK8	kallikrein 8 (neuropsin/ovasin)	protease, serine	-	*	*
MSLN	mesothelin	cell adhesion receptor	*	*	-
MUC1	mucin 1, transmembrane	tumor antigen, epithelial cell antigen	*	*	*
NMU	neuromedin U	cell signaling, muscle contraction	-	-	-
PAX8	paired box gene 8	transcription factor	*	-	*
PNOC	prepronociceptin	cell signaling, neurotransmitter	*	-	-
PRAME	preferentially expressed antigen in melanoma	tumor antigen	*	-	*
PRKCI	protein kinase C, iota	cell signaling	-	-	*
PRSS21	protease, serine, 21 (testisin)	protease, serine	-	*	*
S100A1	S100 calcium binding protein A1	ligand-binding protein, divalent cations	*	-	*
SALL4	sal-like 4 (Drosophila)	transcription factor	-	-	-
SCARA3	scavenger receptor class A, member 3	scavenger receptor	-	-	-
SCGB2A1	secretoglobin, family 2A, member 1	ligand-binding protein	*	-	*
SGPL1	sphingosine-1-phosphate lyase 1	enzyme, metabolism	-	-	-
SLC4A11	solute carrier family 4, sodium bicarbonate transporter-like, member 11	ion transport	-	-	-
SOX11	SRY (sex determining region Y)-box 11	transcription factor	-	-	*
SPON1	spondin 1, (f-spondin) extracellular matrix protein	cell adhesion, ECM	*	-	-
TMPRSS3	transmembrane protease, serine 3	protease, serine	-	*	-
UBE2H	ubiquitin-conjugating enzyme E2H (UBC8 homolog, yeast)	enzyme, ubiquitination	-	-	-

The known gene fragments expressed at ≥2-fold higher levels in the set of ovarian carcinoma than in the set of normal ovaries and other tissue sets were analyzed by Contrast Analysis™. Genes were ranked based on the degree of increase in expression, and e-Northern Analysis™ was performed on the top 400 genes. This table is an alphabetical listing of the 40 genes most specific to ovarian carcinoma, as well as the cellular function of their gene products.

Table 3: Genes upregulated in ovarian carcinoma tissue samples and some other tissues

Known Gene Symbol	Known Gene Name	Function	Previously referenced as upregulated in ovarian carcinoma		Previously referenced as expressed in other types of cancers
			Determined by gene arrays	Determined by another technique (e.g. IH, PCR)	
ATP6V1B1	ATPase, H+ transporting, lysosomal 56/58kDa, V1 subunit B, isoform 1	ion transport, H+	-	-	-
C20orf1	chromosome 20 open reading frame 1	cell cycle	-	-	*
CD47	CD47 antigen (Rh-related antigen, integrin-associated signal transducer)	cell adhesion receptor	-	*	-
CENPF	centromere protein F, 350/400ka (mitosin)	cell cycle, mitosis	-	-	-
CLDN4	claudin 4	cell-cell adhesion receptor	*	*	*
COL8A2	collagen, type VIII, alpha 2	cell adhesion, ECM	-	-	*
CRABP1	cellular retinoic acid binding protein 1	accessory protein	*	-	*
CRABP2	cellular retinoic acid binding protein 2	accessory protein	-	-	*
DD96	epithelial protein up-regulated in carcinoma, membrane associated protein 17	tumor antigen	-	-	*
ETV4	ets variant gene 4 (E1A enhancer binding protein, E1AF)	transcriptional activator	-	*	*
FOXM1	forkhead box M1	transcriptional activator	-	-	*
GPR49	G protein-coupled receptor 49	cell signaling, receptor	*	-	-
GRB7	growth factor receptor-bound protein 7	accessory protein, adaptor protein	-	-	*
H2BFB	H2B histone family, member B	histone	-	-	-
IFRG28	28kD interferon responsive protein	unknown	-	-	-
ITGB4	integrin, beta 4	cell-cell/ECM adhesion receptor	-	*	*
KLK10	kallikrein 10	protease, serine	*	*	*
KNSL6	kinesin-like 6 (mitotic centromere-associated kinesin)	motor protein, mitosis	-	-	-
LNIR	Ig superfamily receptor LNIR	cell adhesion receptor	-	-	-
SCNN1A	sodium channel, nonvoltage-gated 1 alpha	ion transport, Na+	-	-	-
SIAHBP1	fuse-binding protein-interacting repressor	ligand-binding protein, Ro RNP	-	-	*
SLC34A2	solute carrier family 34 (sodium phosphate), member 2	ion transport, phosphate	-	-	-
TFAP2A	transcription factor AP-2 alpha (activating enhancer binding protein 2 alpha)	transcriptional activator	-	-	*
TFAP2C	transcription factor AP-2 gamma (activating enhancer binding protein 2 gamma)	transcriptional activator	-	-	*
USP18	ubiquitin specific protease 18	protease	-	-	-
XPR1	xenotropic and polytropic retrovirus receptor	cell signaling, receptor	-	-	-

The known gene fragments expressed at ≥2-fold higher levels in the set of serous papillary ovarian cancer than in the set of normal ovaries were analyzed by Contrast Analysis™. Genes were ranked based on the degree of increase in expression, and e-Northern™ analysis was performed on the top 400 genes. The 26 genes listed alphabetically in this table were highly expressed in ovarian carcinoma samples, but were also expressed by one or more other tissues. Thus, these genes may not be as specific to ovarian cancer as those in Table 2.

Table 4: *Specificity, sensitivity, and Youden's misclassification index (J) for seven genes*

Gene Name	Comparison I: Normal ovary tissues vs. ovarian carcinoma tissues			Comparison II: Normal ovary tissues vs. metastatic ovarian carcinoma tissues			Comparison III: Ovarian carcinoma tissues vs. metastatic ovarian carcinoma tissues		
	Specificity[a]	Sensitivity[b]	J[c]	Specificity[a]	Sensitivity[b]	J[c]	Specificity[d]	Sensitivity[d]	J
β8 integrin	0.867	0.8	**0.667**	0.867	0.8	**0.667**	0.2	0.8	0
BMP-7	0.667	0.6	0.267	0.667	0.6	0.267	0.4	0.867	0.267
Claudin-4	0.933	0.993	**0.867**	0.933	1	**0.933**	0.067	1	0.067
COL IX α2	1	0.2	0.2	1	0.2	0.2	0.067	1	0.067
CRABP-1	0.533	0.533	0.067	1	0.133	0.133	0.933	0.133	0.067
FOX J1	0.333	0.933	0.267	0.333	1	0.333	0.067	1	0.067
S100A1	0.6	1	**0.6**	0.6	0.933	**0.533**	0.667	0.333	0

Seven genes were analyzed for their ability to distinguish the following: Comparison I, 15 normal ovary tissues from 15 serous papillary ovarian carcinoma tissues; Comparison II, 15 normal ovary tissues from 15 ovarian carcinoma tissues metastatic to the omentum; and Comparison III, 15 serous papillary ovarian tumor tissues from 15 ovarian tumor tissues metastatic to the omentum. All three statistical measures were based on the protein staining intensities as determined by immunohistochemical analysis. For the purpose of these statistical measures, tissue staining intensities were classified as positive if they had scored +, ++, or +++, and they were classified as negative if they had scored – or +/-.

[a]Specificity indicates the probability that a negative protein classification correctly identifies the tissue as normal ovary tissue (i.e. not as carcinoma).

[b]Sensitivity indicates the probability that a positive protein classification correctly identifies the tissue as ovarian carcinoma tissue (i.e. tumor being present);

[c]Youden's misclassification index (J) indicates the overall probability of correct classifications. Genes with a J value of 0.5 or greater (in bold) were considered to be predictive of cancer.

[d]ROC curves (plots of sensitivity vs. specificity) were constructed to determine the optimal staining intensities for each gene at which the two tissue types could be distinguished from each other. Specificity and sensitivity indicate the probability that the optimal staining intensities could correctly distinguish ovarian carcinoma from ovarian carcinoma metastases to the omentum.

Appendix 4

Ovarian Carcinoma Ascites Spheroids Adhere to Extracellular Matrix Components and Mesothelial Cell Monolayers

Kathryn M. Burleson[§], Rachael C. Casey[§], Keith M. Skubitz[†], Stephan E. Pambuccian[§], Theodore R. Oegema, Jr. [‡], and Amy P.N. Skubitz[§]

From the Departments of Laboratory Medicine and Pathology[§], Medicine[†], and Orthopedic Surgery [‡], University of Minnesota, Basic Sciences and Biological Engineering Building, 312 Church St S.E., Minneapolis, Minnesota.

Correspondence and reprint requests to: Amy P. N. Skubitz, Department of Laboratory Medicine and Pathology, MMC 609, 420 Delaware St. S.E., University of Minnesota, Minneapolis, MN 55455, USA. Tel: 612-625-5920; Fax 612-625-1121; email: skubi002@umn.edu

Abstract

Objective Ovarian carcinoma cells form multicellular aggregates, or spheroids, in the peritoneal cavity of patients with advanced disease. The current paradigm that ascites spheroids are non-adhesive leaves their contribution to ovarian carcinoma dissemination undefined. Here, spheroids obtained from ovarian carcinoma patients' ascites were characterized for their ability to adhere to molecules encountered in the peritoneal cavity, with the goal of establishing their potential to contribute to ovarian cancer spread.

Methods Spheroids were recovered from the ascites fluid of eleven patients with stage III ovarian carcinoma. Adhesion assays to extracellular matrix proteins and human mesothelial cell monolayers were performed for each of the ascites spheroid samples. Subsequently, inhibition assays were performed to identify the cell receptors involved.

Results Most ascites samples adhered moderately to fibronectin and type I collagen, with reduced adhesion to type IV collagen and laminin. Monoclonal antibodies against the β1 integrin subunit partially inhibited this adhesion. Ascites spheroids also adhered to hyaluronan. Additionally, spheroids adhered to live, but not fixed, human mesothelial monolayers, and this adhesion was partially mediated by β1 integrins.

Conclusions The cellular content of the ascites fluid has often been considered non-adhesive, but our findings are the first to suggest that patient-derived ascites spheroids can adhere to mesothelial extracellular matrix via β1 integrins, indicating that spheroids should not be ignored in the dissemination of ovarian cancer.

Keywords

Cell adhesion molecules, extracellular matrix, integrins, ovarian carcinoma, spheroids

Introduction

Ovarian carcinoma remains the fifth leading cause of cancer death for women in the United States.[1] Due to the lack of reliable tumor markers and vague or absent symptoms in the early stages of the disease, seventy percent of patients initially present with advanced disease, with tumor spread beyond the ovary. [2] As ovarian cancer progresses, the peritoneal cavity of the patients frequently accumulates malignant ascites fluid containing tumor cells, which exist both singly and as multicellular aggregates, or spheroids. In the current model of ovarian cancer spread, tumor cells shed from the surface of the ovary into the ascites fluid and can subsequently attach to and invade through the mesothelial cell monolayers that line the organs of the peritoneal cavity. However, because the cellular content of the ascites fluid exists in suspension rather than attached to peritoneal surfaces, ascites cells and spheroids are generally considered a non-adhesive subset of the tumor cells. Furthermore, as ovarian cancer research has traditionally focused on the metastatic behavior of single cells, little is known about the role of spheroids in ovarian carcinoma progression.

Most spheroid research has focused on response to cancer therapy since Sutherland and associates showed spheroids are a more accurate model system than monolayers for the study of tumor biology.[3, 4] Spheroids can be created from many different cell lines and types, and their successful manipulation has led to the discovery of a multicellular-associated resistance of spheroids to treatment.[5, 6] As tumor models, ovarian carcinoma spheroids have been shown to be protected from apoptosis induced by radiation or Taxol,[7-10] but the potential of ascites spheroids to implant on peritoneal surfaces remain unexplored.

The mesothelial cell monolayer that lines the peritoneal cavity and its organs is the major site of ovarian carcinoma dissemination.[2] Mesothelial cells express a number of extracellular matrix (ECM) proteins and adhesion molecules, including integrins and CD44, which promote ovarian carcinoma cell adhesion.[11-13] Additionally, mesothelial cells secrete factors that induce ovarian carcinoma cell migration.[14] A variety of adhesion molecules, including integrins, ECM proteins, glycosaminoglycans, and proteoglycans have been detected in spheroids.[15-18] We have previously demonstrated that ovarian carcinoma spheroids generated from the NIH:OVCAR5 cell line adhere to fibronectin, type IV collagen, and laminin, although at a slower rate than single cell suspensions of NIH:OVCAR5 cells, and that this adhesion is mediated by the $\alpha 2$, $\alpha 5$, $\alpha 6$, and $\beta 1$ integrin subunits.[15] Taken together, our findings are the first to suggest that primary patient ascites spheroids may also possess the ability to adhere to secondary tumor sites, rather than comprise a non-adherent population of tumor cells.

In the present study, we examined the ability of eleven ovarian carcinoma patient-derived ascites spheroid samples to adhere to a variety of components frequently found in the ECM of mesothelial cells. We also determined whether a monoclonal antibody (mAb) against the $\beta 1$ integrin subunit or CD44 could block this adhesion. Furthermore, we assessed the ability of patients' ascites spheroids to adhere to live or paraformaldehyde-fixed human mesothelial monolayers and whether this adhesion was partially dependent upon $\beta 1$ integrin or CD44 interactions. Given the propensity of spheroids to exhibit a multicellular resistance to therapy,[4-9] our findings suggest that ovarian carcinoma ascites spheroids should be considered a potential source of secondary tumor growth in ovarian cancer patients.

Materials and Methods

ECM Components

Type IV collagen from mouse Engelbreth Holm-Swarm (EHS) tumor was purchased from Trevigen (Gaithersburg, MD). Type I collagen from human placenta was purchased from Southern Biotech (Birmingham, AL). Mouse EHS laminin was purchased from Invitrogen (Carlsbad, CA). Human plasma fibronectin, purified as described,[19] was provided by Dr. James McCarthy, University of Minnesota. Human umbilical cord hyaluronan and ovalbumin were purchased from Sigma Chemical Co. (St. Louis, MO). Hyaluronan oligomers were prepared as previously described. Briefly, 175 U of bovine testicular hyaluronidase per mg hyaluronan was incubated for 18 hours at 37°C, followed by boiling at 100°C for 10 minutes to inactivate the hyaluronidase.

Antibodies

Purified immunoglobulin (IgG) of mouse mAb P5D2, which blocks the adhesive activity of the human β1 integrin subunit, was provided by Dr. Leo Furcht (University of Minnesota). Affinity-purified IgG of mAb IM7, which blocks the hyaluronan-binding site of CD44, was purchased from Pharmigen (San Diego, CA). Normal mouse IgG was purchased from Sigma Chemical Co. CD 15 mAb MMA, CA-125 mAb OV185:1, and CD45 mAb LCA were purchased from Ventana Medical Systems. B72.3 mAb was purchased from Signet Laboratories, Inc. (Dedham, MA). Polyclonal antibodies against CEA and a mAb against Ber-EP4 were purchased from DakoCytomation (Carpinteria, CA). A polyclonal antibody against calretinin was purchased from Zymed Laboratories (South San Francisco, CA).

Cell Culture

The ovarian carcinoma cell line NIH:OVCAR5 was obtained from Dr. Judah Folkman (Harvard Medical School, Boston, MA),[20] and was chosen for its ability to mimic ovarian carcinoma progression *in vivo* when injected into mice.[21] This cell line was maintained in RPMI 1640 media with 10% fetal bovine serum (FBS, from Nova-Tech, Inc, Grand Island, NE), 2 mM L-glutamine, 0.2 U/ml insulin, and 50 U/ml penicillin G/streptomycin. The human peritoneal mesothelial cell line LP9 was purchased from the Coriell Cell Repository (Camden, NJ), and maintained in a 1:1 ratio of M199 and MCDB110 media, supplemented with 15% FBS, 2 mM glutamine, 5 ng/ml EGF, 0.4 μg/ml hydrocortisone, and 50 U/ml penicillin/streptomycin. Both cell lines were cultured in 75 mm^2 tissue culture flasks in a 5% CO_2 humidified incubator at 37°C.

Purification of Primary Ovarian Carcinoma Cells

Ascites fluid samples from eleven patients diagnosed with stage III or IV ovarian carcinoma were obtained through the University of Minnesota Cancer Center Tissue Procurement Facility with approval of the University of Minnesota Institutional Review Board. Ascites tumor cells and spheroids were collected by centrifugation at 100 x g for 10 minutes. Erythrocytes were lysed by resuspending the cells in lysis buffer (10 nM potassium bicarbonate, 155 mM ammonium chloride, 0.1 mM EDTA, pH 7.4) for 5 minutes. The remaining cells were collected by centrifugation at 100 x g for 10 minutes, then layered upon Ficoll-Paque Plus (Pharmacia Biotech, Uppsala, Sweden) and centrifuged again at 400 x g for 15 minutes. The tumor cells were removed from the top

of the Ficoll layer and washed in RPMI 1640 media. Aliquots of ascites ($1x10^7$ cells/ml) were suspended in 10% DMSO and 90% FBS, and stored in liquid nitrogen.

Immunohistochemistry

For immunohistochemical analysis, paraffin blocks were made from thrombin clots of purified ovarian carcinoma patient ascites fluid. Thrombin clots were prepared by adding 2-3 µl of ascites cell pellet to 100 µl human plasma and 50 µl thrombin (Sigma Chemical Co). The thrombin clots were fixed with 10% formaldehyde in PBS, and were paraffin-embedded in the Fairview University Medical Center Pathology Laboratory. 4-5 micron sections were stained with a panel of antibodies against ovarian carcinoma (CA-125), epithelial cells (Ber-Ep4, CD15, B72.3, CEA), mesothelial cells (calretinin), and inflammatory cells (CD45) on an automated immunostainer (Benchmark, Ventana Medical Systems, Tucson, AZ). A pathologist evaluated each sample and verified the presence of 90% ovarian carcinoma cells in all cases.

Spheroid Culture

Spheroids were generated using a liquid overlay technique as previously described.[15] 24-well tissue culture plates were coated with 500 µl of 0.5% SeaKem LE agarose in serum-free media, and allowed to solidify for 30 minutes at room temperature. NIH:OVCAR5 cells were released from monolayer cultures with 0.5% trypsin/2 mM ethylenediaminetetraacetic acid (EDTA), resuspended in complete media, transferred to agarose-coated wells at 50,000 cells/well, and incubated for 48 hours at 37°C.

Archived patient ascites samples, consisting of heterogeneous populations of single cells and spheroids, were rapidly thawed, washed with complete media, and centrifuged at 100 x g for 5 minutes. The cells were resuspended in complete media, and cultured in suspension on top of solidified agarose overnight to equilibrate. Prior to use in assays, both NIH:OVCAR5 and patient ascites spheroids were centrifuged at 10 x g for 3 minutes to remove single cells.

Spheroid Adhesion Assays

Glass 8-well chamber slides (Nalge Nunc International, Naperville, IL) were coated with 50 μg/ml of laminin, fibronectin, type I collagen, type IV collagen, ovalbumin, or 1 mg/ml of hyaluronan, or hyaluronan fragments (6 and 8-mer's), in phosphate buffered saline (PBS) overnight in a humidified incubator at 37°C. The slides were blocked with 2 mg/ml ovalbumin in PBS for at least one hour, and then gently washed with PBS. Patient ascites spheroids were resuspended in RPMI media, and 200 μl aliquots of the suspension were transferred to each well, to yield 50-100 spheroids/well. The number of spheroids per well was counted manually under a light microscope, and the slides were incubated for 1-4 hrs at 37°C. The slides were rinsed in PBS, fixed and stained with Diff-Quik (Dade Behring, Inc., Newark, DE) according to manufacturer's instructions, and the number of adherent spheroids in each well was counted. Percent adhesion was determined as the number of spheroids per well remaining after fixation divided by the number of spheroids originally added per well, multiplied by 100.

For inhibition assays, patient ascites spheroids were incubated in RPMI media with 10 μg/ml of a blocking mAb against the β1 integrin subunit, a mAb that blocks the

Archived patient ascites samples, consisting of heterogeneous populations of single cells and spheroids, were rapidly thawed, washed with complete media, and centrifuged at 100 x g for 5 minutes. The cells were resuspended in complete media, and cultured in suspension on top of solidified agarose overnight to equilibrate. Prior to use in assays, both NIH:OVCAR5 and patient ascites spheroids were centrifuged at 10 x g for 3 minutes to remove single cells.

Spheroid Adhesion Assays

Glass 8-well chamber slides (Nalge Nunc International, Naperville, IL) were coated with 50 μg/ml of laminin, fibronectin, type I collagen, type IV collagen, ovalbumin, or 1 mg/ml of hyaluronan, or hyaluronan fragments (6 and 8-mer's), in phosphate buffered saline (PBS) overnight in a humidified incubator at 37°C. The slides were blocked with 2 mg/ml ovalbumin in PBS for at least one hour, and then gently washed with PBS. Patient ascites spheroids were resuspended in RPMI media, and 200 μl aliquots of the suspension were transferred to each well, to yield 50-100 spheroids/well. The number of spheroids per well was counted manually under a light microscope, and the slides were incubated for 1-4 hrs at 37°C. The slides were rinsed in PBS, fixed and stained with Diff-Quik (Dade Behring, Inc., Newark, DE) according to manufacturer's instructions, and the number of adherent spheroids in each well was counted. Percent adhesion was determined as the number of spheroids per well remaining after fixation divided by the number of spheroids originally added per well, multiplied by 100.

For inhibition assays, patient ascites spheroids were incubated in RPMI media with 10 μg/ml of a blocking mAb against the β1 integrin subunit, a mAb that blocks the

hyaluronan-binding site of CD44, or mouse IgG for 30 minutes at 37°C prior to addition to the chamber slides. The spheroids were then transferred to the slides in the presence of the antibodies, in which they remained for the duration of the 1-hour adhesion assay. Inhibition was determined as: (% adhesion in mIgG - % adhesion in test mAb) / (% adhesion in mIgG), multiplied by 100. To block adhesion to hyaluronan, spheroids were incubated with 0-1000 μg/ml of soluble hyaluronan, or 0-500 μg/ml hyaluronan fragments, for 30 minutes. The spheroids were then transferred to the slides in the presence of the soluble inhibitor for 2 hours. Inhibition was determined as: (% adhesion in 0 HA - % adhesion in test HA) / (% adhesion in 0 HA), multiplied by 100. The experiments were performed at least three times in quadruplicate.

Spheroid Adhesion to Mesothelial Monolayers

To quantitate the adhesion of patient ascites spheroids to mesothelial monolayers, LP9 human mesothelial cells were grown to confluence in glass Falcon 8-well chamber slides (BD Biosciences, Bedford, MA). For some assays, monolayers were fixed with 4% paraformaldehyde in PBS at room temperature for 10 minutes, then rinsed three times with 50 mM ammonium chloride in PBS, and blocked with 1% BSA in RPMI for 30 minutes to quench excess aldehyde from the fixation step.[22] Patient ascites spheroids were labeled with 5-chloromethylfluorescein diacetate (CMFDA) (Molecular Probes, Eugene, OR) by incubating the spheroids in a solution of 0.01 μg/ml CMFDA in RPMI for 45 minutes at 37°C. Spheroids were rinsed twice and incubated for 30 minutes in RPMI. Following a final rinse, spheroids were added in RPMI to the wells of either live or fixed mesothelial cell monolayers. The number of spheroids/well was counted under a

fluorescent microscope, and the spheroids were allowed to adhere for 1-4 hours at 37°C. Non-adherent spheroids were gently rinsed away with PBS, and the remaining spheroids were fixed with Diff-Quik fixative. The percent of adherent spheroids was determined by dividing the number of spheroids remaining after fixation by the number of spheroids added to each well originally, multiplied by 100. These experiments were performed at least three times in quadruplicate.

For inhibition assays, CMFDA-labeled patient ascites spheroids were incubated in RPMI in the presence of 10 ug/ml of a blocking mAb against the β1 integrin subunit, a mAb that blocks the hyaluronan-binding site of CD44, or mouse IgG for 30 minutes at 37°C prior to their addition to the chamber slides. The spheroids were then transferred in the presence of the antibody to wells containing live, confluent monolayers of mesothelial cells for the duration of the 2-hour adhesion assay. Inhibition was determined as: (% adhesion in mIgG - % adhesion in test mAb) / (% adhesion in mIgG), multiplied by 100. The experiments were performed at least three times in quadruplicate.

Results

Characterization of ovarian carcinoma spheroids from the peritoneal cavity of patients. Ovarian carcinoma spheroids were isolated from ascites samples obtained from eleven patients with ovarian carcinoma. The isolated spheroids were stained with a panel of immunohistochemical markers to verify that the spheroids consisted of over 90% epithelial ovarian carcinoma cells that expressed CA-125, the clinical marker of ovarian carcinoma. Immunohistochemical analysis also revealed that some spheroids incorporated up to 10% mesothelial cells and inflammatory cells into the aggregates along with the tumor cells. All samples were viable as determined by trypan blue stain exclusion (data not shown). The eleven ascites samples were relatively similar in composition, containing a mix of single cells and spheroid aggregates ranging in size from 30-200 μm in diameter (Fig.1, #1-11). Spheroids generated *in vitro* from NIH:OVCAR5 cells (Fig.1, OVCAR5) resembled spheroids recovered from patient ascites samples in terms of size and general appearance.

Adhesion of ascites spheroids to ECM proteins. We have previously shown that spheroids generated *in vitro* from the ovarian carcinoma cell line NIH:OVCAR5 have the ability to adhere to ECM components.[15] To establish the relevance of this adhesion to ovarian carcinoma patients, spheroids obtained from the ascites fluid of eleven patients were tested for their ability to adhere to ECM proteins (Fig. 2A). To quantitate adhesion, ovarian carcinoma ascites spheroids were allowed to adhere for up to four hours to glass chamber slides coated with 50 μg/ml fibronectin, type I collagen, type IV collagen, laminin, or ovalbumin. In most cases, maximal adhesion was observed by 2 hours, with a

decrease in adhesion observed at 4 hours in serum-free conditions. Therefore, the 2-hour time-point was selected for the remainder of the experiments. Patient ascites spheroids segregated into three adhesion groups based on their levels of adhesion to ECM proteins at 2 hours (Fig. 2B). Patient samples #1 and #2 showed high levels of adhesion, with 35-70% of the spheroids adhering to the CM proteins. Patient samples #3-7 displayed moderate levels of adhesion, with 10-20% of the spheroids adhering. Patient samples #8-11 consisted of low or non-adherent spheroids, with <10% adhesion (Fig. 2B). Overall, the samples showed greater levels of adhesion to fibronectin and type I collagen than to laminin or type IV collagen. In many cases, spheroid adhesion to ovalbumin was almost as high as that to laminin.

Ascites spheroid adhesion to ECM proteins is partially mediated by β1 integrin subunits. We have previously shown that NIH:OVCAR5 spheroids have the ability to adhere to ECM components via multiple integrin receptors.[15] Therefore, the contribution of integrin subunits in mediating patients' ascites spheroid adhesion to ECM components was evaluated (Fig. 3). The four most adhesive ascites spheroid samples overall (patient samples #1-4) were selected in order to ensure detection of significant levels of inhibition. Ascites spheroids were allowed to adhere to ECM proteins or ovalbumin for 1 hour in the presence of a blocking mAb against the β1 integrin subunit or a mIgG control. Ascites spheroid adhesion to laminin was decreased by >80% for all four patient samples when incubated with the mAb against the β1 integrin subunit when compared to mIgG. Adhesion to fibronectin and type IV collagen was inhibited by 40-60% for patient samples #1-3, and by >80% for patient sample #4. Adhesion to type I collagen was

decreased by 65-85% in the presence of the mAb against the β1 integrin subunit. These results suggest that patients' ascites spheroid adhesion to laminin, fibronectin, type I collagen, and type IV collagen is mediated partially by β1 integrins. Spheroid adhesion to ovalbumin remained unchanged in the presence of the blocking mAb against the β1 integrin subunit, demonstrating that patients' ascites spheroid adhesion to ovalbumin is not mediated by β1 integrins and is most likely non-specific.

Adhesion of patients' ascites spheroids to hyaluronan. Ovarian carcinoma cells have been shown to express CD44, which can mediate their adhesion to hyaluronan in the pericellular matrix of mesothelial cells.[12, 13] To examine the role of hyaluronan in the adhesion of ascites spheroids, glass chamber slides were coated with 1 mg/ml hyaluronan or hyaluronan oligomers. The oligomers were chosen since they are the shortest hyaluronan fragments that will bind to CD44. Ascites spheroids (samples #1-11) and NIH:OVCAR5 spheroids (OVCAR5) were allowed to adhere for 1-4 hours. Similar to the results seen in the ECM protein adhesion assays (Fig. 2), maximum spheroid adhesion occurred at 2 hours (Fig. 4). For the ascites spheroids (patient samples #1-11), adhesion to hyaluronan surpassed that of adhesion to ECM glycoproteins, with few exceptions (Fig 4., samples #1, 5, and 6.) Ascites spheroids generally adhered to hyaluronan oligomers as readily as they did to intact hyaluronan. Interestingly, NIH:OVCAR5 spheroids typically exhibited very low levels of adhesion (Fig. 4, OVCAR5).

To determine the specificity of hyaluronan adhesion, we performed a competition assay of ascites spheroid adhesion to hyaluronan by adding either soluble hyaluronan or

hyaluronan fragments. Adhesion to hyaluronan decreased in a dose-dependent manner (Fig 5). Addition of 100 μg/ml of soluble hyaluronan reduced adhesion of patient sample #1 to hyaluronan by 30%, and reduced adhesion of patient samples #2-4 by 20% (Fig 5A). Both 500 and 1000 μg/ml of soluble hyaluronan eliminated adhesion for all four patient ascites samples. Addition of 80 mg/ml of hyaluronan fragments had no effect on patient samples #1 and 3, but reduced hyaluronan adhesion of patient sample #2 by 20% and patient sample #4 by 40% (Fig 5B). Increasing the concentration to 500 μg/ml of hyaluronan fragments completely blocked adhesion of patient samples #1-3 to hyaluronan, and adhesion of patient sample #4 was inhibited by approximately 90%.

We next wished to determine the contribution of the cell surface receptor CD44 in ascites spheroid adhesion to hyaluronan. The most adhesive patient ascites spheroid samples, #1-4, were allowed to adhere to hyaluronan for 1 hour in the presence of a mAb against the CD44 receptor. The mAb failed to inhibit hyaluronan adhesion, and in several experiments increased the adhesion of the spheroids by as much as 20% (data not shown). These data suggest that hyaluronan may play a role in ascites spheroid adhesion, but the involvement of CD44 in mediating this adhesion remains to be determined.

Adhesion of NIH:OVCAR5 and patient ascites spheroids to human mesothelial cell monolayers. We examined the ability of patient ascites spheroids to adhere to mesothelial cell monolayers, the primary site of secondary tumor growth in ovarian cancer. LP9 human mesothelial cells were grown to confluence on glass chamber slides. NIH:OVCAR5 or patient ascites spheroids were labeled with CMFDA, resuspended in RPMI, and allowed to adhere to live mesothelial cell monolayers for 1–4 hours (Fig. 6A,

a-d). For all eleven patient ascites samples, adhesion at 2 hours to live mesothelial monolayers was comparable or greater than adhesion to individual ECM glycoproteins (Fig. 6B). The two patient samples (#1 and 2) that adhered at highest levels to ECM proteins (Fig. 2) also adhered well to mesothelial cells (Fig. 6B). Interestingly, the two ascites spheroid samples that exhibited the least adhesion to ECM glycoproteins (patient samples #10 and 11) were among the most adhesive to mesothelial cells (Fig. 6B). Adhesion typically increased from 1-2 hours, and then remained constant up to 4 hours. NIH:OVCAR5 spheroids also adhered to live monolayers, although to degree than to individual ECM glycoproteins at 2 hours.[15] To determine if the presence of mesothelial ECM or cell receptors alone was necessary to facilitate adhesion, ascites spheroids were also added to paraformaldehyde-fixed mesothelial monolayers for 1-4 hours. For all samples, spheroid adhesion to fixed mesothelial cells was less than 10% (Fig. 6B).

β1 integrin subunits partially mediate ascites spheroid adhesion to mesothelial monolayers. To investigate the role of β1 integrins in mediating the adhesion of ascites spheroids to mesothelial cells, the four highest adhering patient spheroid samples (#1, 2, 10, and 11) were allowed to adhere for 2 hours in the presence of a blocking mAb against the β1 integrin subunit (Fig. 7). The mAb against the β1 integrin subunit reduced adhesion of samples #1, #10 and #11 by over 60%, while approximately 40% inhibition was observed for sample #2. Addition of the mAb against CD44 had no effect on adhesion (data not shown.) These data indicate that while β1 integrins play a significant role in mediating adhesion of ascites spheroids to mesothelial cells, it is likely that other cell receptors are involved.

Discussion

In advanced stages of ovarian carcinoma, a malignant ascites fluid accumulates in the peritoneal cavity, populated by tumor cells that exist singly or as multicellular spheroids, with mesothelial and inflammatory cells. Cultures derived from ovarian carcinomas have been difficult to establish, as the tumor cells will often fail to attach to a tissue-culture substrata. [11, 23, 24] Often, the free-floating tumor cells form spheroid aggregates, mimicking those observed in the peritoneal effusions of ovarian carcinoma patients.[25, 26] Despite these difficulties, a number of ovarian carcinoma cell lines have successfully been established and utilized in extensive studies focusing on monolayer culture and single cell suspensions, while largely overlooking the role of spheroids in ovarian cancer progression. However, established cell lines do not necessarily reflect the most accurate approximation of *in vivo* conditions since they represent only a limited outgrowth of select tumor cells and not the heterogeneity seen *in vivo*. Additionally, monolayers and spheroids display altered properties,[27, 28] indicating a need for further investigation into the differences between these two morphologies. In this study, we characterized the adhesive ability of ascites spheroids from eleven ovarian carcinoma patients, and investigated the adhesion molecules involved in mediating ascites spheroid adhesion to both ECM components and mesothelial cells.

Here, we report that spheroids recovered from the ascites fluid of eleven ovarian carcinoma patients demonstrate the ability to adhere to ECM proteins. Patient ascites spheroids adhered preferentially to type I collagen and fibronectin, and exhibited lower levels of adhesion to type IV collagen and laminin. In ECM protein adhesion assays, the patient samples segregated into three groups at 2 hours; a highly adhesive group with 35-

70% adhesion, a moderately adhesive group showing 10-20% adhesion, and a low- or non-adhesive group with less than 10% adhesion to ECM proteins. Since the ascites spheroids are similar in morphology from one sample to the next, shear forces likely do not contribute to the differences in adhesion between groups.

The ability of single ovarian carcinoma cells to adhere to ECM proteins has been studied by several groups. A number of ovarian cancer cells lines[29] and cultured ovarian cancer cells recovered from ascites fluid have demonstrated preferential adhesion to type I collagen.[30] Ovarian cancer cell lines and primary cultures have also been shown to adhere to laminin, fibronectin, vitronectin, and type IV collagen.[29-31] Our previous studies have shown that spheroids created from the ovarian carcinoma cell line NIH:OVCAR5 can adhere to type IV collagen, fibronectin, and laminin in a time-dependent manner. In this study, adhesion levels of ascites spheroids were somewhat lower than those reported for single ovarian carcinoma cells,[10, 27, 29-31] which possibly reflects a change in cell adhesive ability upon acquisition of the spheroid morphology. It is plausible that cells in spheroids prefer to maintain their homotypic interactions, rather than disseminating and establishing heterotypic interactions with a matrix. It has also been observed that ovarian cancer cells form distinctly different adhesion complexes when grown on laminin versus fibronectin.[32] It is thus possible that low adhesion levels by spheroids to some ECM glycoproteins may be due to formation of more structurally weak adhesion complexes that are more sensitive to shear forces than single cells, resulting in decreased attachment to substrata. The spheroid geometry may also result in smaller surface area for attachment. Using patient samples versus established cell lines also presents the opportunity for alterations in the type and

levels of adhesion molecules expressed, or cell receptors already bound with matrix ligand. Furthermore, the ascites spheroids used here were not passaged prior to adhesion assays, which avoided select outgrowth of adhesive tumor cells.

In this study, we show that β1 integrins partially mediate the adhesion of ovarian carcinoma ascites spheroids to ECM proteins. Ascites spheroid adhesion to laminin was nearly eliminated by blocking the β1 integrin subunit, while adhesion to fibronectin, type IV collagen, and type I collagen was reduced by approximately 60% in the presence of the same mAb. While this suggests the importance of β1 integrins in mediating ascites spheroid attachment to ECM glycoproteins, the incomplete inhibition of adhesion indicates that other cell adhesion molecules likely play a role, albeit minor, in spheroid adhesion. Ovarian carcinoma cells have been shown to produce chondroitin sulfate and heparan sulfate proteoglycans, which they use to facilitate their adhesion to interstitial matrix components.[33] It is possible that proteoglycans present on the patient ascites' spheroids may be responsible for mediating some adhesion to the ECM glycoproteins used in our assays. Our previous studies with NIH:OVCAR5 spheroids demonstrated that blocking the β1 integrin subunit function with a mAb completely inhibited adhesion to laminin, fibronectin, and type IV collagen.[15] Similarly, Kawano et al showed that squamous cell carcinoma spheroids adhere to type I collagen, laminin 1, laminin 5, and fibronectin, and that this adhesion is mediated by multiple integrin-ligand interactions.[34] These data indicate a significant role for integrins in spheroid adhesion, although identifying the contribution of other cell receptors will also be relevant.

A number of ovarian cancer cell lines have been shown to adhere to hyaluronan via the cell surface molecule CD44.[35, 36] Based on their levels of adhesion to ECM

glycoproteins, we investigated the ability of ascites spheroids to adhere to hyaluronan. In general, the eleven patient ascites spheroid samples adhered at higher levels to hyaluronan than to ECM glycoproteins. Ascites spheroids adhered at comparable levels to fragmented as well as intact hyaluronan. Interestingly, NIH:OVCAR5 spheroids did not significantly adhere to hyaluronan, which may indicate altered CD44 expression between the NIH:OVCAR5 cell line and patient cells. Soluble hyaluronan and hyaluronan fragments were able to compete with the ability of patient ascites spheroids to adhere to hyaluronan in a dose-dependent manner. A blocking mAb against CD44 did not significantly inhibit adhesion to hyaluronan, and often had the effect of increasing adhesion of the patient's spheroids to hyaluronan. Other cell adhesion molecules besides CD44 are known to mediate cellular adhesion to hyaluronan.[37-39] It is possible that the lack of inhibition seen here by a blocking antibody against CD44 may be due to expression of alternate receptors that mediate hyaluronan adhesion. However, it has been reported that some anti-CD44 antibodies can actually activate binding to hyaluronan through cross-linking of CD44 receptors.[40] Thus, a role for CD44 in mediating ascites spheroid adhesion cannot be ruled out.

Ovarian carcinoma spreads by tumor cell attachment to the peritoneal mesothelium. A number of groups have shown that both ovarian cancer cell lines and some primary cultures are capable of adhering to a monolayer of mesothelial cells, via both β1 integrin-ligand interactions and CD44-hyaluronan interactions.[12, 13, 41] We report here that ascites spheroids from eleven ovarian carcinoma patients adhere to monolayers of living, but not fixed, mesothelial cells. This data implies that ascites spheroid adhesion requires feedback from the mesothelial cells. Paraformaldehyde

treatment gently fixes the cells, preserving surface epitopes. Quenching excess aldehyde helps guarantee that the spheroids will not be accidentally fixed when added to the assays. The low levels of spheroid adhesion we observed to fixed cells suggests the presence of mesothelial cell receptors and matrix components alone are not sufficient to achieve significant adhesion. Further study will be needed to identify factors that can contribute to this apparent cross-talk.

Surprisingly, while those patient ascites spheroid samples that exhibited high levels of adhesion to ECM proteins also adhered to mesothelial cells, the patients' samples that were the least adhesive on individual ECM proteins were also among the most adhesive samples to mesothelial cell monolayers. This may reflect variability in the expression of cell receptors between patient samples. On the other hand, because it is difficult to do an exhaustive study of all of the cell adhesion molecules tumor cells might encounter *in vivo*, live mesothelial cells may present unique epitopes that have a greater avidity for these patients' samples than the ECM proteins tested in this study. Mesothelial cells synthesize a variety of ECM proteins, including laminin, fibronectin, type I collagen, and hyaluronan that tumor cells can use to support their attachment.[12, 42] Additionally, mesothelial cells have been shown to induce the migration of ovarian carcinoma cells.[14] Taken together, the data presented here suggests that ascites spheroids present the potential to contribute to ovarian carcinoma dissemination by their ability to attach to mesothelial monolayers.

To address the role of integrins in mediating ascites spheroid adhesion to mesothelial cells, we incubated the spheroids with a mAb against β1 integrin subunits prior to their addition to the adhesion assays. Blocking the β1 integrin subunit reduced

adhesion by 60% for three of the ascites spheroid samples tested, and reduced adhesion to the fourth sample by 40%. Again, due to variation between patient samples, the composition of cell receptors capable of facilitating mesothelial attachment may differ between patients. A mAb that blocks the hyaluronan-binding site of CD44 failed to inhibit adhesion of ascites spheroids to mesothelial cells. In light of the difficulty in obtaining an effective anti-CD44 antibody, the contribution of CD44 in mediating ascites spheroid adhesion cannot be ruled out. These data specify a role for β1 integrins in mediating ascites spheroid adhesion to mesothelium, though the role of other cell receptors will require further exploration.

While the levels of ascites spheroid adhesion shown here may not be 100%, the fact that these experiments were performed in serum-free conditions must not be overlooked. Ascites fluid from ovarian carcinoma patients has been shown to contain a number of factors that may stimulate tumor cell growth in the patient, including lysophosphatidic acid, colony-stimulating factor, tumor necrosis factor α, interleukin-1β, interleukin-6, vascular endothelial growth factor, and matrix metalloproteinases.[41, 43-45] Moreover, cell-free ascites fluid has been shown to improve ovarian tumor growth in a clonogenic assay.[46] Considering the many growth factors present in the ascites fluid, it is conceivable that enhanced levels of ascites spheroid adhesion may occur *in vivo*.

Follow-up data on some patients was available, but no association could be made between spheroid adhesion levels and patient survival or the recurrence of disease at this time. However, we will be continuing to monitor these patients to see if any future correlations can be established.

Evidence of spheroid multicellular resistance to radio- and chemotherapy has been reported.[6, 47] In particular, ovarian carcinoma cells exhibit protection from both radiation and Taxol-induced apoptosis when grown as spheroids in comparison to monolayers.[9, 10, 27] We have previously reported decreased proliferation of ovarian carcinoma cells when cultured as spheroids in contrast to the same cells grown as monolayers.[15] Due to this reduced proliferative ability, which may ultimately cause an altered response to cytotoxic agents, the potential for ascites spheroids to escape treatment-induced apoptosis and contribute to peritoneal implantation needs to be addressed.

Taken together, the data presented here implicate ascites spheroids as a potentially overlooked threat in ovarian carcinoma spread. Their ability to attach to ECM glycoproteins, hyaluronan, and mesothelial cells, as well as their inherent resistance to chemo- and radiation therapies indicate that spheroids may be clinically relevant in the progress of ovarian cancer. Further studies into the migrational and invasive properties of ascites spheroids will be necessary to establish their role in the dissemination of ovarian carcinoma.

Acknowledgements

We thank Dr. James McCarthy for providing fibronectin, Dr. Leo Furcht for providing laminin and the mAb P5D2 against the β1 integrin subunit, and Dr. Judah Folkman for providing the NIH:OVCAR5 cell line. We thank Diane Rauch and Sarah Bowell of Tissue Procurement Facility of the University of Minnesota for their assistance in collecting and processing the ascites samples. This project was supported by a grant from

the Department of the Army (DA/DAMD17-99-1-9564). The content of the information presented in this manuscript does not necessarily reflect the position of the Government.

Figure Legends

Figure 1. Morphologic appearance of ovarian carcinoma spheroids. Spheroids were obtained from the ascites fluid of eleven patients (designated #1-11, respectively) diagnosed with stage III/IV serous ovarian carcinoma. Photographs of the ascites spheroids were taken prior to adhesion assays while still in agarose-coated plates. NIH:OVCAR5 ovarian carcinoma cell lines were cultured in 0.5% agarose-coated 24-well plates to form multicellular spheroids (OVCAR5), and photographed at 48 hours. The size of the NIH:OVCAR5 and patient ascites spheroids ranged from 30-200 μm in diameter. Scale bar, 100 μm.

Figure 2. Adhesion of ovarian carcinoma patient ascites spheroids to extracellular matrix proteins. Patient ascites spheroids were incubated in serum-free media for 2 hours on glass chamber slides coated with 50 μg/ml laminin, fibronectin, type IV collagen, or type I collagen. Non-adherent spheroids were rinsed away, and the remaining adherent spheroids were fixed and stained. Panel A: Patient sample #1 adhering to: (a) laminin, (b) fibronectin, (c) type IV collagen, and (d) type I collagen. Panel B: Patient samples adhering to laminin (black bars), fibronectin (white), type IV collagen (striped), and type I collagen (gray). Values are expressed as a percentage of the total number of spheroids that adhered to each substrate. Data of a representative experiment are expressed as mean ± standard deviation for quadruplicate wells.

Figure 3. Adhesion of ovarian carcinoma patient ascites spheroids to extracellular matrix is dependent upon the β1 integrin subunit. The four most adhesive patient

spheroids samples (#1-4) were incubated for 30 minutes with 10 μg/ml blocking antibody against the β1 integrin subunit or normal mouse IgG before being added to glass chamber slides coated with 50 μg/ml laminin (black bars), fibronectin (white), type IV collagen (striped), type I collagen (gray), or ovalbumin (stippled). Assays were performed in the continued presence of the antibody for 1 hour. Non-adherent spheroids were rinsed away, and the remaining adherent spheroids were fixed and stained. Values are expressed as the percent inhibition. Data of a representative experiment are shown as mean ± standard deviation for quadruplicate wells.

Figure 4. Patient ascites spheroids adhere to hyaluronan. Patient ascites spheroids (#1-11) and NIH:OVCAR5 spheroids (OVCAR5) were added to glass chamber slides coated with 1 mg/ml hyaluronan (black) or hyaluronan fragments (white) and allowed to adhere for 2 hours. Non-adherent spheroids were rinsed away, and the remaining spheroids were fixed and stained. Values are expressed as a percentage of the total number of spheroids that adhered to each substrate. Data of a representative experiment are expressed as mean ± standard deviation for quadruplicate wells.

Figure 5. Adhesion of patient ascites spheroids to hyaluronan can be inhibited by soluble hyaluronan and hyaluronan fragments. The four most adhesive patient spheroids samples, patient #1 (diamonds), #2 (squares), #3 (circles), or #4 (triangles), were incubated for 30 minutes with 0, 100, 500, or 1000 μg/ml hyaluronan (panel A), or 0, 80, or 500 μg/ml hyaluronan fragments (panel B) before being added to glass chamber slides coated with 1 mg/ml hyaluronan. Assays were performed in the continued

presence of the soluble inhibitor for 2 hours. Non-adherent spheroids were rinsed away, and the remaining adherent spheroids were fixed and stained. Values are expressed as the percent inhibition. Data of a representative experiment are shown as mean ± standard deviation for quadruplicate wells.

Figure 6. Adhesion of spheroids to live or fixed human mesothelial monolayers. Patient ascites spheroids and NIH:OVCAR5 spheroids were labeled with CMFDA and added to LP9 human mesothelial monolayers grown to confluence on glass chamber slides. Spheroids were incubated in the wells 2 hours, then non-adherent spheroids were rinsed away and remaining spheroids were fixed with Diff-Quik fixative. Panel A: Brightfield (a, b) and fluorescence microscopy (c, d) of patient ascites spheroids adhering to live mesothelial monolayers at 2 hours; patient sample #1 (a, c) and patient sample #2 (b, d). Magnification at 200X. Panel B: Adhesion assay of patient ascites spheroids (#1-11) and NIH:OVCAR5 spheroids (OVCAR5) to live (black bars) and fixed (white) mesothelial monolayers. Values are expressed as a percentage of the total number of spheroids that adhered. Data of a representative experiment are expressed as mean ± standard deviation for quadruplicate wells.

Figure 7. Inhibition of patient ascites spheroid adhesion to mesothelial cell monolayers. The four most adhesive patient ascites spheroid samples (#1-2, #10-11) were labeled with CMFDA and incubated for 30 minutes with 10 μg/ml blocking antibody against the β1 integrin subunit or mouse IgG. The spheroids were then added in

the presence of the antibody for 1 hour to live confluent LP9 human mesothelial monolayers on glass chamber slides. Non-adherent spheroids were rinsed away, and the remaining adherent spheroids were fixed and stained. Values are expressed as the percent inhibition. Data of a representative experiment are expressed as mean ± standard deviation for quadruplicate wells.

References

1. Ahmedin J, Murray T, Samuels A, Ghafoor A, Ward E, Thun MJ. Cancer Statistics, 2003. CA: A Cancer Journal for Clinicians 2003;53:5-26.

2. Cannistra SA. Cancer of the ovary. New England Journal of Medicine 1993;329(21):1550-1559.

3.Sutherland RM, McCredie JA, Inch WR. Growth of multicell spheroids in tissue culture as a model of nodular carcinoma. Journal of the National Cancer Institute 1971;46:113-120.

4. Sutherland RM, MacDonald HR, Howell RL. Multicellular spheroids: a new model target for *in vitro* studies of immunity to solid tumor allografts. Journal of the National Cancer Institute 1977;58(6):1849-1853.

5. Durand RE, Sutherland RM. Effects of intercellular contact on repair of radiation damage. Experimental Cell Research 1972;71:75-80.

6. Graham CH, Kobayashi H, Stankiewicz KS, Man S, Kapitain SJ, Kerbel RS. Rapid acquistion of multicellular drug resistance after a single exposure of mammary tumor cells to antitumor alkylating agents. Journal of the National Cancer Institute 1994;86(13):975-982.

7.Bardiès M, Thedrez P, Gestin J-F, Marcille B-M, Guerreau D, Faivre-Chauvet A, et al. Use of multi-cell spheroids of ovarian carcinoma as an intraperitoneal radio-immunotherapy model: uptake, retention kinetics and dosimetric evaluation. International Journal of Cancer 1992;50:984-991.

8. Becker JL, Prewett TL, Spaulding GF, Goodwin TJ. Three-dimensional growth and differentiation of ovarian tumor cell line in high ascpect rotating-wall vessel: morphologic and embryological considerations. Journal of Cellular Biochemistry 1993;51:283-289.

9. Filipovich IV, Sorokina NI, Robillard N, Chatal J-F. Radiation-induced apoptosis in human ovarian carcinoma cells growing as a monolayer and as multicell spheroids. International Journal of Cancer 1997;72:851-859.

10. Makhija S, Taylor DD, Gibb RK, Gerçel-Taylor Ç. Taxol-induced Bcl-2 phosphorylation in ovarian cancer cell monolayer and spheroids. International Journal of Oncology 1999;14:515-521.

11. Niedbala MJ, Crickard K, Bernacki RJ. Interactions of human ovarian tumor cells with human mesothelial cells grown on extracellular matrix. Experimental Cell Research 1985;160:499-513.

12.Lessan K, Aguiar DJ, Oegema T, Siebenson L, Skubitz APN. CD44 and β1 integrin mediate ovarian carcinoma cell adhesion to peritoneal mesothelial cells. American Journal of Pathology 1999;154(5):1525-1537.

13.Cannistra SA, Kansas GS, Niloff J, DeFranzo B, Kim Y, Ottensmeier C. Binding of ovarian cancer cells to peritoneal mesothelium *in vitro* is partly mediated by CD44H. Cancer Research 1993;53:3830-3838.

14. Rieppi M, Vergani V, Gatto C, Zanetta G, Allavena P, Taraboletti G, et al. Mesothelial cells induce the motility of human ovarian carcinoma cells. International Journal of Cancer 1999;80:303-307.

15.Casey RC, Burleson KM, Skubitz KM, Pambuccian SE, Oegema TR, Ruff LE, et al. β1-integrins regulate the formation and adhesion of ovarian carcinoma multicellular spheroids. American Journal of Pathology 2001;159(6):2071-2080.

16. Glimelius B, Norling B, Nederman T, Carlsson J. Extracellular matrices in multicellular spheroids of human glioma origin: increased incorporation of proteoglycans and fibronectin as compared to monolayer cultures. APMIS 1988;96:433-444.

17. Nederman T, Norling B, Glimelius B, Carlsson J, Brunk U. Demonstration of an extracellular matrix in multicellular tumor spheroids. Cancer Research 1984;44:3090-3097.

18.Rainaldi G, Calcabrini A, Arancia G, Santini MT. Differential expression of adhesion molecules (CD44, ICAM-1 and LFA-3) in cancer cells grown in monolayer or as multicellular spheroids. Anticancer Research 1999;19:1769-1778.

19.Smith DE, Mosher DF, Johnson RB, Furcht LT. Immunological identification of two sulfhydryl-containing fragments of human plasma fibronectin. Journal of Biological Chemistry 1982;257(10):5831-5838.

20.Hamilton TC, Young RC, Ozols RF. Experimental model systems of ovarian cancer: applications to the design and evaluation of new treatment approaches. Seminars in Oncology 1984;11:285-298.

21. Molpus KL, Koelliker D, Atkins L, Kato DT, Buczek-Thomas J, Fuller AF, et al. Characterization of a xenograft model of human ovarian carcinoma which produces intraperitoneal carcinomatosis and metastasis in mice. International Journal of Cancer 1996;67:588-595.

22. Semler EJ, Ranucci CS, Moghe PV. Mechanochemical manipulation of hepatocyte aggregation can selectively induce or repress liver-specific function. Biotechnology and Bioengineering 2000;69(4):359-369.

23. Monif GRG, Daly JW. "Living cytology" in the diagnosis of intraabdominal adenocarcinoma. Obstetrics and Gynecology 1975;46(1):80-83.

24.Verschraegen CF, Hu W, Du Y, Mendoza J, Early J, Deavers M, et al. Establishment and charcterization of cancer cell cultures and xenografts derived from primary or metastatic mullerian cancers. Clinical Cancer Research 2003;9:845-852.

25.Allen HJ, Porter C, Gamarra M, Piver MS, Johnson EAZ. Isolation and morphological characterization of human ovarian carcinoma cell clusters present in effusions. Experimental Cell Biology 1987;55:194-208.

26. Woods LK, Morgan RT, Quinn LA, Moore GE, Semple TU, Stedman KE. Comparison of four new cell lines from patients with adenocarcinoma of the ovary. Cancer Research 1979;39:4449-4459.

27. Frankel A, Buckman R, Kerbel RS. Abrogation of Taxol-induced G_2-M arrest and apoptosis in human ovarian cancer cells grown as multicellular tumor spheroids. Cancer Research 1997;57:2388-2393.

28. Paulus W, Huettner C, Tonn JC. Collagens, integrins and the mesenchymal drift in glioblastomas: a comparison of biopsy specimens, spheroid and early monolayer cultures. International Journal of Cancer 1994;58:841-846.

29.Cannistra SA, Ottensmeier C, Niloff J, Orta B, DiCarlo J. Expression and function of $\beta 1$ and $\alpha v\beta 3$ integrins in ovarian cancer. Gynecologic Oncology 1995;58:216-225.

30.Fishman DA, Kearns A, Chilukuri K, Bafetti LM, O'Toole EA, Georgacopoulos J, et al. Metastatic dissemination of human ovarian epithelial carcinoma is promoted by α2β1-intgrin-mediated interaction with type I collagen. Invasion and Metastasis 1998;18:15-26.

31.Buczek-Thomas JA, Chen N, Hasan T. Integrin-mediated adhesion and signalling in ovarian cancer cells. Cellular Signaling 1998;10(1):55-63.

32. Gimond C, Mercier I, Weber I, Aumailley M. Adhesion complexes formed by OVCAR-4 cells on laminin 1 differ from those observed on fibronectin. Cell Adhesion and Communication 1996;3:527-539.

33.Kokenyesi R. Ovarian carcinoma cells synthesize both chondroitin sulfate and heparan sulfate cell surface proteoglycans that mediate cell adhesion to interstitial matrix. Journal of Cellular Biochemistry 2001;83:259-270.

34.Kawano K, Kantak SS, Murai M, Yao C-C, Kramer RH. Integrin α3β1 engagement dirupts intercellular adhesion. Experimental Cell Research 2001;262:180-196.

35.Gardner MJ, Catterall JB, Jones LMH, Turner GA. Human ovarian tumour cells can bind hyaluronic acid via membrane CD44: a possible step in peritoneal metastasis. Clinical and Experimental Metastasis 1996;14:325-334.

36. Catterall JB, Jones LMH, Turner GA. Membrane protein glycosylation and CD44 content in the adhesion of human ovarian cancer cells to hyaluronan. Clinical and Experimental Metastasis 1999;17(583-591).

37.Day AJ, Prestwich GD. Hyaluronan-binding proteins: tying up the giant. Journal of Biological Chemistry 2002;277:4585-4588.

38.Bono P, Rubin K, Higgins JM, Hynes RO. Layilin, a novel integral membrane protein, is a hyaluronan receptor. Molecular Biology of the Cell 2001;12:891-900.

39. Hardwick C, Hoare K, Owens R, Hohn HP, Hook M, Moore D, et al. Molecular cloning of a novel hyaluronan receptor that mediates tumor cell motility. Journal of Cell Biology 1992;117:1343-1350.

40.Lesley J, Hyman R, Kincade PW. CD44 and its interaction with extracellular matrix. Advances in Immunology 1983;54:271-335.

41.Mills GB, May C, Hill M, Campbell S, Shaw P, Marks A. Ascitic fluid from human ovarian cancer patients contains growth factors necessary for intraperitoneal growth of human ovarian adenocarcinoma cells. Journal of Clinical Investigation 1990;86:851-855.

42. Stylianou E, Jenner LA, Davies M, Coles GA, Williams JD. Isolation, culture and characterization of human peritoneal mesothelial cells. Kidney International 1990;37:1563-1570.

43.Westermann AM, Beijnen JH, Moolenaar WH, Rodenhuis S. Growth factors in human ovarian cancer. Cancer Treatment Reviews 1997;23:113-131.

44.Westermann AM, Havik E, Postma FR, Beijnen JH, Dalesio O, Moolenaar WH, et al. Malignant effusions contain lysophosphatidic acid (LPA)-like activity. Annals of Oncology 1998;9:437-442.

45. Davidson B. Ovarian carcinoma and serous effusions. Changing views regarding tumor progression and review of current literature. Analytical Cellular Pathology 2001;23:107-128.

46.Uitendaal MP, Hubers HAJM, McVie JG, Pinedo HM. Human tumour clonogenicity in agar is improved by cell-free ascites. British Journal of Cancer 1983;48:55-59.

47. Sutherland RM. Cell and environment interactions in tumor microregions: the multicell spheroid model. Science 1988;240:177-184.

Article Précis

Ascites spheroids from eleven ovarian carcinoma patients adhered to extracellular matrix proteins and mesothelial cell monolayers, implicating spheroids as potential sources of secondary tumor growth.

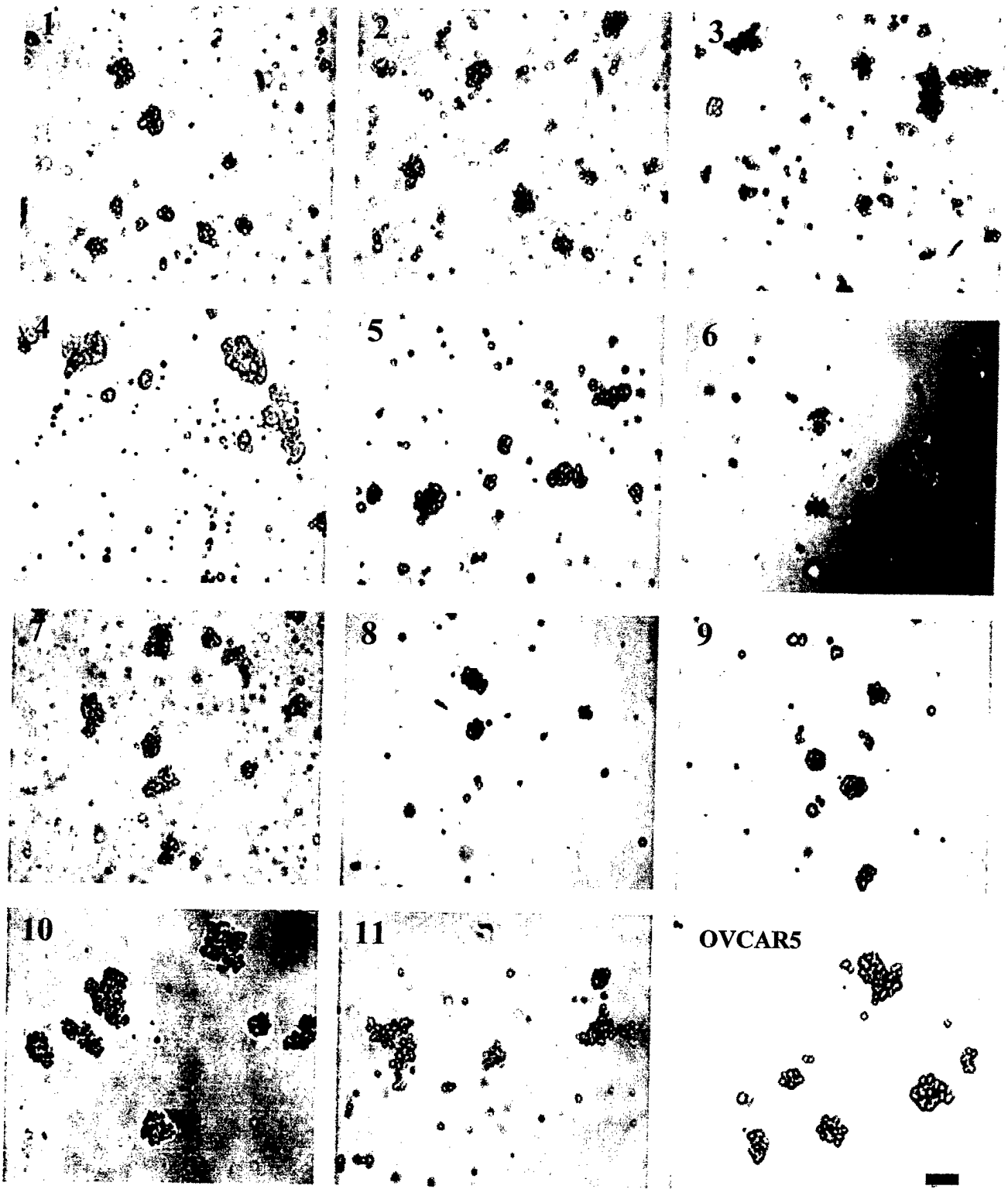
1
2
3
4
5
6
7
8
9
10
11
OVCAR5

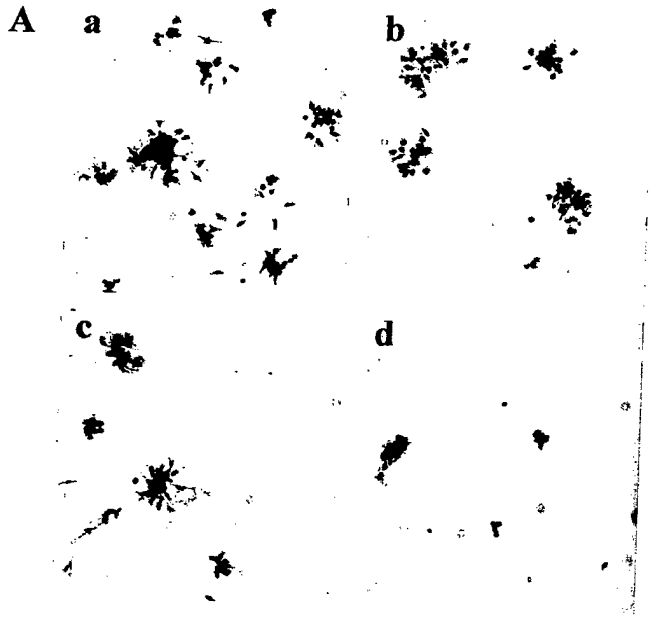

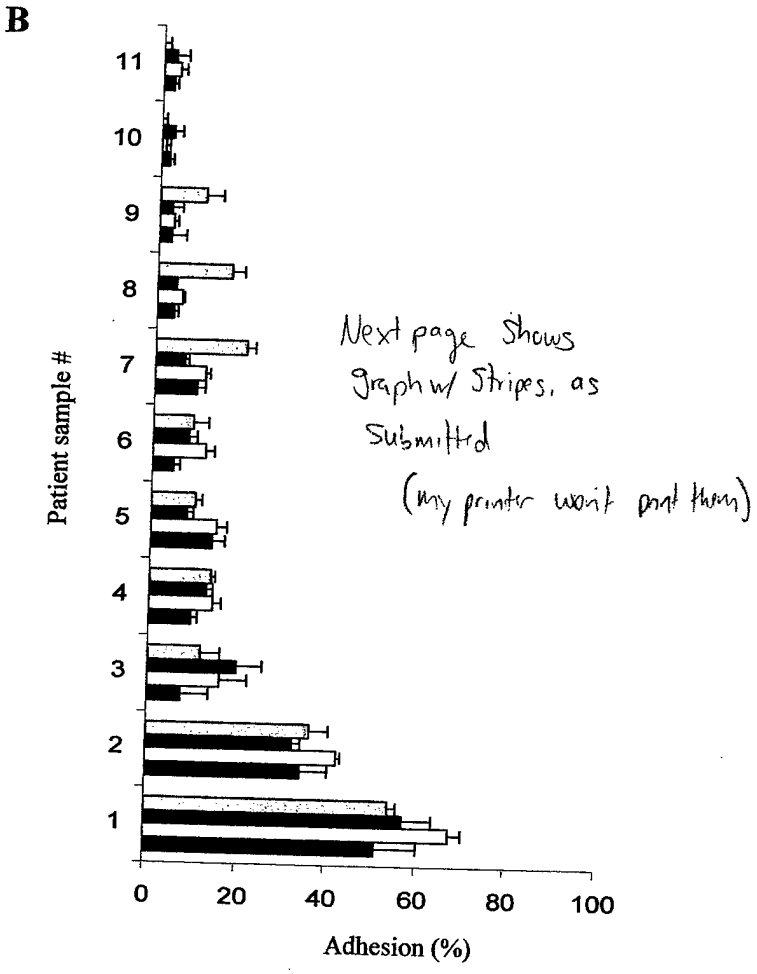

Next page shows graph w/ stripes, as submitted (my printer won't print them)

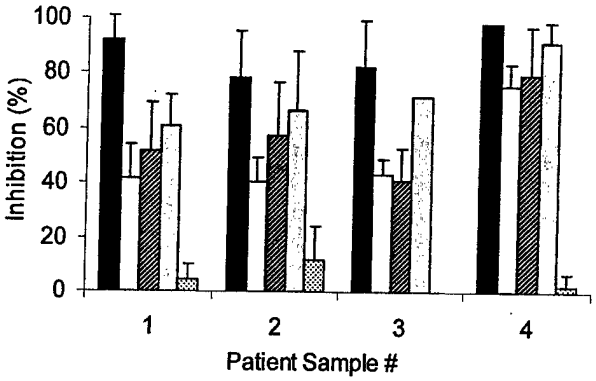
100
80
60
40
20
0
Inhibition (%)
1
2
3
4
Patient Sample #

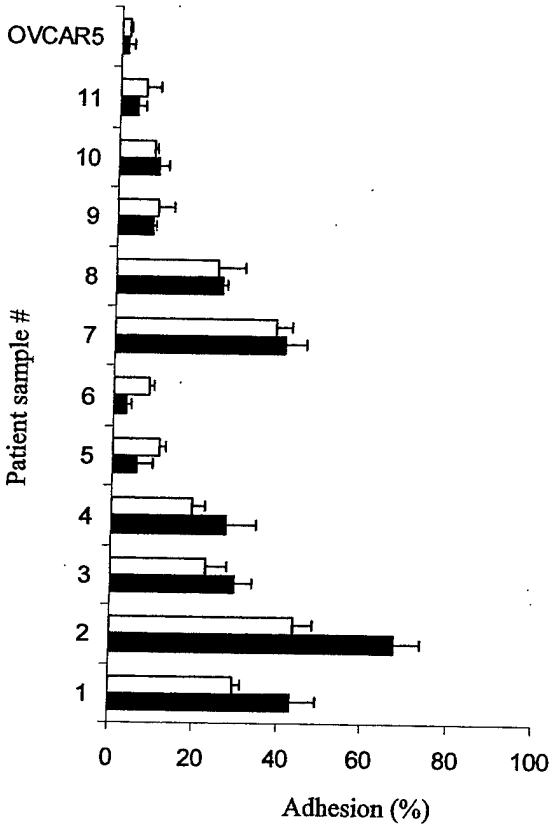
OVCAR5
11
10
9
8
7
6
5
4
3
2
1
Patient sample #
0
20
40
60
80
100
Adhesion (%)

A

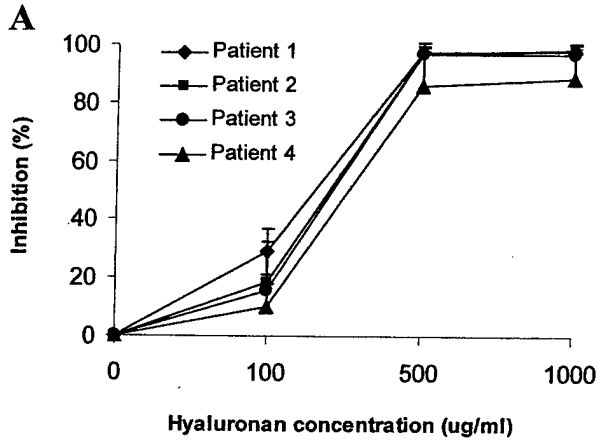
100
80
60
40
20
0
Inhibition (%)
Patient 1
Patient 2
Patient 3
Patient 4
0
100
500
1000
Hyaluronan concentration (ug/ml)

B

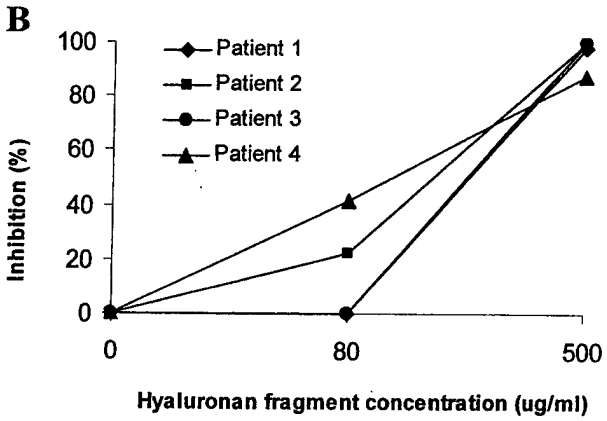
100
80
60
40
20
0
Inhibition (%)
Patient 1
Patient 2
Patient 3
Patient 4
0
80
500
Hyaluronan fragment concentration (ug/ml)

A

B

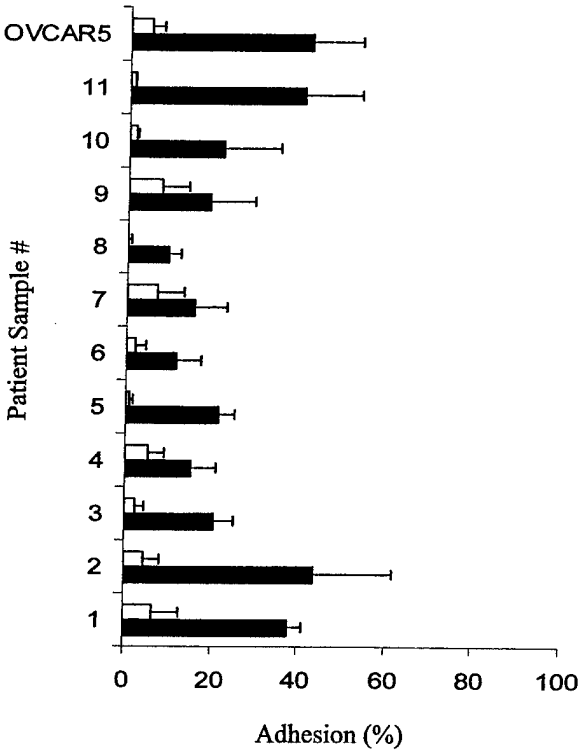
OVCAR5
11
10
9
8
7
6
5
4
3
2
1
Patient Sample #
0
20
40
60
80
100
Adhesion (%)

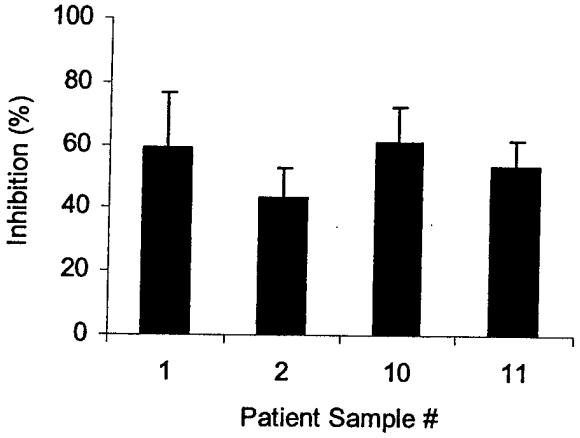
100
80
60
40
20
0
Inhibition (%)
1
2
10
11
Patient Sample #